
ETD Archive

Spring 4-13-2022

Biochemical Characterization Of Induced Pluripotent Stem Cell-Derived Cardiomyocytes As A Model Of Barth Syndrome

Alisha J. House
Cleveland State University

Follow this and additional works at: <https://engagedscholarship.csuohio.edu/etdarchive>

 Part of the [Chemistry Commons](#)

[How does access to this work benefit you? Let us know!](#)

Recommended Citation

House, Alisha J., "Biochemical Characterization Of Induced Pluripotent Stem Cell-Derived Cardiomyocytes As A Model Of Barth Syndrome" (2022). *ETD Archive*. 1331.
<https://engagedscholarship.csuohio.edu/etdarchive/1331>

This Dissertation is brought to you for free and open access by EngagedScholarship@CSU. It has been accepted for inclusion in ETD Archive by an authorized administrator of EngagedScholarship@CSU. For more information, please contact library.es@csuohio.edu.

BIOCHEMICAL CHARACTERIZATION OF INDUCED PLURIPOTENT STEM
CELL-DERIVED CARDIOMYOCYTES AS A MODEL OF BARTH SYNDROME

ALISHA J HOUSE

Bachelor of Science in Nuclear Engineering Technology

Excelsior College

June 2012

Submitted in partial fulfillment of requirements for the degree

DOCTOR OF CLINICAL-BIOANALYTICAL CHEMISTRY

at the

CLEVELAND STATE UNIVERSITY

MAY 2022

We hereby approve this dissertation

for

ALISHA J HOUSE

Candidate for the Doctorate degree in Clinical and Bioanalytical Chemistry

for the Department of Chemistry and

CLEVELAND STATE UNIVERSITY'S

College of Graduate Studies by

Committee Chairperson: Dr. Yana Sandlers
Chemistry Department at Cleveland State University

Date

Committee Member: Dr. Michael Kalafatis
Chemistry Department at Cleveland State University

Date

Committee Member: Dr. Aimin Zhou
Chemistry Department at Cleveland State University

Date

Committee Member: Dr. Bin Su
Chemistry Department at Cleveland State University

Date

Committee Member: Dr. Roman Kondratov
Biology Department at Cleveland State University

Date

Date of Defense: April 13, 2022

DEDICATION

To God, for always seeing me through life's challenges, to my wonderful family for their endless support, and to Ethan, the brightest-shining light in my life – I love you to infinity and back!

BIOCHEMICAL CHARACTERIZATION OF INDUCED PLURIPOTENT STEM
CELL-DERIVED CARDIOMYOCYTES AS A MODEL OF BARTH SYNDROME

ALISHA J HOUSE

ABSTRACT

Barth Syndrome (BTHS) is an X-linked inborn error of metabolism (IEM) which manifests as a multi-systemic disease. One of the primary symptoms is dilated cardiomyopathy, and alongside the cardiovascular disease that arises, patients often experience metabolic abnormalities such as 3-methylglutaconic aciduria, growth retardation, and neutropenia. There has been a need for the development of a suitable *in-vitro* modeling system which will accurately recapitulate the biochemical and physical nature of BTHS. The purpose of this project has been to develop a model for studying the biochemical pathogenesis of Barth Syndrome using human induced pluripotent stem cell-derived cardiomyocytes (hiPSC-CMs). To achieve this, groundwork was laid in developing differentiation methods for producing ventricular hiPSC-CMs from hiPSCs. Simultaneously, a group of methods utilizing mass spectrometry in the biochemical analysis of hiPSC-CMs was developed, and this has provided a novel platform for the detection of many metabolites for the purpose of analyzing the metabolic abnormalities due to BTHS. Biochemical characterization of hiPSC-CMs is a novel tool to be used in assessing biochemical abnormalities and has not previously been achieved.

TABLE OF CONTENTS

	Page
ABSTRACT.....	iv
LIST OF TABLES	ix
LIST OF FIGURES	x
INNOVATION	xiv
 CHAPTER	
I. INTRODUCTION	1
1.1 Barth Syndrome	2
1.1.1 Cardiolipin and BTHS Mitochondria.....	4
1.1.2 Dilated Cardiomyopathy	7
1.2 Cardiac Metabolism	9
1.2.1 Fatty Acid β -Oxidation	9
1.2.2 Glycolysis	11
1.2.3 Ketone Bodies, Lactate, and Pyruvate	12
1.2.4 Citric Acid Cycle	13
1.2.5 Amino Acids	14
1.2.6 Other Organic Acids	16
1.3 Metabolomics.....	18
1.3.1 Untargeted Metabolomics.....	19
1.3.2 Targeted Metabolomics	20
II. DEVELOPMENT OF VENTRICULAR hiPSC-CM DIFFERENTIATION	
PROTOCOLS	21

2.1	Human Induced Pluripotent Stem Cells (hiPSCs)	22
2.1.1	Differentiation to Cardiomyocytes	26
2.1.2	hiPSC-CM Subtype.....	27
2.2	Small Molecules Manipulate Signaling Pathways During Differentiation.....	27
2.2.1	CHIR99021	28
2.2.2	IWR-1	29
2.2.3	Y-27632	31
2.2.4	Activin-A and BMP4	32
2.2.5	Ascorbic Acid	33
2.3	Materials and Methods.....	33
2.3.1	Cell Lines	33
2.3.2	Culture of hiPSCs	34
2.3.3	Cardiomyocyte Differentiation Protocol Development	36
2.4	Results.....	48
2.4.1	hiPSC-CM Differentiation Protocols.....	48
2.4.2	CHIR-Activin-E/IWR	48
2.4.3	9 μ M/24hrs CHIR-IWR	54
2.4.4	Immunohistochemical Analysis.....	60
2.5	Conclusion	65
III.	MASS SPECTROMETRY ASSAYS FOR EVALUATING METABOLIC ACTIVITY	66

3.1	Introduction.....	66
3.1.1	LC-MS/MS	67
3.1.2	GC-MS.....	68
3.2	Derivatization Methods.....	68
3.2.1	MOX-TMS Derivatization.....	69
3.2.2	Butyl-Esterification.....	69
3.3	Mass Spectrometry Assays	71
3.3.1	Cell Harvesting and Metabolite Extraction.....	72
3.3.2	Small Metabolite Scan and Citric Acid Cycle Intermediates	74
3.3.3	Amino Acids and Acylcarnitines	79
3.4	Conclusion	86
IV.	RANOLAZINE STUDY	88
4.1	Ranolazine.....	88
4.2	Methods.....	89
4.3	TAZ ^{517delG} -hiPSC-CMs vs. TAZ ^{WT} -hiPSC-CMs (BTHS vs. Control) – (cell media - ¹ H-NMR).....	92
4.4	Ranolazine-treated vs. Non-treated TAZ ^{517delG} -hiPSC-CMs – (cell media - ¹ H-NMR)	98
4.5	Technical Feasibility	104
4.5.1	Detection of Metabolic Abnormalities Due to TAZ Mutation and Effect of Ranolazine Treatment on TAZ ^{517delG} hiPSC-CMs (cell lysate –	

LC-MS/MS)	104
4.6 Conclusion	108
V. CONCLUSION AND FUTURE DIRECTIONS	109
BIBLIOGRAPHY	111
APPENDIX	125

LIST OF TABLES

Table	Page
1. Structures of Lactate, Pyruvate, Acetoacetate, and β -hydroxybutyrate	12
2. Wild-Type hiPSC Cell Lines	34
3. TAZ-Mutation hiPSC Cell Lines	34
4. Differentiation Methods Attempted (a)	44
5. Differentiation Methods Attempted (b)	45
6. Differentiation Methods Attempted (c)	46
7. Differentiation Methods Attempted (d)	47
8. Successful Differentiation Methods.....	59
9. GC-MS Parameters for Small Metabolites	75
10. GC-MS Parameters for Citric Acid Cycle Intermediates	77
11. LC-MS/MS Parameters for FIA of Acylcarnitines.....	82
12. LC-MS/MS Parameters for FIA of Amino Acids.....	85

LIST OF FIGURES

Figure	Page
1. Cardiolipin Structure.....	5
2. Cardiolipin's Supportive Role within the Electron Transport Chain.....	6
3. Example of Dilated Cardiomyopathy with Left Ventricular Non-Compaction.....	8
4. Red Blood Cell Fatty Acids	10
5. Multivariate Analysis of Case vs Control for Acylcarnitines	11
6. Interrelationship between AcAc/BhB, pyruvate/lactate, and NADH/NAD ⁺ in the mitochondria and cytosol.	13
7. Plasma Citric Acid Cycle Intermediates by LC-MS/MS	14
8. Plasma Amino Acid Levels	15
9. Multivariate Statistical Analysis of Case vs Control for Amino Acids	16
10. GC-MS Spectra of Urine Organic Acids in BTHS	17
11. Urine Organic Acids by GC-MS.....	17
12. Reprogramming of Fibroblasts to hiPSCs	24
13. Workflow of Investigation of BTHS Using hiPSCs	25
14. Structure of CHIR99021	29
15. Wnt/ β -catenin pathway with CHIR 99021	29
16. Structure of IWR-1	30
17. Wnt/ β -catenin pathway with IWR-1	31
18. Structure of Y-27632	32
19. Immunohistochemical analysis of hiPSCs to verify pluripotency	35
20. Colony of hiPSCs.....	36

21.	Timeline of CHIR-Activin-E/IWR Protocol.....	50
22.	Timeline of 9 μ M/24hrs CHIR-IWR Protocol.....	55
23a.	TNNI3, IRX4, and DAPI Staining of hiPSC-CMs.....	62
23b.	TNNI3, IRX4, and DAPI Staining of hiPSC-CMs.....	63
24.	α -actinin and DAPI Staining of Multi-nucleated hiPSC-CMs.....	63
25a.	α -actinin Staining of hiPSC-CMs	64
25b.	α -actinin Staining of hiPSC-CMs	64
26.	MOX-TMS Derivatization.....	69
27.	MOX-TBDMS Derivatization	69
28.	Butyl-Esterification of Amino Acids	70
29.	Fragmentation of Amino Acids	70
30.	Butyl-Esterification of Acylcarnitines	71
31.	Fragmentation of Acylcarnitines.....	71
32.	Equation for Determining Metabolite Levels in iPSC-CM	75
33.	Small Metabolite Scan by GC-MS	76
34.	Citric Acid Cycle Intermediates via GC-MS	78
35.	Acylcarnitines Assay	81
36.	Amino Acids Analysis	83
37.	LC-MS/MS spectra of amino acids detected in hiPSC-CMs.....	84
38.	Glycolysis Intermediates in BTHS hiPSC-CMs with respect to WT hiPSC-CMs (cell media)	92
39.	Citric Acid Cycle Intermediates in BTHS hiPSC-CMs with respect to WT hiPSC-CMs (cell media).....	93

40.	Pentose Phosphate Pathway Intermediates in BTHS hiPSC-CMs with respect to WT hiPSC-CMs (cell media).....	94
41.	Sugar Phosphates in BTHS hiPSC-CMs with respect to WT hiPSC-CMs (cell media)	95
42.	Nucleotides/Hexose Amines in BTHS hiPSC-CMs with respect to WT hiPSC-CMs (cell media).....	96
43.	Miscellaneous Metabolites in BTHS hiPSC-CMs with respect to WT hiPSC-CMs (cell media).....	97
44.	Glycolysis Intermediates in BTHS hiPSC-CMs treated with 100 mM Ranolazine with respect to Non-treated BTHS hiPSC-CMs (cell media)	98
45.	Citric Acid Cycle Intermediates in BTHS hiPSC-CMs treated with 100 mM Ranolazine with respect to Non-treated BTHS hiPSC-CMs (cell media)	99
46.	Pentose Phosphate Pathway Intermediates in BTHS hiPSC-CMs treated with 100 mM Ranolazine with respect to Non-treated BTHS hiPSC-CMs (cell media)	100
47.	Sugar Phosphates in BTHS hiPSC-CMs treated with 100 mM Ranolazine with respect to Non-treated BTHS hiPSC-CMs (cell media)	101
48.	Nucleotides/Hexose Amines in BTHS hiPSC-CMs treated with 100 mM Ranolazine with respect to Non-treated BTHS hiPSC-CMs (cell media)	102
49.	Miscellaneous Metabolites in BTHS hiPSC-CMs treated with 100 mM Ranolazine with respect to Non-treated BTHS hiPSC-CMs (cell media)	103
50.	Succinate Levels in TAZ517delG vs. TAZ517delG 100 mM Ranolazine-Treated hiPSC-CMs (cell lysate)	105

51.	GSH + GSSG Levels in TAZ517delG, and TAZ517delG 100 mM Ranolazine-Treated hiPSC-CMs (cell lysate)	106
52.	GSH+GSSG Levels in Undifferentiated iPSCs (WT vs. BTHS)	107
53.	Cysteine Levels in WT, TAZ ^{517delG} , and TAZ ^{517delG} 100 mM Ranolazine-Treated hiPSC-CMs	107
54.	Complete list of compounds measured by GC-MS small metabolite scan.....	125
55.	hiPSC-CM: TAZWT vs. TAZ517delG (cell lysate).....	126
56.	hiPSC-CM: TAZ517delG vs. TAZ517delG Ranolazine-treated (cell lysate)	127

INNOVATION

This project has several technical aspects which are innovative to their respective fields. Cardiac differentiation from stem cells has long been a challenge for scientists in the context of producing a highly pure and fully functional population of stem cell-derived cardiomyocytes. Furthermore, differentiation of iPSCs is highly dependent on the cell line used, and the challenge is increased when a particular subtype of cardiomyocyte is desired. In this project, several cell lines are used, and two differentiation protocols were developed that worked well for our cell lines to produce ventricular iPSC-CMs. These protocols produced functional cardiomyocytes which could survive in culture for at least 90 days and were confirmed to be of human ventricular lineage, demonstrated by positive staining for IRX4. They also displayed signs of a higher level of maturity such as being rod-shaped and having organized myocardial z-bands.

The mass spectrometry assays developed are innovative in a way that provides a new method for evaluating the biochemical nature of *in-vitro* cellular material, of iPSC-CM. Biochemical analysis of iPSC-CM has never been used to characterize either wild type or diseased cells, and these methods have the potential to provide a complementary analysis with regard to other types of biomolecular characterization such as protein or genetic analysis of cells. Of the ‘omics’ fields, metabolomics remains to be the less explored in the context of *in-vitro* cellular models, and this project has produced headway in the development of such methods.

CHAPTER I

INTRODUCTION

Inborn errors of metabolism are diseases which arise from genetic defects related to metabolism. These genetic defects manifest as aberrant metabolic pathway functioning. IEM can be wide-ranging, and affect various biological processes to include: carbohydrate processing, fatty acid oxidation, mitochondrial metabolism, DNA synthesis, and organic and amino acid metabolism (*About Inborn Errors of Metabolism*, n.d.). Dysfunction may be present not only at the site of the defect in a metabolic pathway but may also cause malfunction in other body systems which act in concert with the affected pathway.

Barth Syndrome is notable in that it presents as a multi-systemic disease. Although the genetic cause of the disease miscodes for a single protein, many areas of the body are affected – the heart, skeletal muscles, blood, and urine, and is associated with other symptoms which are inherently multi-systemic, such as growth delay and neutropenia (Jefferies, 2013). Additionally, patients have also reported that fatigue and tiredness with muscle weakness is a significant symptom of BTHS (Gwaltney et al., 2021). Although the specific biochemical symptoms of the disease have been identified, it has been a challenge for clinicians to discover the exact mechanisms of the disease.

1.1 Barth Syndrome

Barth Syndrome (BTHS) is an X-linked multi-system disorder which presents at a young age. The disease is due to defects in the TAZ gene which encodes the Tafazzin protein, and manifests primarily as dilated cardiomyopathy, skeletal myopathy, and neutropenia. Since it is X-linked recessive, it generally only affects males (Finsterer, 2019).

The TAZ gene (G4.5) is located on Xq28, contains 11 exons, and has 4 major mRNA splice variants. Alternative splicing caused by insertions, deletions, or point mutations leads to the defects in the formation of the TAZ protein, and it has been found that approximately 90% of cases are caused by point mutations (Finsterer, 2019), which can then lead errors such as frameshift or missense errors.

The Tafazzin protein, which is 292 amino acids in size with a molecular weight of 33.5 kDa, is an acyltransferase which remodels the phospholipid Cardiolipin (CL) in the mitochondria. CL is highly expressed in cardiac and skeletal tissue (Clarke et al., 2013; Yan & Kang, 2012), and serves as the structural building block of the mitochondria. Cardiolipin is crucial for ATP production and the proper functioning of the electron transport chain in the mitochondria, and plays a part in the control of reactive oxygen species (Paradies et al., 2019).

The pathogenesis of BTHS is difficult to predict on an individual basis, which makes the disease difficult to treat as well. There is a lack of clear genotype-phenotype correlation, and patients with the same mutation often have very different symptoms (*OMIM Entry - # 302060 - BARTH SYNDROME; BTHS*, n.d.). Given the wide variability of age of onset, expression of symptoms, and the progression of the disease from one patient to another, it is often difficult to make a correct diagnosis and has even been called

a “mystery disease” by health professionals (Schlame & Ren, 2006). Currently, the reported incidence of BTHS is 1:300,000, however it is believed to be significantly underdiagnosed (Clarke et al., 2013; Schlame & Ren, 2006). Many questions are still unanswered about BTHS, and with the variability of symptoms and progression of disease, much is left to be discovered about the pathophysiology behind BTHS.

Symptoms of BTHS typically manifest from between birth to within a few months of life. The most prominent of the symptoms are usually heart-related and present as dilated cardiomyopathy with a variable degree of left ventricular non-compaction, and endocardial fibroelastosis. Other symptoms include neutropenia, skeletal myopathy, growth retardation, and 3-methylglutaconic aciduria (3-MGA), which can be fatal if not diagnosed early (*OMIM Entry - # 302060 - BARTH SYNDROME; BTHS*, n.d.). Biochemical characteristics of BTHS include increased levels of monolysocardiolipin (MLCL, which is the precursor to mature CL) and decreased levels of mature CL. There also tends to be seen an abnormal acyl chain composition of the remaining CL (Saric et al., 2016). Other biochemical characteristics include decreased plasma arginine, decreased total serum cholesterol, and increased plasma proline. Diagnosis of BTHS is made based on the presentation of clinical symptoms, which include existence of cardiomyopathy and prominent neutropenia. Biochemically, elevated levels of 3-MGA in urine and plasma, and measurement of the concentration of cardiolipin in cultured skin fibroblasts and platelets (Valianpour et al., 2002) aid in the diagnosis. The disease is confirmed via genetic analysis for a Tafazzin mutation.

To date, several models of the BTHS genotype exist. Although no model is ever a perfect replica of the native disease, there are promising models which have provided

valuable information as to the mechanisms of BTHS. These include murine TAZ gene knock-out and knockdown models, and cellular models using shRNAs in rodent heart cells. Additionally, models for the BTHS genotype have been provided by yeast, *Drosophila*, and Zebrafish. More recently, mouse embryonic fibroblasts (MEFs) and human induced pluripotent stem cells (hiPSCs) have been used to model BTHS, in addition to patient-derived fibroblasts and platelets (*Barth Syndrome Foundation : Research : Animal and Cellular Models of Barth Syndrome*, n.d.).

Electrophysical studies of BTHS cardiomyocytes have been performed using iPSC-CMs, however there remained to be developed a platform for the metabolic study of BTHS using iPSC-CMs – the goal of this study has been to produce such a platform. Due to the unlimited self-renewal of iPSCs and the ability to insert gene mutations, the iPSC-CM model holds great promise to the future study of BTHS. The goals of this project have been to differentiate iPSCs into cardiomyocytes of ventricular origin for the purpose of modeling the BTHS phenotype of dilated cardiomyopathy with left-ventricular non-compaction more closely, and to develop and perform biochemical assays on the iPSC-CMs using mass spectrometry in order to further elucidate the biochemical pathogenesis of BTHS.

1.1.1 Cardiolipin and BTHS Mitochondria

Cardiolipin is a phospholipid found exclusively in the mitochondria and peroxisomes (Raja & Greenberg, 2014; Raval & Kamp, 2014) of cells. Its abundance is high in tissues which have a high energy demand – CL constitutes 15-20% of the total phospholipid phosphorus mass of the heart (Lu & Claypool, 2015), and unlike other phospholipids which are synthesized in the endoplasmic reticulum, cardiolipin is synthesized exclusively in the mitochondria (Schlame & Greenberg, 2017). It is a dimer,

composed of two phosphatidylglycerol units connected via a glycerol backbone. The predominant, mature form of cardiolipin has four fatty acid chains composed of 18:2 linoleic acid, forming the tetralinoleoyl-CL species (Lu & Claypool, 2015). Following initial synthesis, CL must undergo remodeling in order to produce the mature form of cardiolipin. First, it is de-acylated by a lipase to form monolysocardiolipin (MLCL), and then re-acylated with the appropriate fatty acid chains. Tafazzin is one of the three proteins responsible for this remodeling, and the only one of which has been conserved across species (Saric et al., 2015). A defect in tafazzin results in the majority of cellular cardiolipin species not containing the correct fatty acid composition or the high degree of symmetry found in mature cardiolipin – characteristics which are vital to it fulfilling its role within the mitochondria. These roles include stabilizing respiratory supercomplexes and maintaining the correct structure of mitochondria, initiating apoptosis, mitochondrial replication, cell cycle regulation, and iron-sulfur cluster biosynthesis (Saric et al., 2015; Schlame & Ren, 2006).

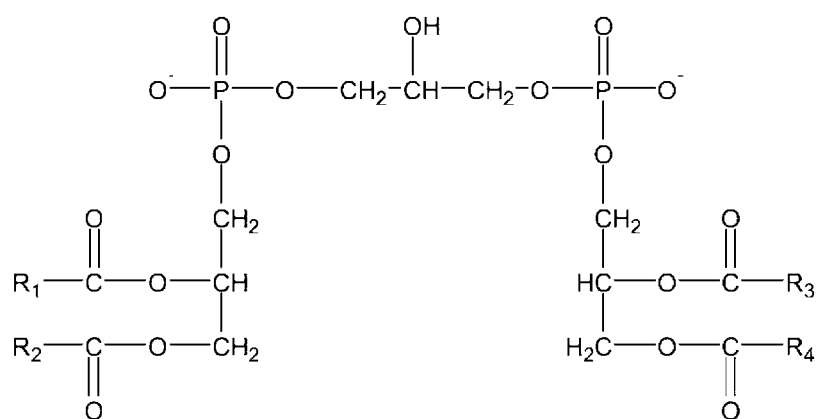


Figure 1: Cardiolipin Structure (Vaz et al., 2003)

The main purpose of mitochondria in the cell is for the production of energy and ATP for the cell, and cardiolipin has been described as the “glue that holds the machinery together” (Saric et al., 2015) for the processes of energy and ATP production in the cell, thus ensuring that electron flow and proton transport are efficient. CL is able to associate with and modify the functions of several key enzymes of the inner mitochondrial membrane, including Complex III (Schlame & Ren, 2006), Complex IV (cytochrome C oxidase), ATP/ADP translocase, ATP synthase, and creatine phosphokinase (Saric et al., 2015). The interactions of CL with the supercomplex proteins are specific, and CL is required in order for some enzymes to be active. It has been shown that Complex IV of the respiratory chain contains precise CL binding sites at the entrance of the proton channel, which may indicate that CL plays a role in the transport of protons across the complex (Saric et al., 2015). This activity is not able to be rescued by other phospholipids (Saric et al., 2015), thus cardiolipin is essential to the correct functioning and structure of the respiratory supercomplexes and cannot be compensated for by other endogenous biological means (Saric et al., 2016).

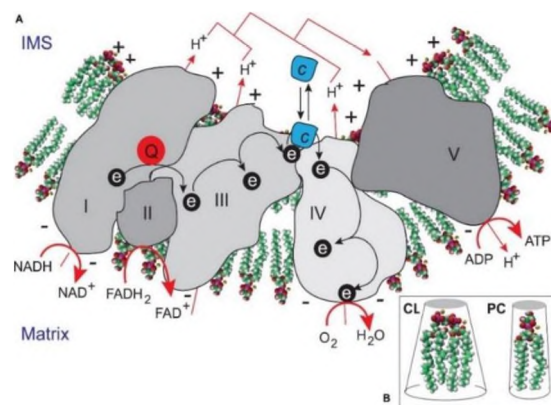


Figure 2: Cardiolipin’s Supportive Role within the Electron Transport Chain (Saric et al., 2015)

Biopsies of heart, liver, and skeletal tissue from BTHS patients have shown malformed mitochondria and tightly stacked or circular bundles of cristae (Lu & Claypool, 2015). BTHS lymphoblast mitochondria have reduced inner membranes, collapsed cristae, and are fragmented. Although the structural and functional abnormalities of BTHS mitochondria have been well-described, it is still unclear as to *how* or *why* these abnormalities lead to the diverse clinical manifestations of BTHS, in particular the 3-methylglutaconic aciduria that is a hallmark phenotype of BTHS (Schlame & Ren, 2006).

1.1.2 Dilated Cardiomyopathy

Cardiomyopathy is an abnormal functioning of the heart muscle and is accompanied by abnormal structural characteristics. It is a leading cause of heart failure – accounting for around half of all of the heart failure cases in the United States (Hershberger et al., 2010). Cardiomyopathies are categorized based on their morphologies, and the four main types include: dilated cardiomyopathy (DCM), hypertrophic cardiomyopathy (HCM), arrhythmogenic cardiomyopathy (AC), and restrictive cardiomyopathy (RCM) (McNally et al., 2013).

Cardiomyopathies can be caused by both genetic and as well as non-genetic factors. The cause of DCM can vary greatly from genetic mutations in 20-30% of cases (Hershberger et al., 2010) to non-genetic factors such as myocardial ischemia, immunologic or metabolic sources such as hypertension (Hershberger et al., 2010), or have a mixed etiology. Other non-genetic factors include toxins, pharmaceuticals, inflammatory diseases, and valve disease (Jain et al., 2021).

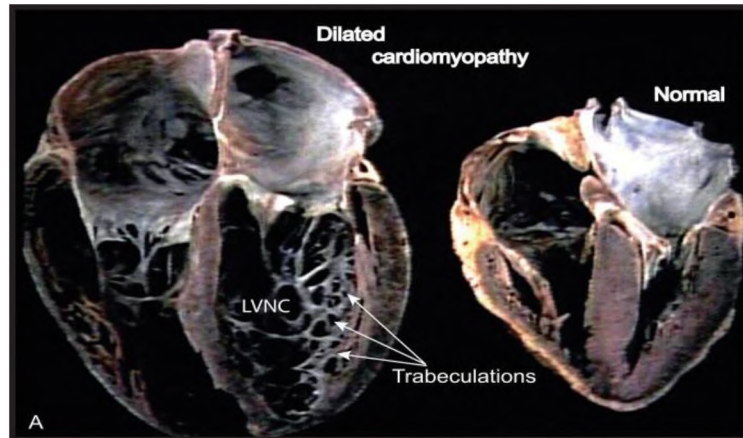


Figure 3: Example of Dilated Cardiomyopathy with Left Ventricular Non-Compaction (Saric et al., 2015)

Dilated Cardiomyopathy (DCM) is a type of cardiomyopathy which is characterized by enlargement of the heart, particularly of the left ventricle. This causes poor ventricular contraction, leading to reduced systolic function. Early in the disease, left ventricular enlargement (LVE) is present, and later in the disease all chambers may be enlarged (Hershberger et al., 2010). Compromised systolic function is also present, which results in an ejection fraction (EF) of $<40\%$ (Katsuragi & Ikeda, 2021). DCM is diagnosed via echocardiography or cardiac MRI (CMR). Occasionally a biopsy is used in the diagnosis of other forms of cardiomyopathy (McNally & Mestroni, 2017). The effects of DCM can be detrimental to the structure and function of the heart and can be seen in the form of increased myocardial fibrosis which leads to ventricular remodeling. Additionally, severe arrhythmias, perturbed signaling pathways, and decreased contractile force result due to dysregulated calcium homeostasis (Burke et al., 2016).

1.2 Cardiac Metabolism

The human heart, due to its high energy demands and limited storage capacity, must maintain flexibility in its ability to utilize energy resources. Although fatty acids, via β -oxidation, are the preferred energy source of the heart, the heart can also use carbohydrates such as glucose, amino acids, and ketone bodies as sources of fuel in times of need. This alternative use of fuel depends on the balance of substrates at hand, current energy needs, and the health of the tissue (Taegtmeyer, 2004).

1.2.1 Fatty Acid β -Oxidation

Fatty acids are the preferred fuel source of the human heart (Kolwicz et al., 2013; Neely & Morgan, 1974). Under aerobic conditions, the oxidation of fatty acids suppresses glycolysis by the inhibition of enzymes in the glycolysis pathway (Neely & Morgan, 1974). Exceptions to the normal function of the heart do exist, such as during times of increased energy demand - the heart will use glucose (via glycolysis) as well, but perfused heart studies have shown that β -oxidation is the preferred method of energy utilization (Neely & Morgan, 1974). Under anaerobic or hypoxic conditions, glucose use is stimulated, and fatty acid utilization is down-regulated (Neely & Morgan, 1974).

Acylcarnitines are vital to the metabolism of fatty acids, which takes place in the mitochondria. For fatty acid β -oxidation to occur, fatty acids (acyl-CoAs) must first be transported into the mitochondria, however the organelle lacks such transporters. The solution to this is by activating fatty acids to form acyl-CoA thioesters, and subsequently transferring the acyl group to carnitine, thus producing acylcarnitine. The mitochondria contain acylcarnitine transporters, and once inside the matrix, carnitine and acyl-CoA are regenerated and the acyl-CoA can undergo β -oxidation.

Studies have shown a link between cardiolipin and carnitine transport proteins. Both Carnitine acyltransferase (CAT) and carnitine/acylcarnitine translocase (CACT) have been shown to either associate with or require CL for activity (Raja & Greenberg, 2014), and this could provide an additional link between BTHS and aberrant fatty acid levels that have been observed (Vernon et al., 2014) in patients:

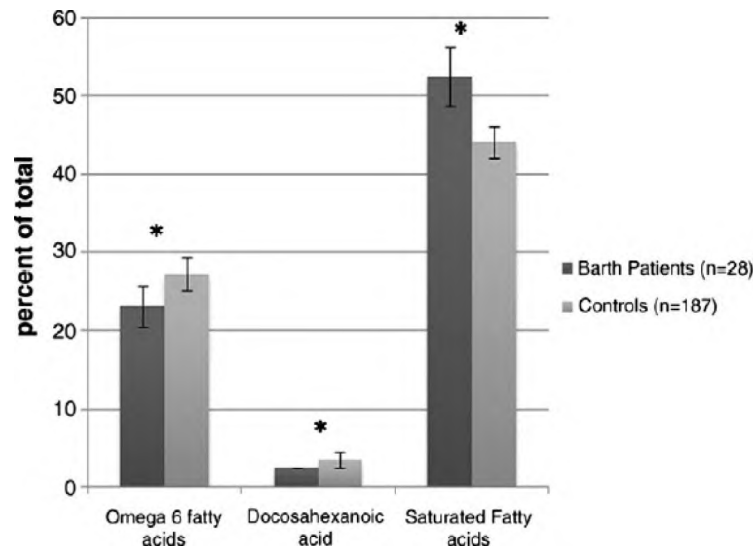


Figure 4: Red Blood Cell Fatty Acids (Vernon et al., 2014)

A recent study has shown statistically significant differences in acylcarnitine levels in plasma between BTHS patients and control subjects (Sandlers et al., 2016). Deeper analysis of acylcarnitines at the cardiomyocyte level may provide additional insight as to the mechanism of disturbances in the utilization of fatty acids as a primary fuel source.

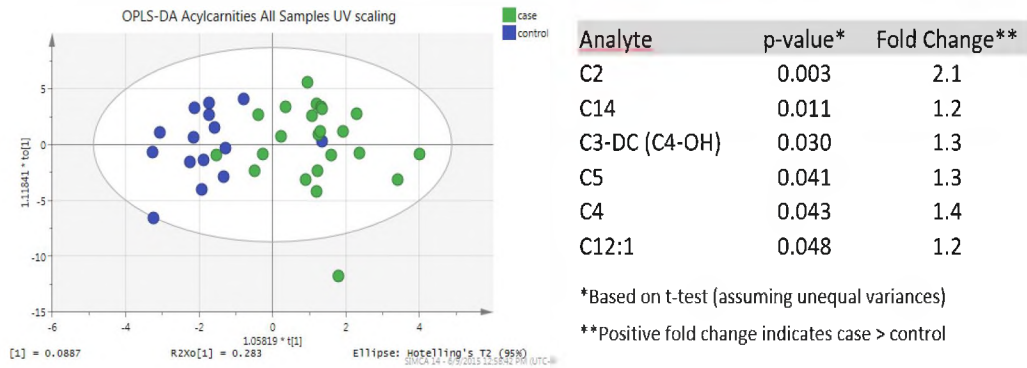


Figure 5: Multivariate Analysis of Case vs Control for Acylcarnitines (Sandlers et al., 2016)

1.2.2 Glycolysis

Throughout all of the human body, tissues take up the carbohydrate glucose from the blood to be broken down into pyruvate as its end-product. Pyruvate then is converted to acetyl-CoA to enter the citric acid cycle and generate ATP for energy production. The only exception to this rule is in the heart, where fatty acid β -oxidation is the preferred source of generating acetyl-CoA. This rule is not hard-and-fast, as the heart will use glycolysis in some of its energy production.

After the formation of pyruvate as the terminal product of glycolysis, four differing pathways may be followed by pyruvate: either the formation of acetyl-CoA via decarboxylation, the formation of lactate via reduction, or the formation of citric acid cycle intermediates oxaloacetate or malate via carboxylation, or amination to form alanine. The last two processes are under the antipleuritic category, which are not used under normal circumstances. The formation of oxaloacetate or malate would occur due to low levels of TCA cycle intermediates (Werner et al., 2016).

Under normal conditions, the enzyme pyruvate dehydrogenase (PDH) controls the conversion of pyruvate to acetyl-CoA and is controlled by the substrate levels of acetyl-

CoA (feedback regulation) and NADH generated by the TCA cycle. PDH is also controlled by phosphorylation via pyruvate dehydrogenase kinase, which is activated by high levels of acetyl-CoA and the conversion of ADP to ATP (Werner et al., 2016). Although the breakdown of fatty acids is the preferred method of deriving energy from fuel by cardiac muscle, it is estimated that cardiac tissue derives approximately 5% of its energy production from glycolysis (Doenst et al., 2013), thus it is important to monitor this pathway when investigating the pathogenesis of BTHS-related DCM.

1.2.3 Ketone Bodies, Lactate, and Pyruvate

Metabolites which give indication of cellular redox state include lactate, pyruvate, acetoacetate (AcAc), and β -hydroxybutyrate (BhB). Acetoacetate and β -hydroxybutyrate are ketone bodies, and they hold a specific relationship with each other in the mitochondria, as β -hydroxybutyrate dehydrogenase oxidizes BhB to form AcAc. Likewise, in the cytosol, lactate dehydrogenase reduces lactate to pyruvate (see figure 3). Both enzymes are governed by the relative ratio of NADH/NAD⁺ in the cell. Thus, these metabolites are maintained in a specific ratio which is indicative of the redox state of the cell (Nocito et al., 2015), and changes amongst them will indicate the relative ability of the cell to handle the metabolic loads of the cellular environment.

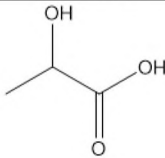
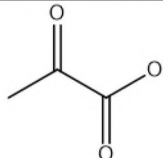
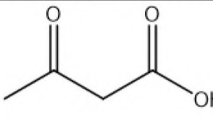
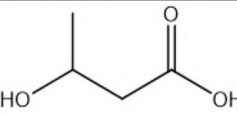
Lactate	Pyruvate	Acetoacetate	β -hydroxybutyrate
			

Table 1: Structures of Lactate, Pyruvate, Acetoacetate, and β -hydroxybutyrate.

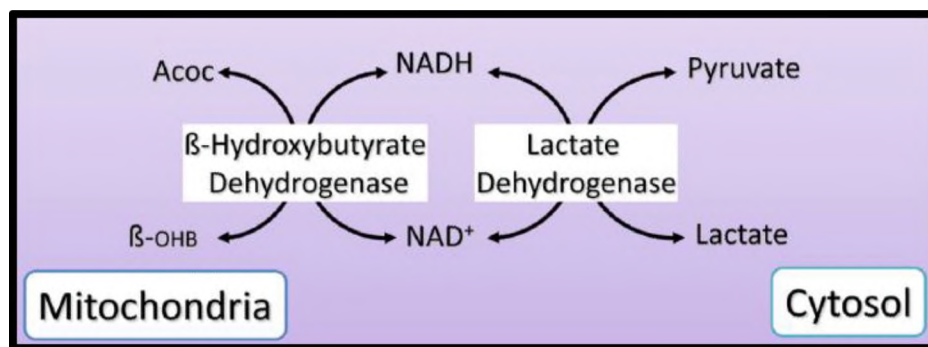


Figure 6: Interrelationship between AcAc/BhB, pyruvate/lactate, and NADH/NAD⁺ in the mitochondria and cytosol. (Corkey & Shirihai, 2012)

1.2.4 Citric Acid Cycle

The citric acid cycle is the method by which cells break down carbon fuel sources to be used for oxidation and ATP production via the electron transport chain. It is also commonly referred to as the tricarboxylic acid (TCA) cycle or the Krebs cycle, and can be thought of as the epicenter of metabolic pathways in cellular metabolism, as several other pathways converge on this one, to include glycolysis and fatty acid β -oxidation. The beginning substrate of the citric acid cycle is acetyl-CoA, and the end product yields two molecules of CO₂, one reducing equivalent of NADH, and one reducing equivalent of FADH₂. These reducing equivalents then go on to deliver energy in the form of electrons to the electron transport chain, in order to generate a proton gradient which is used to generate ATP (Werner et al., 2016). Each round of glycolysis yields two molecules of acetyl-CoA, whereas fatty acid β -oxidation will yield many molecules of acetyl-CoA for use in the citric acid cycle. It is for this reason that fatty acid oxidation is regarded as a more efficient means by which cells can obtain energy and is necessary since the cardiac system requires a constant supply to maintain constant conduction. Unpublished data (below) has shown disturbances in plasma TCA cycle intermediates between BTHS and control subjects, which warrants further investigation at the cellular level.

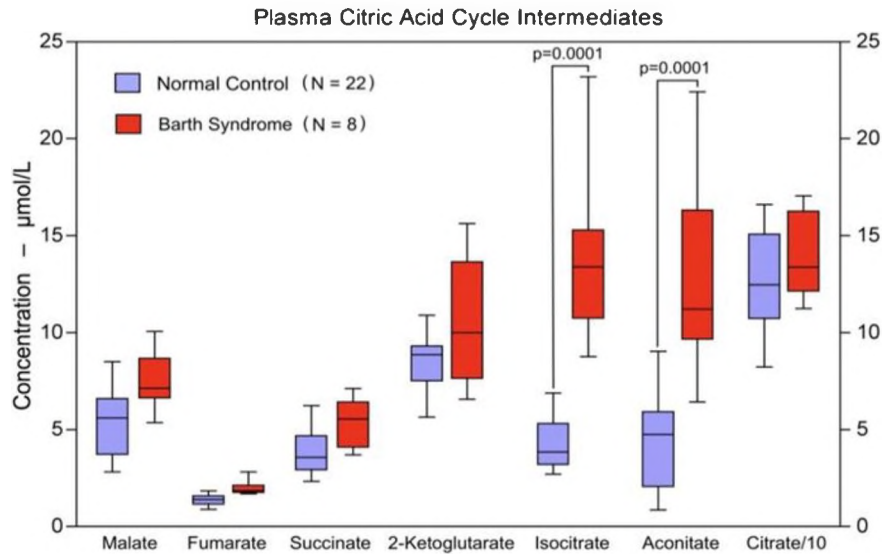


Figure 7: Plasma Citric Acid Cycle Intermediates by LC-MS/MS
(Y. Sandlers, RI. Kelley – unpublished data)

1.2.5 Amino Acids

Amino acids are the building blocks of proteins and are also used by the body for other processes such as those which require nitrogen or for fuel by the breakdown of proteins. The metabolism of most amino acids converge on the citric acid cycle, and the degradation of amino acids requires the production of keto-acids (Kolwicz et al., 2013) and the utilization of the urea cycle, which is also closely linked to the TCA cycle.

The human heart does not regularly utilize amino acids as fuel, as these substrates are not usually high in abundance under normal conditions. Exceptions to this would be during starvation, in which protein would be degraded to be used as fuel. In this case, the amino acids do not require special transport mechanisms to enter the mitochondria to be used (Kolwicz et al., 2013). Specifically, the amino acids that are used are the branched-chain amino acids, which are converted to precursors of glucose and then further metabolized (Werner et al., 2016).

Another exception to the rule of amino acids not being used as fuel by the human heart is during times of low availability of citric acid cycle intermediates. This condition results in a process called anaplerosis (Werner et al., 2016), in which certain amino acids such as glutamate or aspartate are used to regenerate intermediates of the pathway such as α -ketoglutarate and oxaloacetate, respectively. Defects in this pathway have been noted in heart disease (Werner et al., 2016). Due to the central importance of this pathway to cardiac metabolism, we will be monitoring this in our investigation of DCM.

Certain specific amino acid levels have been shown to be disrupted in Barth Syndrome patients. A recent clinical study conducted using plasma and urine has demonstrated low levels of arginine and high levels of proline (Vernon et al., 2014), for which there is yet no explanation. Other amino acid levels were found to be disturbed as well, including increased tyrosine and asparagine, and decreased cysteine:

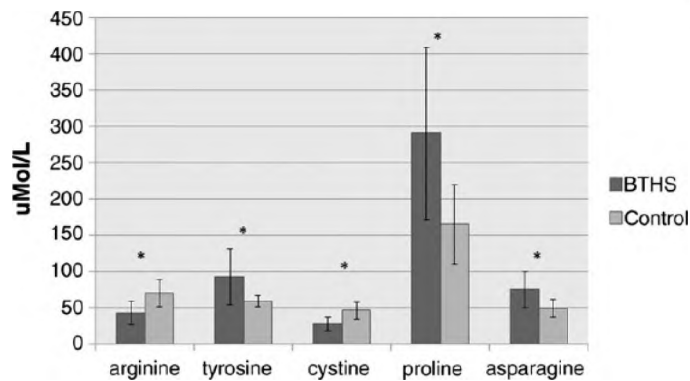


Figure 8: Plasma Amino Acid Levels (Vernon et al., 2014)

A more recent study provided additional insight into disturbances in plasma amino acid levels amongst Barth patients using ^1H nuclear magnetic resonance spectroscopy and liquid chromatography-mass spectrometry (Sandlers et al., 2016). Multivariate data analysis methods were used in evaluating the differences in analyte levels and found

arginine and glycine to be decreased. Levels of proline, methionine, tyrosine, and valine were found to be significantly increased.

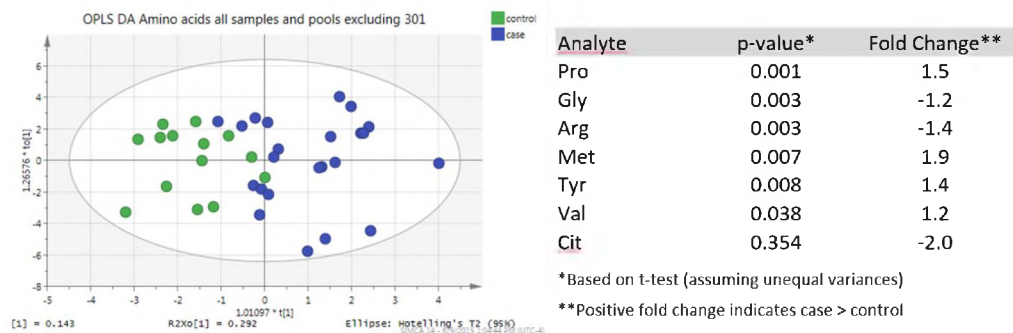


Figure 9: Multivariate Statistical Analysis of Case vs Control for Amino Acids (Sandlers et al., 2016)

Additionally, a TAZ knockdown mouse model has demonstrated changes in substrate utilization of cardiac mitochondria away from fatty acids and towards amino acids, as well as changes in the regulation of amino acid metabolism on the level of gene transcription (Kiebish et al., 2013). This could signify compensatory mechanisms in place due to the inability of BTHS cardiomyocytes to properly utilize normal fuel sources such as fatty acids. These findings have driven our decision to look more closely at amino acid levels in BTHS iPSC-derived cardiomyocytes.

1.2.6 Other Organic Acids

BTHS is also classified as 3-methylglutaconic aciduria (3-MGA) Type II (Wortmann et al., 2012). This condition is characterized by an increase in 3-MGA in the urine. Its presence, however, can be highly variable, with some patients presenting with the syndrome – sometimes with diurnal variations (Wortmann et al., 2012), and others free of 3-MGA. There is no correlation of urine or plasma 3-MGA levels to the severity of clinical

symptoms. Additional urine organic acids markers in Barth Syndrome are elevated 2-ethylhydracrylic acid, aconitate and 2-hydroxybutyrate (BHB):

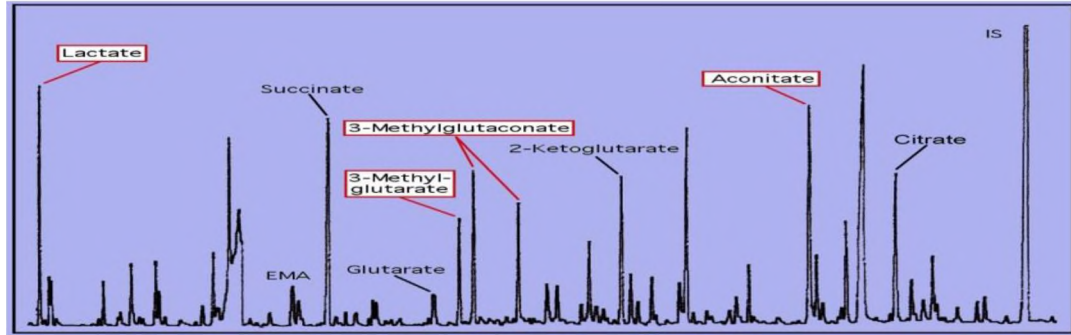
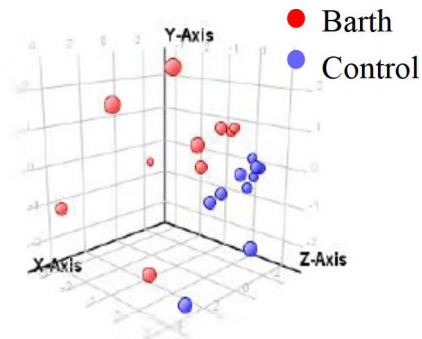


Figure 10: GC-MS Spectra of Urine Organic Acids in BTHS
(Y. Sandlers, RI. Kelley – unpublished data)

Principle Component Analysis



Mass Profiler Professional-Agilent

Metabolite	<i>p</i> value
2OH-butyrate	0.002
Aconitate	0.00058
3MGC	0.00000057
2ethylhydracrylate	0.007
Unknown (m/z 207)	0.00096

Figure 11: Urine Organic Acids by GC-MS
(Y. Sandlers, RI. Kelley – unpublished data)

The molecular mechanism by which 3-MGA/MGC present in the urine remains unknown. 3-MGA-uria Type I has been shown to be caused by a defect in leucine breakdown, but when it comes to BTHS, studies have shown that leucine metabolism is not implicated in 3-MGA Type II (Kelley et al., 1991; Wortmann et al., 2012). Instead, it is hypothesized that a defect in cholesterol metabolism or disturbed oxidative phosphorylation function may be involved (Wortmann et al., 2012).

1.3 Metabolomics

Metabolomics is the study of the molecular products of metabolism in a living system. Out of the four ‘omics’ approaches, it is the one which is regarded as being most representative to the phenotype of the organism which is being studied (Roberts et al., 2012). The other omics approaches include genomics, transcriptomics, and proteomics. Metabolites include vast categories of compounds within the biological system, and include amino acids, acylcarnitines, fatty acids, phospholipids, ceramids, and other organic acids, among many others. Within each category are up to hundreds of individual compounds that can be detected and measured by various metabolomic approaches in the laboratory.

The reason for metabolomics being regarded as the most representative to an organism’s phenotype is several-fold. First, genomics and transcriptomics serve to investigate the existence and expression of wild-type and mutated genes in the biological system. These methodologies have led to vast advances to our understanding of the human genome, particularly how it is differentially expressed within the body. It has also led to understandings of how and why certain diseases manifest. An example of the methodologies behind this includes quantitative reverse transcriptase-polymerase chain

reaction (qRT-PCR) of DNA from tissues of wild-type and diseased cell lines, human subjects, or animals to investigate gene expression patterns.

Proteomics has given insight into which proteins are then actually present in the given system. Although helpful, these ‘omics’ approaches have left many questions unanswered into the manifestation of many disease states. Although proteomics can detect the *presence* of many proteins, it cannot detect the aberrant *functioning* of the proteins. For example, a mass spectrometer may correctly identify a protein, thus indicate in a proteomic sense that the organism has correct function in the pathway in which the protein of interest operates. However, if under biological conditions, the protein has not undergone correct post-translational modifications or is in other ways not able to function correctly, the cause of the clinical disease state will go undetected.

Metabolomics serves to measure the presence and quantity of substrates and products of the metabolism in a biological system, as opposed to the proteins or genes themselves. These substrates and products are the endpoint of the ‘omics’ cascade, as they are the final product of energy utilization in a cell. By knowing the basal, or wild-type, level of metabolites in a cellular system and comparing the levels to the disease state, scientists can elucidate which pathways are disturbed. This allows a work-backward approach – scientists can then hypothesize and investigate which proteins are functioning incorrectly, thus leading them to which genes may be functioning incorrectly.

1.3.1 Untargeted Metabolomics

Untargeted metabolomics is a technique which aims to profile the entire metabolome of the cellular system or organism at hand. This approach is analogous to throwing a wide net out over the entire metabolome and pulling as much data as possible

with regard to metabolite content. It requires the use of multivariate statistics to interpret the full range of data and is semi-quantitative due to the large number of metabolites measured and the limited number of internal standards available. Untargeted metabolomics are typically used for biomarker discovery regarding disease state, at which point other methods of investigating the causes of pathology would be implemented.

1.3.2 Targeted Metabolomics

Targeted metabolomics is a powerful tool in which pre-selected classes of compounds are measured in a cellular or biological system and is the focus of this work. For example, for a disease, untargeted metabolomics may have discovered that acylcarnitine levels are perturbed. This can translate to use in the clinical laboratory with targeted metabolomics. Scientists could then further develop a targeted assay for measuring acylcarnitines in the blood of a patient to determine the existence of a disease state. This targeted approach applies to any classes of compounds for which there are pre-determined analytes which will be measured and applies to the *measurement* of substrates within a class of compounds, whereas untargeted metabolomics generally applies to simply the *detection* of disease biomarkers. The targeted classes which are the subject of this work includes amino acids, acylcarnitines, citric acid cycle intermediates, ketone bodies, and other small organic metabolites.

CHAPTER II

DEVELOPMENT OF hiPSC-CM DIFFERENTIATION PROTOCOLS

The first step of this project was to find a highly efficient method of differentiating cardiomyocytes from iPSCs for the purpose of metabolic characterization of TAZ-iPSC cardiomyocytes. Initial attempts were made to differentiate iPSC-CMs using commercial kits and previously published protocols. The results were not sufficient for metabolic profiling, as we desired a relatively large population of cardiomyocytes per cell well for metabolic analysis. For this reason, the project incorporated an iPSC-CM differentiation protocol development component to generate cardiomyocytes from our laboratory's cell lines. Differentiation efficiency can vary widely between cell line, cell passage number, initial confluency, and concentration of small molecule treatment.

For the purpose of investigating metabolic abnormalities in cardiomyocytes, those with the ventricular subtype are of highest preference due to the fact that dilated cardiomyopathy primarily affects the ventricles (*Dilated Cardiomyopathy - Symptoms and Causes* - Mayo Clinic, n.d.). For this reason, when developing novel protocols, a protocol (Bhattacharya et al., 2014) which has been shown to produce a highly pure population of

ventricular cardiomyocytes was used as a starting point. From there, alterations were made to optimize small molecule dosages and culturing techniques.

2.1 Human Induced Pluripotent Stem Cells

When the use of embryonic stem cells (ESCs) was successfully implemented in the lab, the initial reaction of many researchers and laypeople alike was excitement. Scientists had found cells that could be grown into any type of cell or tissue in the body (known as differentiation) as long as they were familiar with the pathways involved in the growth of the tissue of interest. This meant the potential for huge advances in *in vitro* biological and genetic research. Embryonic stem cells are indefinitely self-replicating, thus provide a virtually inexhaustible supply of cells. And now, if scientists could generate virtually any cell or tissue type in the body, under any experimental conditions desired, the potentials for advances span to any field which even remotely involves research in the biological sciences. However, as news grew, so did ethical concern. ESCs are derived from the inner cell mass of a 4-5 day old human embryo in the blastocyst stage (McLaren, 2001), which some argue that by destroying the embryo, one is also destroying a human life. This led to the United States banning research using ESCs in 2001 (McLaren, 2001). For a time, the promise that was seen in ESC research was lost. Then in 2007, in the lab of Dr. Shinya Yamanaka, human induced pluripotent stem cells (hiPSCs) were developed (Takahashi et al., 2007). hiPSCs are derived from somatic (adult) stem cells, oftentimes fibroblasts or PBMCs (Malik & Rao, 2013; Ross et al., 2017). The fibroblast is reprogrammed to a state of pluripotency which is on many faces indistinguishable from that of ESCs. hiPSCs were found to be able to replicate indefinitely and differentiate into all three germ layers (thus, has the potential to be differentiated into any cell type of the body) in the exact same way

that ESCs were able to be differentiated, using the same pathways. The research that had begun so enthusiastically before on ESCs could continue once more, this time using hiPSCs.

Although hiPSCs are comparable to ESCs, their use holds a key advantage. Perhaps one of the most significant things to happen to the future of personalized medicine, iPSCs retain the genotype of the donor from which they were derived (Kamdar et al., 2015). This allows for the generation of patient-specific iPSC lines which can be further differentiated into many kinds of tissue to model certain genetic mutations or pathological conditions. These cellular models can then be compared to the pathological state at the clinical level in order to help further elucidate the mechanisms of disease. Thus, iPSCs can be thought of as the patient- or disease-specific counterpart to ESCs.

iPSCs are generated by the forced expression of 4 transcription factors which are specific to ESCs, which were determined to be the factors required for the induction of pluripotency. These transcription factors are Oct4 (octamer-binding transcription factor 4), Sox2 (sex determining region Y box 2), Klf4 (Krueppel-like factor 4), c-Myc (v-Myc myelocytomatosis avian viral oncogene homolog) – known as the OSKM factors – (Rony et al., 2015; Takahashi et al., 2007), and Nanog (Rony et al., 2015). There exist several methods of delivery of the reprogramming vectors, and the original method used integrating viral vectors to deliver the reprogramming factors (Rony et al., 2015), which is not optimal for translation to clinical applications. Recent developments have provided viral methods which will not integrate into the host genome, which include the Adenovirus and Sendai Virus (Ebert et al., 2015). There also exist excisable viral methods, non-viral delivery such as plasmid vectors, and direct transfection methods (Rony et al., 2015).

In short, the fibroblasts are exposed to the reprogramming factors for a short period of time, followed by culture in media compatible with ESC/iPSC survival. After several weeks, assuming a successful reprogramming, iPSC colonies will emerge which can then be selected, expanded, and characterized prior to long-term use. The cells that are expanded from the selected colonies then undergo a characterization process which includes fluorescent staining, embryoid body formation, and teratoma formation. Additionally, cells will be screened for the presence of the appropriate cellular protein markers which indicate pluripotency. The validated iPSCs would then be able to be expanded and used for differentiation.

iPSCs have many of the same properties as ESCs, including their capacity for proliferation. They are capable of unlimited self-renewal (Kamdar et al., 2015; Rony et al., 2015), have a high telomerase activity (Takahashi et al., 2007), and exist in a completely unspecialized state prior to directed differentiation. Both ESCs and iPSCs are pluripotent (Rony et al., 2015; Takahashi et al., 2007), which means that they can be differentiated into many different cell types.

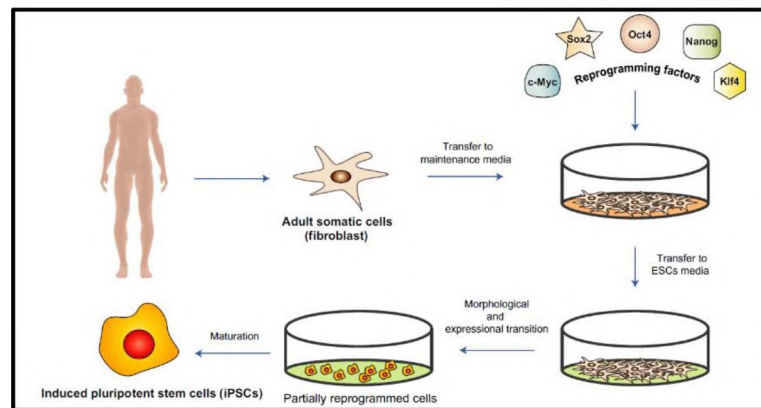


Figure 12: Reprogramming of Fibroblasts to hiPSCs (Rony et al., 2015)

iPSCs have also passed the test for pluripotency in forming embryoid bodies (EBs) into all three germ layers – endoderm, mesoderm, ectoderm (Takahashi et al., 2007).

Teratoma formation when iPSCs are subcutaneously injected into immunodeficient mice result in tumors containing tissue derived of each of the three germ layers (Takahashi et al., 2007). Additionally, iPSCs are similar to ESCs in their morphology, surface antigen expression, and pluripotent state-specific promotor activities, methylation patterns, histone modifications, and gene expression (Rony et al., 2015; Takahashi et al., 2007).

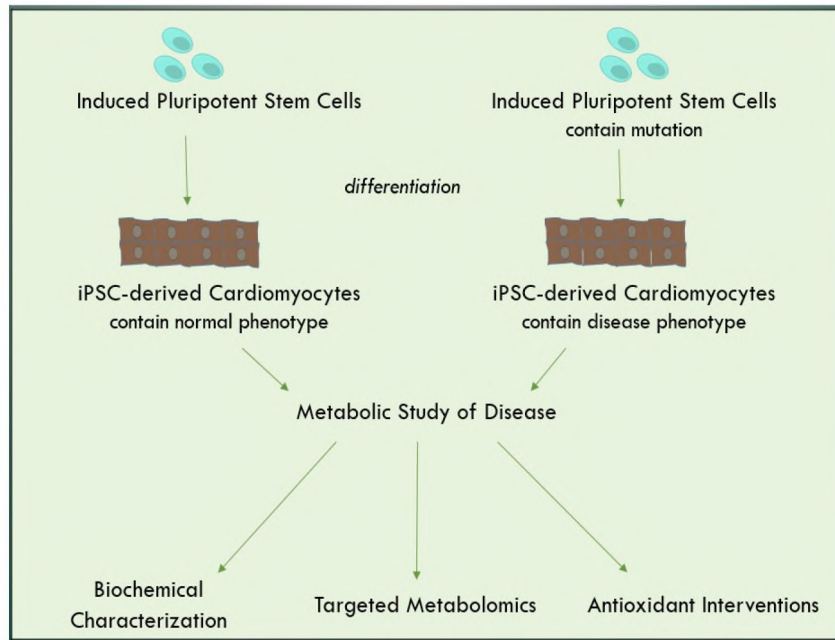


Figure 13: Workflow of Investigation of BTHS Using hiPSCs

Since iPSCs may constitute patient-specific genetic backgrounds and can be differentiated into functional cardiomyocytes containing the same genotype as the undifferentiated iPSCs, these cells provide a unique model to study inherited cardiac disorders. Since our interest lies in the metabolic characterization of a disease which results in cardiomyopathy, our goal was to differentiate iPSCs into cardiomyocytes. There exist several established protocols for generating cardiomyocytes from iPSCs. We chose to manipulate the Wnt/ β -catenin pathway, as this pathway has been shown to produce iPSC-

derived cardiomyocytes with greater than 90% efficiency (Lian et al., 2012). The iPSC-derived cardiomyocytes produced were derived from both wild-type iPSCs as well as iPSCs containing genetic mutations which lead to the inherited metabolic disorder known as Barth Syndrome. This allowed us to study the metabolic consequences of the disease by measuring and comparing metabolite levels in the iPSC-CMs.

2.1.1 Differentiation to Cardiomyocytes

One of the major goals of this project has been to successfully differentiate iPSCs to the ventricular-subtype of iPSC-CM. In accordance with the published protocol upon which our successful differentiation methods are based, iPSC-CM are 90% positive for the cellular protein markers cardiac troponin I (TNNT3), which is only expressed in human adult cardiac cells (Vallins et al., 1990) and iroquois homeobox 4 (IRX4), to indicate that cells are of ventricular (Bruneau et al., 2000) cardiomyocyte origin.

Early differentiation protocols utilized embryoid body formation in the differentiation of ESCs and hiPSCs into cardiomyocytes (Batalov & Feinberg, 2015; Yang et al., 2008). This has proven to be a method with much lower efficiency than the small molecule signaling pathway method developed in recent years. In the latter method, cells are treated with a sequence of small molecules which alter cellular signaling processes, thus directing iPSCs through the mesodermal lineage and then into the cardiac cellular lineage. This method has been shown to potentially generate an hiPSC-CM population of 90% or greater. Directing the specific subtype – whether cardiomyocytes are ventricular or atrial in nature – as well as culturing cardiomyocytes with a more mature growth profile, as demonstrated by their shape, are the most daunting tasks of researchers in the field.

2.1.2 *hiPSC-CM Subtype*

The goal of part of this project has been to develop a successful differentiation protocol for ventricular cardiomyocytes due to the nature of BTHS and the manifestation of DCM involved. It was expected that ventricular cardiomyocytes would provide a clear representation of the phenotype that results from Barth Syndrome, particularly due to the dilated cardiomyopathy and left ventricular non-compaction that occurs with the disease. Several iPSC differentiation methods have been developed by scientists which reliably produce ventricular cardiomyocytes, and our methods have been developed using some of the techniques and small molecule differentiation factors outlined in those protocols.

In the embryo, the three types of cells that can be found are the ectoderm, mesoderm, and endoderm. It has been found that the heart develops from the mesoderm (Yang et al., 2008). Thus, when differentiating iPSCs to cardiomyocytes, it is necessary to first induce the cells to the mesoderm lineage. The challenge is that from mesoderm, many other cell types can potentially develop, such as blood cells, kidney cells, and other types of muscle cells, so it is important to have a fine-tuned cardiomyocyte differentiation protocol based on individual cell line.

2.2 Small Molecules Manipulate Signaling Pathways During Differentiation

When inducing iPSCs to the cardiomyocyte lineage, cells must be treated with a variety of molecules to alter the signaling pathways controlling transcription and translation of the genes which govern pluripotency and lineage specification.

The Wnt3a pathway is heavily involved in regulating the TCF/LEF group of transcription factors, which go on to regulate the pluripotency state of hiPSCs. This pathway is typically controlled by Wnt molecules binding to the Frizzled receptor on the

cell surface. This cell surface binding can be bypassed or inhibited using small synthetic molecules, and by manipulating this pathway during differentiation, researchers can direct cells to various cell lineages.

In the so-called ‘off’ state, the β -catenin destruction complex is formed, and includes Axin, APC, GSK3b, and β -catenin. Upon formation of the destruction complex, β -catenin is ubiquitinated, which leads to its destruction by the proteasome.

The active state of the Wnt3a pathway allows for the movement of β -catenin into the nucleus, where β -catenin binds to the TCF/LEF group of transcription factors. Transcription is activated and pluripotency is inhibited, thus cells are now directed to differentiation. The challenge for researchers at this stage is directing the cells toward the specific lineage which is desired.

2.2.1 CHIR99021

CHIR99021 (CHIR) is a synthetic small molecule which is an inhibitor of the Wnt3a pathway. It is used at the beginning of differentiation from iPSCs to cardiomyocytes and directs iPSCs towards the mesodermal lineage (Mazzotta et al., 2016). CHIR works by inhibiting GSK3 β so that it will not bind to β -catenin. This prevents the formation of the β -catenin destruction complex, thus preventing β -catenin from being ubiquitinated, or marked for destruction by the cell. This allows β -catenin to migrate into the nucleus and activate the TCF/LEF family of transcription factors, thus ending the pluripotency state of the iPSCs.

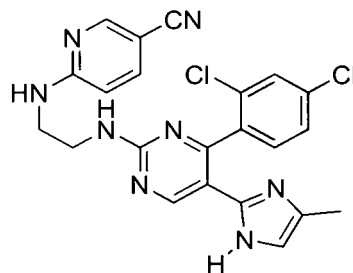


Figure 14: Structure of CHIR99021
(STEMCELL Technologies, n.d.)

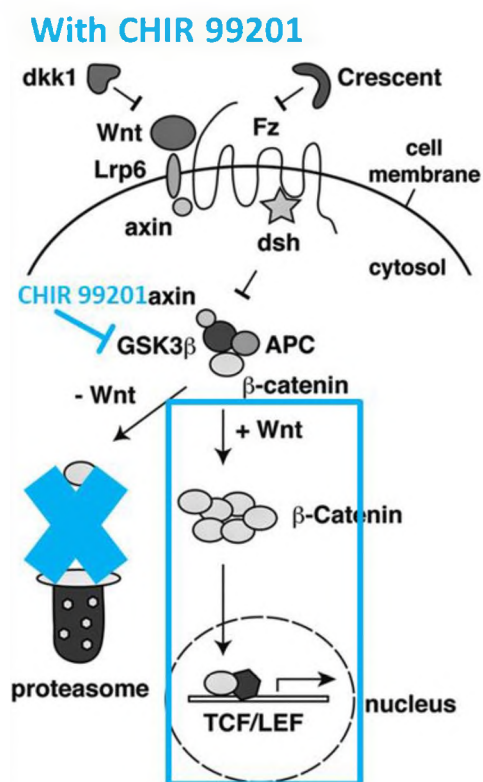


Figure 15: Wnt/ β -catenin pathway with CHIR 99021
Adapted from (Gessert & Kuhl, 2010)

2.2.2 IWR-1

IWR-1 is a synthetic small molecule which is used after CHIR in the small-molecule differentiation method. It also acts on the Wnt/3a pathway; however, this

molecule inhibits β -catenin-associated gene transcription by stabilizing Axin1 as part of the β -catenin destruction complex. As the amount of Axin in the cell increases, the β -catenin destruction complex is more easily formed due to easier binding with APC and GSK3b, thus ubiquitinating β -catenin and leading to its destruction. The ‘shutting off’ of the Wnt/3a pathway essentially turns off the transcription of the TCF/LEF-associated genes which were activated at the initiation of differentiation. This part of differentiation is thought to be what leads the cells into the cardiomyocyte, specifically ventricular, lineage (Bhattacharya et al., 2014).

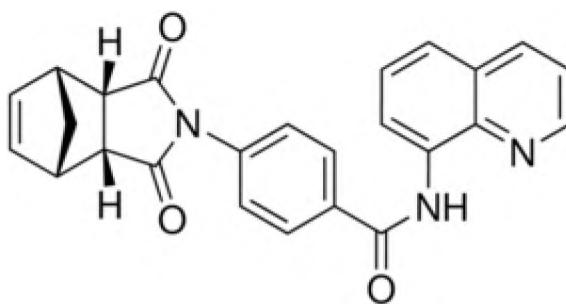


Figure 16: Structure of IWR-1
(Sigma Aldrich, n.d.)

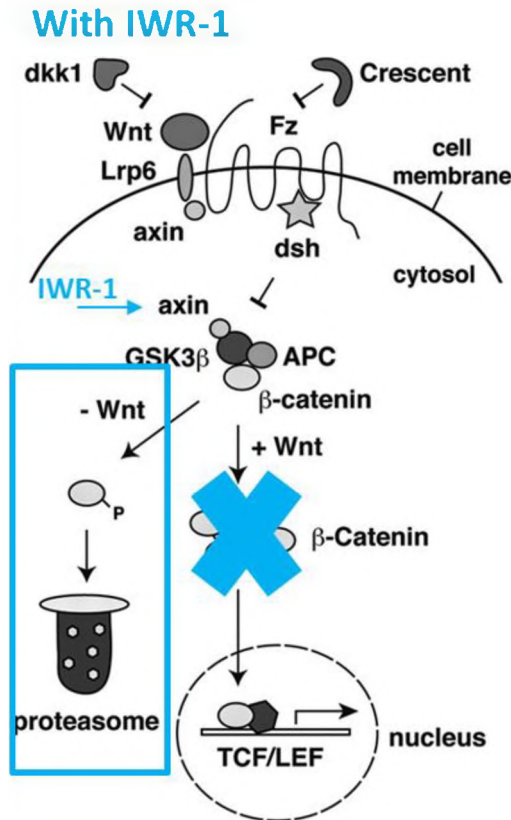


Figure 17: Wnt/β-catenin pathway with IWR-1
Adapted from (Gessert & Kuhl, 2010)

2.2.3 Y-27632

Y-27632 (ROCK inhibitor, or ((R)-trans-4-(1-Aminoethyl)-N-(4-pyridyl)cyclohexanecarboxamide) is a small molecule used commonly in stem cell research for the purpose of maintaining the integrity of stem cell populations. This small molecule maintains stem cells in a pluripotent state by preventing differentiation and apoptosis after passaging, and is used by our group routinely during our culturing of iPSCs.

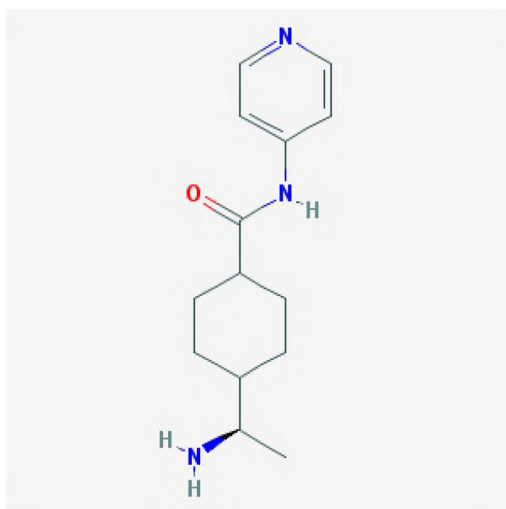


Figure 18: Structure of Y-27632
(National Center for Biotechnology Information, n.d.)

2.2.4 *Activin A and BMP4*

Activin A is a growth factor and one type of the Inhibin dimers, and functions as one signaling protein out of many that can activate the TGF- β /SMAD signaling pathway in iPSCs. Specifically, it has been found that Activin A is able to control mesoderm specification and is involved in cardiac development (Kim et al., 2015).

The TGF- β /SMAD signaling transduction pathway is a complex and diverse-functioning pathway which is active in development, differentiation, and cell-cycle progression. This pathway has been found to have an important role in cardiac development, and by manipulating the signaling of these pathways, cardiac mesoderm can be formed.

The receptors are serine-threonine kinases which dimerize upon ligand activation, thus phosphorylating either SMAD 2/3 for Activin A, or SMAD 1/5/8 for BMP4. Both SMAD2/3 and SMAD1/5/8 cofactor with SMAD4, and then enter the nucleus to bind with transcription factors to activate genes for transcription. Although it is generally accepted

that the SMAD2/3 complex is required to maintain pluripotency, it has been found that it can prime other genes for differentiation by recruiting transcriptional regulators and has been found on many mesodermal genes (Budi et al., 2017).

2.2.5 *Ascorbic Acid/Vitamin C*

Ascorbic acid, commonly known as Vitamin C, has been used in published protocols as a supplement to aid in cardiomyocyte differentiation. It has been shown to increase the number of cardiac progenitor cells. Additionally, as iPSC-CMs are typically less mature than fetal or hESC-CMs, it has been found that treatment with ascorbic acid helps to increase cardiomyocyte maturity (Cao et al., 2012).

Interestingly, ascorbic acid results in an upregulation of cardiac transcription factor expression and downregulation of pluripotency transcription factor expression with ascorbic acid treatment. These properties are due to manipulation of collagen synthesis, however it is not due to Vitamin C's antioxidative properties (Cao et al., 2012).

2.3 Materials and Methods

The following text outlines the process by which hiPSC-CM differentiation methods were developed by our lab.

2.3.1 *Cell Lines*

Control iPSCs. Control iPSCs were obtained from two sources – the Harvard Medical Center and the Duke University Medical Center. These are wild type controls which contain no BTHS-associated mutation and will be used in comparison with the cells that contain the BTHS genotype. DU11 (Duke) is an iPSC line which was derived from BJ fibroblasts (ATCC) and was donated by the Duke iPSC Shared Resource Facility at the Duke University Medical Center. PGP1 is an iPSC line derived from a healthy donor, from

which the BTHH and Clone 37 lines were produced, all of which were donated by Dr. Pu of the Harvard Stem Cell Institute.

Label	Source
DU11	Duke iPSC Shared Resource Facility
PGP1	Harvard Medical Center

Table 2: Wild-Type hiPSC Cell Lines

Engineered BTHS iPSCs. Engineered BTHS iPSCs include BTHH, containing a frameshift TAZ mutation of c.517delG (Zweigerdt et al., 2014) have been generously donated by Dr. Pu (Harvard Medical Center, MA). The cell lines were created by first isolating fibroblasts from a healthy donor and reprogramming them to iPSCs. The healthy iPSCs were then edited with CRISPR/CAS9 genome editing technology to introduce a known mutation of BTHS. The original research group has performed some initial studies which include heart-on-chip electrophysiological studies (Wang et al., 2014), and the goal of this project was to develop and perform the biochemical characterization, which has not previously been conducted on iPSCs or iPSC-CMs.

Label	Source	Mutation
BTHH	Harvard Medical Center	c.517delG
C37	Harvard Medical Center	c.517 ins

Table 3: TAZ-Mutation hiPSC Cell Lines

2.3.2 Culture of hiPSCs

Cells were obtained from passage 3 (PGP1/BTHH) and passage 12 (Duke) and proliferated until between 20-25 passages prior to beginning differentiation. iPSCs are cultured in Essential 8 Flex medium (Gibco), on Matrigel-coated (1:200) plates. Medium is changed every other day as prescribed by manufacturer's protocol, and iPSC colonies

are passaged at a 1:12 ratio once ~80% confluency is reached, using 0.5 mM EDTA solution.

The pluripotency state of iPSCs was verified upon initial receipt of cell lines and is repeated periodically throughout culture. iPSCs are characterized based on protein expression of the pluripotency markers OCT4 (nuclear) and SSEA4 (surface). DAPI is also used to image the nucleus of cells.

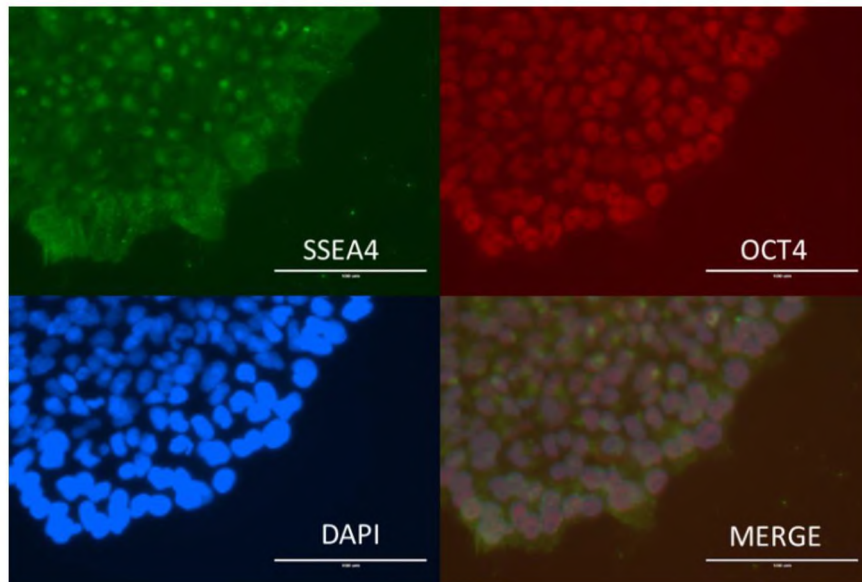


Figure 19: Immunohistochemical analysis of hiPSCs to verify pluripotency

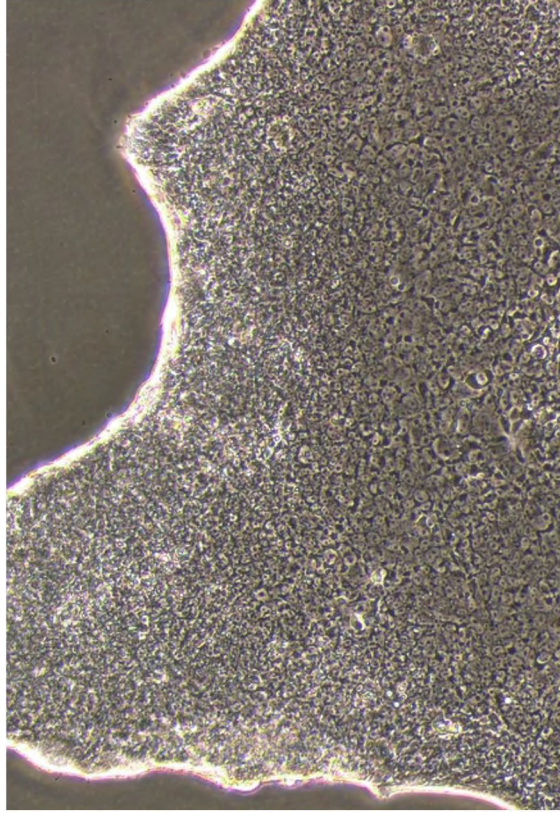


Figure 20: Colony of hiPSCs

2.3.3 Cardiomyocyte Differentiation Protocol Development

In determining whether a differentiation attempt has been successful, the first step is to analyze the cells for functionality. This is a relatively easy task, as the functional cardiomyocytes can be seen spontaneously contracting in the cell culture dish. After that, the cells undergo immunohistochemical analysis, to detect cardiac specific markers. The proteins which are stained for include TNNI3 (specific to human cardiac troponin – found only in cardiac cells), IRX4 (specific to ventricular subtype), and α -actinin (to view the myosin fibrils of the cardiomyocytes). Together, the functionality and positive staining of the cells for ventricular specific cardiac markers gives us confidence that the hiPSCs have

successfully been differentiated into hiPSC-CMs of ventricular subtype. The following section describes the development of iPSC-CM differentiation methods for this project.

Commercial: Gibco PSC Cardiomyocyte Differentiation Kit. iPSCs are singularized when passaged and expanded to 30-70% confluency. On day 0, Essential 8 medium is removed from wells and 2 mL of Cardiomyocyte Differentiation Medium A is added. Cells are incubated overnight and through the next day. On day 2, Medium A is removed, and 2 mL of Cardiomyocyte Differentiation Medium B is added to each well. The cells are again incubated overnight and through the next day. On day 4, Medium B is removed, and 2 mL of Cardiomyocyte Maintenance Medium is added to each well, and cells will be incubated further, with replacement of Maintenance Medium every other day. Beating cardiomyocytes should be able to be seen by day 10.

Commercial kit was used on the Duke line of iPSCs. Differentiation of iPSCs into cardiomyocytes was at an insufficient level for performing biochemical analysis. Additionally, a large amount of cellular death and detachment was observed.

Initially, differentiation was performed with iPSCs in culture on a matrix of vitronectin (ThermoFisher). The benefit of vitronectin over the established use of Matrigel matrix (Corning) was that in vitronectin, the synthetic proteins are fully defined, whereas Matrigel is a basement-membrane matrix derived from mouse sarcomas, and is poorly defined and highly variable in composition (Aisenbrey & Murphy, 2020). Due to the detachment of the small number of differentiated cardiomyocytes obtained from this differentiation attempt, the matrix used was switched from vitronectin to Matrigel (1:200) (Corning).

Wnt/ β -catenin Modulation Protocol (from (Lian et al., 2013). On the first attempt at differentiation using this method, the protocol was followed exactly as written. hiPSCs (passage >20) were singularized for 5 passages prior to differentiation, passed at a 1:12 ratio, and cultured in Essential 8 Flex medium until ~80 % confluency, at which point began Day 0. Medium was changed to RPMI 1640 (11875, Life Technologies) with B27 minus insulin supplement (A1895601, Life Technologies) with 6 μ M CHIR99021 (Sigma). On day 2, medium was changed to RPMI 1640 with B27 minus insulin supplement. On day 4, medium was changed to basal differentiation supplement and 5 μ M IWR-1 (Sigma). Medium was changed on Day 6 RPMI 1640 with B27 minus insulin supplement (without IWR-1). On Day 8, and every other day thereafter, medium was refreshed with RPMI 1640 with B27 supplement and 2% FBS. A small amount of spontaneously contracting cardiomyocytes was first observed on day 11 in one of the three cell lines. Next, small changes to this previously published protocol were made to optimize differentiation conditions specifically for our cell lines. The concentration of IWR-1 was increased to 10 μ M, and the concentration and amount of time which the iPSCs were treated with CHIR 99201 was altered to find an optimal combination of differentiation conditions, and a method of purification of iPSC-CM by lactate feeding was added (Sharma et al., 2015).

Alteration of Wnt/ β -catenin Modulation Protocol (adapted from (Lian et al., 2013)). hiPSCs (passage >20) were singularized for 5 passages prior to differentiation, passed at a 1:12 ratio, and cultured in Essential 8 Flex medium until ~80 % confluency, at which point began Day 0. Medium was changed to RPMI 1640 (11875, Life Technologies) with B27 minus insulin supplement (A1895601, Life Technologies) with 6 μ M CHIR99021 (Sigma) for 24 hours. On day 1, medium was changed to RPMI 1640 with

B27 minus insulin supplement for 24 hours. On day 2, medium was then changed to basal differentiation supplement and 10 μ M IWR-1 (Sigma). On day 4, basal differentiation supplement with 10 μ M IWR-1 was replenished. On day 6, Medium was changed to basal differentiation medium *without* IWR-1. Beginning on day 8, medium was changed to RPMI 1640 with B27 plus insulin supplement. Lactate purification was performed on day 10 by culturing cells in RPMI 1640 with B27 plus insulin supplement *minus glucose* supplemented with 4 mM lactate for 2 days. On day 12, and every other day thereafter, media was replenished with RPMI 1640 with B27 plus insulin supplement as cardiomyocyte maintenance medium. Small amounts of spontaneously contracting cardiomyocytes were first observed by day 8, or not at all (cell line and small molecule concentration dependent). This protocol was followed simultaneously in several cell culture wells at different small molecule concentrations and treatment times:

- 6 μ M/24 hrs CHIR-10 μ M IWR:
- 9 μ M/24 hrs CHIR-10 μ M IWR
- 12 μ M/24 hrs CHIR-10 μ M IWR
- 6 μ M/48 hrs CHIR-10 μ M IWR
- 9 μ M/48 hrs CHIR-10 μ M IWR
- 12 μ M/48 hrs CHIR-10 μ M IWR

Beating cardiomyocytes were seen in several of the small molecule treatment conditions, however efficiency was not high enough to perform biochemical characterization. From there, several other attempts were made to develop a differentiation protocol which produced a sufficient number of contracting cardiomyocytes for analysis.

It has been established that the addition of ascorbic acid (Vitamin C) increases the number of cardiac progenitor cells in culture, so this was added to the protocol (Cao et al., 2012). There have been published protocols which utilize the growth factor BMP4 (Weng et al., 2014) for differentiation of cardiomyocytes, so this was attempted in a manner similar to the previous protocol, with varying the concentration and time of treatment with small molecules:

CHIR-IWR/BMP(+). hiPSCs (passage >20) were passed at a 1:12 ratio and cultured in Essential 8 Flex medium until ~80 % confluency, at which point began Day 0. Medium was changed to RPMI 1640 (11875, Life Technologies) with B27 plus insulin supplement (Life Technologies) with 6 μ M CHIR99021 (Sigma), 50 ug/mL ascorbic acid, and 25 ng/mL BMP4. On Day 1, medium was changed to RPMI 1640 with B27 minus insulin supplement (11875, Life Technologies). On day 2, medium was changed to RPMI 1640 with B27 minus insulin supplement and 10 μ M IWR-1 (Sigma) or XAV939. On day 4, medium was refreshed (RPMI 1640 with B27 minus insulin supplement and 10 μ M IWR-1 (Sigma) or XAV939. Medium was switched on day 6 to RPMI 1640 with B27 minus insulin supplement (no IWR-1). On day 8, medium was changed, and every other day thereafter, to RPMI 1640 with B27 plus insulin supplement. Small amounts of spontaneously contracting cardiomyocytes for the 6 μ M/24 hrs and 6 μ M/48 hrs combination, however efficiency was not high enough to perform biochemical characterization.

- 6 μ M/24 hrs CHIR/BMP(+)
- 9 μ M/24 hrs CHIR/BMP(+)
- 12 μ M/24 hrs CHIR/BMP(+)

- 6 μ M/48 hrs CHIR/BMP(+)
- 9 μ M/48 hrs CHIR/BMP(+)
- 12 μ M/48 hrs CHIR/BMP(+)

There are published protocols which utilize the growth factor Activin A (Kattman et al., 2011) for differentiation of cardiomyocytes, so this was attempted in a manner similar to the previous protocol:

CHIR-Activin/IWR. hiPSCs (passage >20) were passed at a 1:12 ratio and cultured in Essential 8 Flex medium until ~80 % confluency. At Day 0, medium was changed to RPMI 1640 (11875, Life Technologies) with B27 minus insulin supplement (A1895601, Life Technologies) with 9 μ M CHIR99021 (Sigma), 10 ng/ml Activin A, and 50 μ g/ml ascorbic acid. On day 1, medium was changed to RPMI 1640 with B27 minus insulin supplement (referred to as basal differentiation supplement). On day 2, medium was changed to basal differentiation supplement and 10 μ M IWR-1 (Sigma). On day 4, medium was refreshed with basal supplement and 10 μ M IWR-1. Medium was changed on Day 6 to basal differentiation supplement (without IWR-1). On Day 8, and every other day thereafter, medium was refreshed with RPMI 1640 with B27 plus insulin supplement (referred to as cardiomyocyte maintenance media). Spontaneously contracting cardiomyocytes were first observed on day 11. Approximately 2 days after observing initial cardiomyocyte contractions, medium was changed to RPMI 1640 without glucose supplemented with 4 μ M lactate. Medium was changed 72 hours later to cardiomyocyte maintenance media. This protocol produced a decent number of contracting cardiomyocytes, and the goal was to further enhance the differentiation efficiency. Due to published literature which utilizes both Activin A *and* BMP4 in producing ventricular

cardiomyocytes with the use of CHIR 99201 (Kim et al., 2015), a couple of attempts were made at using this method:

CHIR-Activin-BMP/IWR. hiPSCs (passage >20) were passed at a 1:12 ratio and cultured in Essential 8 Flex medium until ~80 % confluency, at which point began Day 0. Medium was changed to RPMI 1640 (11875, Life Technologies) with B27 plus insulin supplement (Life Technologies) with 6 μ M CHIR99021 (Sigma), 50 ug/mL ascorbic acid, and 10 ng/mL Activin A. On day 1, medium was then changed to RPMI 1640 (11875, Life Technologies) with B27 minus insulin supplement with 6 uM CHIR, 50 ug ascorbic acid, and 25 ng/mL BMP-4. On day 2, medium was then changed to RPMI 1640 (11875, Life Technologies) with B27 minus insulin supplement (A1895601, Life Technologies). On day 3, medium was changed to RPMI 1640 with B27 minus insulin supplement and 10 uM IWR-1 (Sigma). On day 5, medium was refreshed (RPMI 1640 with B27 minus insulin supplement and 10 uM IWR-1 (Sigma) or XAV939). On day 7, medium was changed to RPMI 1640 without glucose supplemented with 4 μ M lactate. On day 9, medium was changed, and every other day thereafter, to RPMI 1640 with B27 plus insulin supplement. No spontaneously contracting cardiomyocytes were observed.

CHIR-Activin-BMP 2/IWR. hiPSCs (passage >20) were passed at a 1:12 ratio and cultured in Essential 8 Flex medium until ~80 % confluency, at which point began Day 0. Medium was changed to RPMI 1640 (11875, Life Technologies) with B27 minus insulin supplement (Life Technologies) with 7 μ M CHIR99021 (Sigma), 50 ug/mL ascorbic acid, and 10 ng/mL Activin A. On day 1, medium was then changed to RPMI 1640 (11875, Life Technologies) with B27 minus insulin supplement with 7 uM CHIR, 50 ug ascorbic acid, and 25 ng/mL BMP-4. On day 2, medium was then changed to RPMI 1640 (11875, Life

Technologies) with B27 minus insulin supplement (A1895601, Life Technologies). On day 3, medium was changed to RPMI 1640 with B27 minus insulin supplement and 10 uM IWR-1 (Sigma). On day 5, medium was refreshed (RPMI 1640 with B27 minus insulin supplement and 10 uM IWR-1 (Sigma). On day 6, medium was changed, and every other day thereafter, to RPMI 1640 with B27 plus insulin supplement. No spontaneously contracting cardiomyocytes were observed.

After the failure of the Activin A/BMP4 combination protocol, it was decided that CHIR/IWR either with or without Activin A were the most successful and promising of the protocols which had been attempted. Both protocols had produced a sufficient number of contracting cardiomyocytes for biochemical characterization, and the next step was to reproduce the results and to validate these cells with the methods discussed at the beginning of the section.

Differentiation Attempts:

Thermo Kit (Commercial)	DAY 0	DAY 1	DAY 2	DAY 3	DAY 4	DAY 5	DAY 6	DAY 7	DAY 8	DAY 9	DAY 10	DAY 11	DAY 12	DAY 13	DAY 14	DAY 15
Differentiation Medium A	2 mL	2 mL	x	x	x	x	x	x	x	x	x	x	x	x	x	x
Differentiation Medium B	x	x	2 mL	2 mL	x	x	x	x	x	x	x	x	x	x	x	x
Cardiomyocyte Maintenance Medium	x	x	x	x	2 mL	2 mL	2 mL	2 mL	2 mL	2 mL	2 mL	2 mL	2 mL	2 mL	2 mL	2 mL
(Jove) CHIR-IWR	DAY 0	DAY 1	DAY 2	DAY 3	DAY 4	DAY 5	DAY 6	DAY 7	DAY 8	DAY 9	DAY 10	DAY 11	DAY 12	DAY 13	DAY 14	DAY 15
Basal Media Formulation:	B27 (-) Ins.								B27 (+) Ins.		B27 (+) Ins. No glu		B27 (+) Ins.			
CHIR99021	6 uM	6 uM	x	x	x	x	x	x	x	x	x	x	x	x	x	x
IWR-1	x	x	x	x	5 uM	5 uM	x	x	x	x	x	x	x	x	x	x
Lactate	x	x	x	x	x	x	x	x	x	x	4 mM	4 mM	x	x	x	x
6 uM/24 hrs CHIR-IWR	DAY 0	DAY 1	DAY 2	DAY 3	DAY 4	DAY 5	DAY 6	DAY 7	DAY 8	DAY 9	DAY 10	DAY 11	DAY 12	DAY 13	DAY 14	DAY 15
Basal Media Formulation:	B27 (-) Ins.								B27 (+) Ins.		B27 (+) Ins. No glu		B27 (+) Ins.			
CHIR99021	6 uM	x	x	x	x	x	x	x	x	x	x	x	x	x	x	x
IWR-1	x	x	10 uM	10 uM	10 uM	10 uM	x	x	x	x	x	x	x	x	x	x
Lactate	x	x	x	x	x	x	x	x	x	x	4 mM	4 mM	x	x	x	x
9 uM/24 hrs CHIR-IWR	DAY 0	DAY 1	DAY 2	DAY 3	DAY 4	DAY 5	DAY 6	DAY 7	DAY 8	DAY 9	DAY 10	DAY 11	DAY 12	DAY 13	DAY 14	DAY 15
Basal Media Formulation:	B27 (-) Ins.								B27 (+) Ins.		B27 (+) Ins. No glu		B27 (+) Ins.			
CHIR99021	9 uM	x	x	x	x	x	x	x	x	x	x	x	x	x	x	x
IWR-1	x	x	10 uM	10 uM	10 uM	10 uM	x	x	x	x	x	x	x	x	x	x
Lactate	x	x	x	x	x	x	x	x	x	x	4 mM	4 mM	x	x	x	x
12 uM/24 hrs CHIR-IWR	DAY 0	DAY 1	DAY 2	DAY 3	DAY 4	DAY 5	DAY 6	DAY 7	DAY 8	DAY 9	DAY 10	DAY 11	DAY 12	DAY 13	DAY 14	DAY 15
Basal Media Formulation:	B27 (-) Ins.								B27 (+) Ins.		B27 (+) Ins. No glu		B27 (+) Ins.			
CHIR99021	12 uM	x	x	x	x	x	x	x	x	x	x	x	x	x	x	x
IWR-1	x	x	10 uM	10 uM	10 uM	10 uM	x	x	x	x	x	x	x	x	x	x
Lactate	x	x	x	x	x	x	x	x	x	x	4 mM	4 mM	x	x	x	x
6 uM/48 hrs CHIR-IWR	DAY 0	DAY 1	DAY 2	DAY 3	DAY 4	DAY 5	DAY 6	DAY 7	DAY 8	DAY 9	DAY 10	DAY 11	DAY 12	DAY 13	DAY 14	DAY 15
Basal Media Formulation:	B27 (-) Ins.								B27 (+) Ins.		B27 (+) Ins. No glu		B27 (+) Ins.			
CHIR99021	6 uM	6 uM	x	x	x	x	x	x	x	x	x	x	x	x	x	x
IWR-1	x	x	x	10 uM	10 uM	10 uM	10 uM	x	x	x	x	x	x	x	x	x
Lactate	x	x	x	x	x	x	x	x	x	x	x	4 uM	4 uM	x	x	x

Table 4: Differentiation Methods Attempted (a)

Differentiation Attempts (cont'd):																
9 uM/48 hrs CHIR-IWR	DAY 0	DAY 1	DAY 2	DAY 3	DAY 4	DAY 5	DAY 6	DAY 7	DAY 8	DAY 9	DAY 10	DAY 11	DAY 12	DAY 13	DAY 14	DAY 15
Basal Media Formulation:	B27 (-) Ins.									B27 (+) Ins.		B27 (+) Ins. No glu		B27 (+) Ins.		
CHIR99021	9 uM	9 uM	x	x	x	x	x	x	x	x	x	x	x	x	x	x
IWR-1	x	x	x	10 uM	10 uM	10 uM	10 uM	x	x	x	x	x	x	x	x	x
Lactate	x	x	x	x	x	x	x	x	x	x	x	4 uM	4 uM	x	x	x
12 uM/48 hrs CHIR-IWR	DAY 0	DAY 1	DAY 2	DAY 3	DAY 4	DAY 5	DAY 6	DAY 7	DAY 8	DAY 9	DAY 10	DAY 11	DAY 12	DAY 13	DAY 14	DAY 15
Basal Media Formulation:	B27 (-) Ins.									B27 (+) Ins.		B27 (+) Ins. No glu		B27 (+) Ins.		
CHIR99021	12 uM	12 uM	x	x	x	x	x	x	x	x	x	x	x	x	x	x
IWR-1	x	x	x	10 uM	10 uM	10 uM	10 uM	x	x	x	x	x	x	x	x	x
Lactate	x	x	x	x	x	x	x	x	x	x	x	4 mM	4 mM	x	x	x
6 uM/24 hrs CHIR/BMP(+)	DAY 0	DAY 1	DAY 2	DAY 3	DAY 4	DAY 5	DAY 6	DAY 7	DAY 8	DAY 9	DAY 10	DAY 11	DAY 12	DAY 13	DAY 14	DAY 15
Basal Media Formulation:	B27 (+) Ins.	B27 (-) Ins.							B27 (+) Ins.		B27 (+) Ins. No glu		B27 (+) Ins.			
CHIR99021	6 uM	x	x	x	x	x	x	x	x	x	x	x	x	x	x	x
BMP4	25 ng/ml	x	x	x	x	x	x	x	x	x	x	x	x	x	x	x
Ascorbic acid	50 ug/ml	x	x	x	x	x	x	x	x	x	x	x	x	x	x	x
IWR-1	x	x	10 uM	10 uM	10 uM	10 uM	x	x	x	x	x	x	x	x	x	x
Lactate	x	x	x	x	x	x	x	x	x	x	4 mM	4 mM	x	x	x	x
9 uM/24 hrs CHIR/BMP(+)	DAY 0	DAY 1	DAY 2	DAY 3	DAY 4	DAY 5	DAY 6	DAY 7	DAY 8	DAY 9	DAY 10	DAY 11	DAY 12	DAY 13	DAY 14	DAY 15
Basal Media Formulation:	B27 (+) Ins.	B27 (-) Ins.							B27 (+) Ins.		B27 (+) Ins. No glu		B27 (+) Ins.			
CHIR99021	9 uM	x	x	x	x	x	x	x	x	x	x	x	x	x	x	x
BMP4	25 ng/ml	x	x	x	x	x	x	x	x	x	x	x	x	x	x	x
Ascorbic acid	50 ug/ml	x	x	x	x	x	x	x	x	x	x	x	x	x	x	x
IWR-1	x	x	10 uM	10 uM	10 uM	10 uM	x	x	x	x	x	x	x	x	x	x
Lactate	x	x	x	x	x	x	x	x	x	x	4 mM	4 mM	x	x	x	x
12 uM/24 hrs CHIR/BMP(+)	DAY 0	DAY 1	DAY 2	DAY 3	DAY 4	DAY 5	DAY 6	DAY 7	DAY 8	DAY 9	DAY 10	DAY 11	DAY 12	DAY 13	DAY 14	DAY 15
Basal Media Formulation:	B27 (+) Ins.	B27 (-) Ins.							B27 (+) Ins.		B27 (+) Ins. No glu		B27 (+) Ins.			
CHIR99021	12 uM	x	x	x	x	x	x	x	x	x	x	x	x	x	x	x
BMP4	25 ng/ml	x	x	x	x	x	x	x	x	x	x	x	x	x	x	x
Ascorbic acid	50 ug/ml	x	x	x	x	x	x	x	x	x	x	x	x	x	x	x
IWR-1	x	x	10 uM	10 uM	10 uM	10 uM	x	x	x	x	x	x	x	x	x	x
Lactate	x	x	x	x	x	x	x	x	x	x	4 mM	4 mM	x	x	x	x

Table 5: Differentiation Methods Attempted (b)

Differentiation Attempts (cont'd):																
6 uM/48 hrs CHIR/BMP(+)	DAY 0	DAY 1	DAY 2	DAY 3	DAY 4	DAY 5	DAY 6	DAY 7	DAY 8	DAY 9	DAY 10	DAY 11	DAY 12	DAY 13	DAY 14	DAY 15
Basal Media Formulation:	B27 (+) Ins.	B27 (-) Ins.								B27 (+) Ins.	B27 (+) Ins. No glu		B27 (+) Ins.			
CHIR99021	6 uM	6 uM	x	x	x	x	x	x	x	x	x	x	x	x	x	x
BMP4	25 ng/ml	x	x	x	x	x	x	x	x	x	x	x	x	x	x	x
Ascorbic acid	50 ug/ml	50 ug/ml	x	x	x	x	x	x	x	x	x	x	x	x	x	x
IWR-1	x	x	x	10 uM	10 uM	10 uM	10 uM	x	x	x	x	x	x	x	x	x
Lactate	x	x	x	x	x	x	x	x	x	x	x	4 mM	4 mM	x	x	x
9 uM/48 hrs CHIR/BMP(+)	DAY 0	DAY 1	DAY 2	DAY 3	DAY 4	DAY 5	DAY 6	DAY 7	DAY 8	DAY 9	DAY 10	DAY 11	DAY 12	DAY 13	DAY 14	DAY 15
Basal Media Formulation:	B27 (+) Ins.	B27 (-) Ins.								B27 (+) Ins.	B27 (+) Ins. No glu		B27 (+) Ins.			
CHIR99021	9 uM	9 uM	x	x	x	x	x	x	x	x	x	x	x	x	x	x
BMP4	25 ng/ml	x	x	x	x	x	x	x	x	x	x	x	x	x	x	x
Ascorbic acid	50 ug/ml	50 ug/ml	x	x	x	x	x	x	x	x	x	x	x	x	x	x
IWR-1	x	x	x	10 uM	10 uM	10 uM	10 uM	x	x	x	x	x	x	x	x	x
Lactate	x	x	x	x	x	x	x	x	x	x	x	4 mM	4 mM	x	x	x
12 uM/48 hrs CHIR/BMP(+)	DAY 0	DAY 1	DAY 2	DAY 3	DAY 4	DAY 5	DAY 6	DAY 7	DAY 8	DAY 9	DAY 10	DAY 11	DAY 12	DAY 13	DAY 14	DAY 15
Basal Media Formulation:	B27 (+) Ins.	B27 (-) Ins.								B27 (+) Ins.	B27 (+) Ins. No glu		B27 (+) Ins.			
CHIR99021	12 uM	12 uM	x	x	x	x	x	x	x	x	x	x	x	x	x	x
BMP4	25 ng/ml	x	x	x	x	x	x	x	x	x	x	x	x	x	x	x
Ascorbic acid	50 ug/ml	50 ug/ml	x	x	x	x	x	x	x	x	x	x	x	x	x	x
IWR-1	x	x	x	10 uM	10 uM	10 uM	10 uM	x	x	x	x	x	x	x	x	x
Lactate	x	x	x	x	x	x	x	x	x	x	x	4 mM	4 mM	x	x	x
CHIR-BMP/IWR	DAY 0	DAY 1	DAY 2	DAY 3	DAY 4	DAY 5	DAY 6	DAY 7	DAY 8	DAY 9	DAY 10	DAY 11	DAY 12	DAY 13	DAY 14	DAY 15
Basal Media Formulation:	B27 (-) Ins.								B27 (+) Ins.		B27 (+) Ins. No glu		B27 (+) Ins.			
CHIR99021	6 uM	6 uM	x	x	x	x	x	x	x	x	x	x	x	x	x	x
BMP4	25 ng/ml	x	x	x	x	x	x	x	x	x	x	x	x	x	x	x
Ascorbic acid	50 ug/ml	50 ug/ml	x	x	x	x	x	x	x	x	x	x	x	x	x	x
IWR-1	x	x	x	10 uM	10 uM	10 uM	10 uM	x	x	x	x	x	x	x	x	x
Lactate	x	x	x	x	x	x	x	x	x	x	x	4 mM	4 mM	x	x	x
CHIR-Activin1/IWR	DAY 0	DAY 1	DAY 2	DAY 3	DAY 4	DAY 5	DAY 6	DAY 7	DAY 8	DAY 9	DAY 10	DAY 11	DAY 12	DAY 13	DAY 14	DAY 15
Basal Media Formulation:	B27 (-) Ins.								B27 (+) Ins.		B27 (+) Ins. No glu		B27 (+) Ins.			
CHIR99021	6 uM	6 uM	x	x	x	x	x	x	x	x	x	x	x	x	x	x
Activin A	10 ng/ml	x	x	x	x	x	x	x	x	x	x	x	x	x	x	x
Ascorbic acid	50 ug/ml	50 ug/ml	x	x	x	x	x	x	x	x	x	x	x	x	x	x
IWR-1	x	x	x	10 uM	10 uM	10 uM	10 uM	x	x	x	x	x	x	x	x	x
Lactate	x	x	x	x	x	x	x	x	x	x	x	4 mM	4 mM	x	x	x

Table 6: Differentiation Methods Attempted (c)

Differentiation Attempts (cont'd):																
CHIR-Activin 2/IWR	DAY 0	DAY 1	DAY 2	DAY 3	DAY 4	DAY 5	DAY 6	DAY 7	DAY 8	DAY 9	DAY 10	DAY 11	DAY 12	DAY 13	DAY 14	DAY 15
Basal Media Formulation:	B27 (-) Ins.								B27 (+) Ins.		B27 (+) Ins. No glu		B27 (+) Ins.			
CHIR99021	9 uM	x	x	x	x	x	x	x	x	x	x	x	x	x	x	x
Activin A	10 ng/ml	x	x	x	x	x	x	x	x	x	x	x	x	x	x	x
Ascorbic acid	50 ug/ml	x	x	x	x	x	x	x	x	x	x	x	x	x	x	x
IWR-1	x	x	10 uM	10 uM	10 uM	10 uM	x	x	x	x	x	x	x	x	x	x
Lactate	x	x	x	x	x	x	x	x	x	x	4 mM	4 mM	x	x	x	x
CHIR-Activin-BMP/IWR	DAY 0	DAY 1	DAY 2	DAY 3	DAY 4	DAY 5	DAY 6	DAY 7	DAY 8	DAY 9	DAY 10	DAY 11	DAY 12	DAY 13	DAY 14	DAY 15
Basal Media Formulation:	B27 (-) Ins.								B27 (+) Ins.		B27 (+) Ins. No glu		B27 (+) Ins.			
CHIR99021	6 uM	x	x	x	x	x	x	x	x	x	x	x	x	x	x	x
Activin A	10 ng/ml	x	x	x	x	x	x	x	x	x	x	x	x	x	x	x
BMP	x	25 ng/ml	x	x	x	x	x	x	x	x	x	x	x	x	x	x
Ascorbic acid	50 ug/ml	50 ug/ml	x	x	x	x	x	x	x	x	x	x	x	x	x	x
IWR-1	x	x	x	10 uM	10 uM	10 uM	10 uM	x	x	x	x	x	x	x	x	x
Lactate	x	x	x	x	x	x	x	x	x	x	x	4 mM	4 mM	x	x	x
CHIR-Activin-BMP 2/IWR	DAY 0	DAY 1	DAY 2	DAY 3	DAY 4	DAY 5	DAY 6	DAY 7	DAY 8	DAY 9	DAY 10	DAY 11	DAY 12	DAY 13	DAY 14	DAY 15
Basal Media Formulation:	B27 (-) Ins.						B27 (+) Ins.									
CHIR99021	7 uM	7 uM	x	x	x	x	x	x	x	x	x	x	x	x	x	x
Activin A	10 ng/ml	x	x	x	x	x	x	x	x	x	x	x	x	x	x	x
BMP	x	25 ng/ml	x	x	x	x	x	x	x	x	x	x	x	x	x	x
Ascorbic acid	50 ug/ml	50 ug/ml	x	x	x	x	x	x	x	x	x	x	x	x	x	x
IWR-1	x	x	x	10 uM	10 uM	10 uM	x	x	x	x	x	x	x	x	x	x
Lactate	x	x	x	x	x	x	x	x	x	x	x	x	x	x	x	x

Table 7: Differentiation Methods Attempted (d)

2.4 Results

2.4.1 *hiPSC-CM Differentiation Protocols*

The work performed on developing working hiPSC-CM differentiation protocols from 21 different attempted methods has led to the two most effective working protocols: *CHIR-Activin-E/IWR* and *9 μ M/24hrs CHIR-IWR*. For our cell lines, the most efficient of the protocols is 6 μ M/CHIR-Activin A-EDTA, in which the iPSCs are treated briefly with EDTA dissociation solution prior to induction of differentiation, however either of these are sufficient for producing a large population of hiPSC-CMs for biochemical analysis.

To optimize the differentiation method which uses Activin A, a happy accident occurred which produced an extremely efficient method for iPSC-CM differentiation. On the day of differentiation induction, iPSCs were at 100% confluency, which is generally considered to be a relatively high population for inducing differentiation. Cells were briefly treated with dissociation reagent (0.5 mM EDTA) for approximately 45 seconds (cells were not pipetted) in order to dislodge only a small amount of cells. This resulted in a lower (approximately 80%) confluency of the iPSCs. After removal of the EDTA solution, differentiation solution was immediately applied to the cell culture well (10 μ M Y-27632 was added to prevent cell death), and cells were incubated as prescribed below for differentiation.

2.4.2 *CHIR-Activin-E/IWR*

A lactate-purified population of induced pluripotent stem cell derived cardiomyocytes was established through a combination growth factor and small molecule-based differentiation protocol. Briefly, iPSCs (passage >20) were passed at a 1:12 ratio and cultured in Essential 8 Flex medium until ~100 % confluency. At Day 0, prior to medium

change, E8 media was aspirated from cells, and they were washed with DPBS. 1 mL of 0.5 mM EDTA in DPBS was added to each culture well. Plate was placed in incubator for approximately 45 seconds. Upon removal from incubator, dish was gently tapped to dislodge only a small amount of cells. EDTA solution was aspirated, however upon addition of differentiation medium care was taken to avoid further removal of cells. The medium was changed to RPMI 1640 (11875, Life Technologies) with B27 minus insulin supplement (A1895601, Life Technologies) with 6 μ M CHIR99021 (Sigma), 10 ng/ml Activin A, and 50 μ g/ml ascorbic acid. 10 μ M Y-27632 was added to prevent cell death. On day 1, medium was changed to RPMI 1640 with B27 minus insulin supplement (referred to as basal differentiation supplement). On day 2, medium was changed to basal differentiation supplement and 10 μ M IWR-1 (Sigma). On day 4, medium was refreshed with basal supplement and 10 μ M IWR-1. Medium was changed on Day 6 to basal differentiation supplement (without IWR-1). On Day 8, and every other day thereafter, medium was refreshed with RPMI 1640 with B27 supplement (referred to as cardiomyocyte maintenance media). Spontaneously contracting cardiomyocytes were first observed on day 7. Approximately 2 days after observing initial cardiomyocyte contractions, medium was changed to RPMI 1640 without glucose supplemented with 4 μ M lactate. Medium was changed 72 hours later to cardiomyocyte maintenance media.

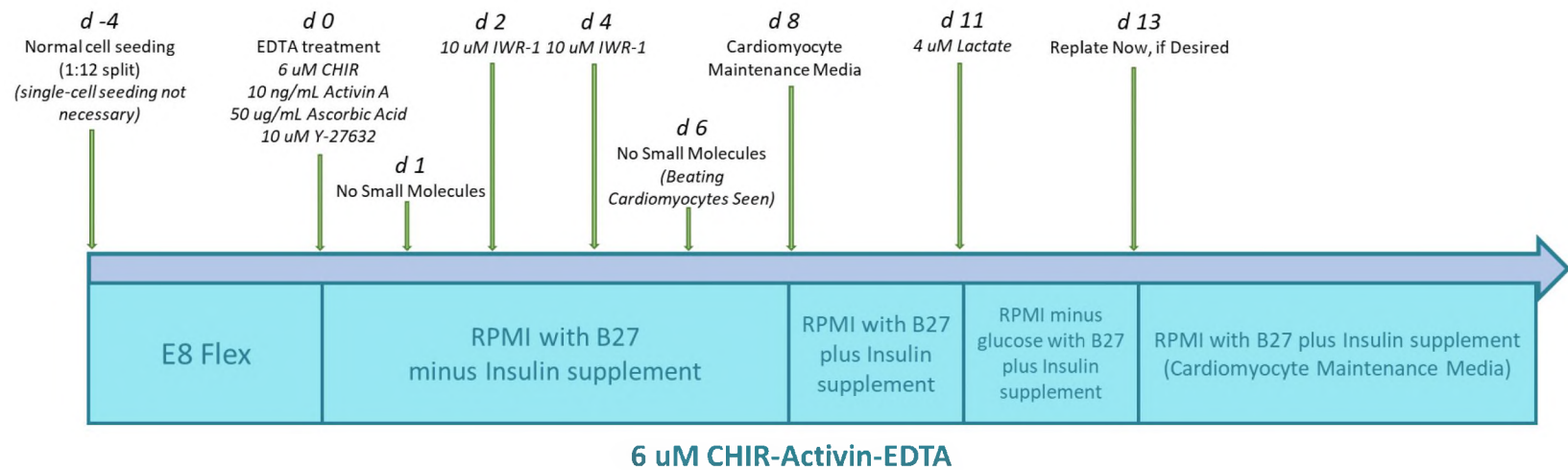


Figure 21: Timeline of CHIR-Activin-E/IWR Protocol

CHIR-Activin-E/IWR Protocol Step-by-Step

- Day -4: Passage cells at 1:12 ratio (single cell seeding not necessary)
 - Use Matrigel matrix at 1:400 ratio
- Day -2: Refresh media with E8 Flex
- Day 0: Perform EDTA treatment to cells and initiate differentiation as follows (iPSCs should be at ~100% confluency):
 - Aspirate cell media.
 - Add 1 mL 0.5 mM EDTA solution to cells.
 - Place cells in incubator for ~45 seconds. *If too many cells have dislodged from culture dish (no less than 70% confluency), protocol must be restarted at day -4.*
 - Remove cells from incubator and gently remove EDTA solution, taking care to not dislodge the cell mass with pipetting.
 - Add 2 mL of the differentiation solution to each cell well:
 - In RPMI with B27 *minus* Insulin:
 - 6 μ M CHIR 99201
 - 10 ng/mL Activin A
 - 50 μ g/mL Ascorbic Acid
 - 10 μ M Y-27632
- Day 1: Change media to RPMI with B27 minus Insulin with *no* small molecules/growth factors.
- Day 2: Change media to RPMI with B27 minus Insulin with:
 - 10 μ M IWR-1

- Day 4: Refresh media with RPMI with B27 minus Insulin with:
 - 10 μ M IWR-1
- Day 6: Contracting cardiomyocytes will be seen. Change media to RPMI with B27 minus Insulin with *no* small molecules.
- Day 8: Change media to cardiomyocyte maintenance media: RPMI with B27 supplement (with Insulin).
- Day 10: Refresh media with cardiomyocyte maintenance media.
- Day 11: Begin lactate purification: Change media to RPMI *minus glucose* with B27 supplement with:
 - 4 μ M lactate
- Day 13: Replate cardiomyocytes now. Cardiomyocytes, if replated, will continue to proliferate in culture for a short time. Change media to cardiomyocyte maintenance media.
 - Prepare centrifuge tubes containing 1 mL cardiomyocyte maintenance media
 - Prepare new culture dishes (coated with Matrigel (1:200)):
 - 2 mL Cardiomyocyte maintenance media with:
 - 10 μ M Y-27632.
 - Dislodge CMs from cell culture well using TrypLE solution:
 - Add 1 mL TrypLE solution to cell well and place in incubator for 1 minute.
 - Remove cells from incubator and gently pipette cells to dislodge from cell well and to break up large clumps of cells.

- Add TrypLE solution (containing cells from the well) to tube of cardiomyocyte maintenance media (CMM neutralizes TrypLE).
- Centrifuge tube at 1000 RPM for 5 minutes (cell pellet will be seen at bottom of centrifuge tube)
- Aspirate media from tube, being careful to not disturb cell pellet.
- To pass at 1:12 ratio:
 - Add 1.2 mL to CMM to cell pellet and pipette gently to singularize cells
 - Add appropriate amount of cell solution to each cell culture well:
 - 12 wells, passed at 1:12 ratio: Add 100 μ L cell-containing solution to each of 12 new wells.
 - Gently shift plates back and forth to evenly distribute cells.
 - Place cells in incubator, and change media the next day to CMM (no Y-27632)
- For remainder of time in culture: supply cells with cardiomyocyte maintenance media every 2 days.

2.4.3 9 μ M/24hrs CHIR-IWR

A lactate-purified population of induced pluripotent stem cell derived cardiomyocytes was established through a small molecule-based differentiation protocol. hiPSCs (passage >20) were singularized for 5 passages prior to differentiation, passed at a 1:12 ratio, and cultured in Essential 8 Flex medium until ~80 % confluency, at which point began Day 0. Medium was changed to RPMI 1640 (11875, Life Technologies) with B27 minus insulin supplement (A1895601, Life Technologies) with 9 μ M CHIR 99021 (Sigma). On day 1 (exactly 24 hours after addition of media with CHIR99021), medium was changed to RPMI 1640 with B27 minus insulin supplement (referred to as basal differentiation supplement). On day 2 (exactly 24 hours after media was changed), medium was changed to basal differentiation supplement with 10 μ M IWR-1 (Sigma). On day 4, medium was refreshed with basal supplement and 10 μ M IWR-1. Medium was changed on Day 6 to basal differentiation supplement (without IWR-1). On Day 8, and every other day thereafter, medium was refreshed with RPMI 1640 with B27 supplement (referred to as cardiomyocyte maintenance media). Spontaneously contracting cardiomyocytes were first observed on day 9. Approximately 2 days after observing initial cardiomyocyte contractions, medium was changed to RPMI 1640 without glucose supplemented with 4 μ M lactate. Medium was changed 72 hours later to cardiomyocyte maintenance media.

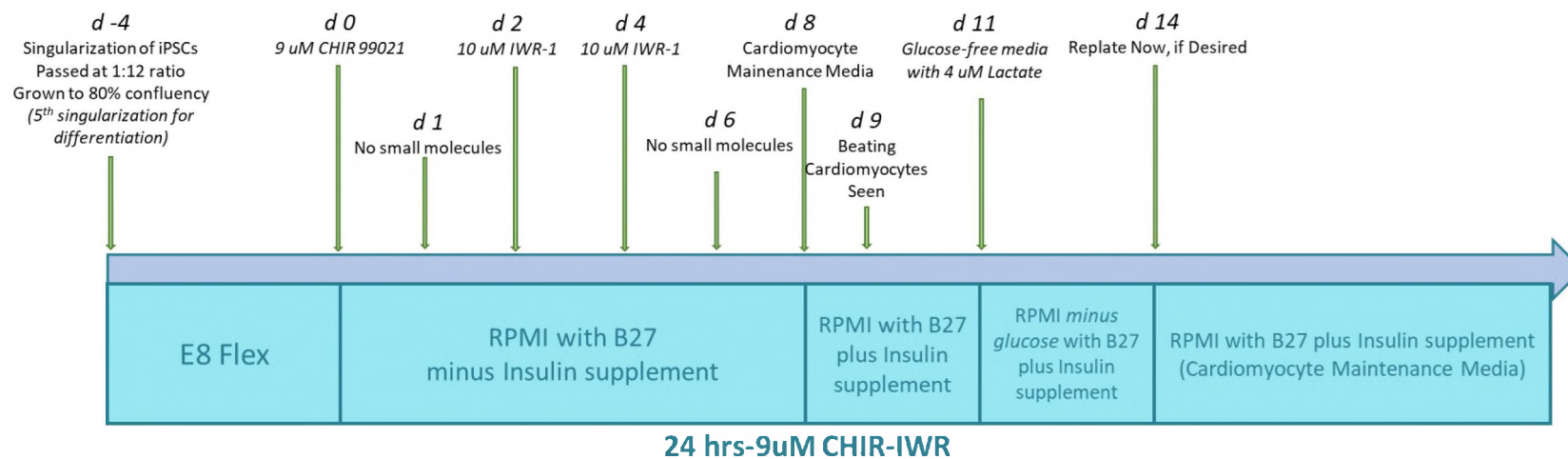


Figure 22: Timeline of 9 μ M/24hrs CHIR-IWR Protocol

9 μ M/24hrs CHIR-IWR Protocol Step-by-Step

- Day -4: Passage cells at 1:12 ratio (single cell seeding not necessary)
 - Use Matrigel matrix at 1:400 ratio
- Day -2: Refresh media with E8 Flex
- Day 0: Initiate differentiation as follows (iPSCs should be at ~80% confluency):
 - Aspirate cell media.
 - Add 2 mL of the differentiation solution to each cell well:
 - In RPMI with B27 *minus* Insulin:
 - 6 μ M CHIR 99201
- Day 1: Change media to RPMI with B27 minus Insulin with *no* small molecules/growth factors.
- Day 2: Change media to RPMI with B27 minus Insulin with:
 - 10 μ M IWR-1
- Day 4: Refresh media with RPMI with B27 minus Insulin with:
 - 10 μ M IWR-1
- Day 6: Change media to RPMI with B27 minus Insulin with *no* small molecules.
- Day 8: Change media to cardiomyocyte maintenance media (CMM): RPMI with B27 supplement (with Insulin).
- Day 9: Contracting cardiomyocytes will be seen.
- Day 10: Refresh media with cardiomyocyte maintenance media.

- Day 11: Begin lactate purification: Change media to RPMI *minus glucose* with B27 supplement with:
 - 4 μ M lactate
- Day 13: Replate cardiomyocytes now. Cardiomyocytes, if replated, will continue to proliferate in culture for a short time.
 - Prepare centrifuge tubes containing 1 mL cardiomyocyte maintenance media
 - Prepare new culture dishes (coated with Matrigel (1:200)):
 - 2 mL Cardiomyocyte maintenance media with:
 - 10 μ M Y-27632.
 - Dislodge CMs from cell culture well using TrypLE solution:
 - Add 1 mL TrypLE solution to cell well and place in incubator for 1 minute.
 - Remove cells from incubator and gently pipette cells to dislodge from cell well and to break up large clumps of cells.
 - Add TrypLE solution (containing cells from the well) to tube of cardiomyocyte maintenance media (CMM neutralizes TrypLE).
 - Centrifuge tube at 1000 RPM for 5 minutes (cell pellet will be seen at bottom of centrifuge tube)
 - Aspirate media from tube, being careful to not disturb cell pellet.
 - To pass at 1:12 ratio:

- Add 1.2 mL to CMM to cell pellet and pipette gently to singularize cells
- Add appropriate amount of cell solution to each cell culture well:
 - 12 wells, passed at 1:12 ratio: Add 100 μ L cell-containing solution to each of 12 new wells.
 - Gently shift plates back and forth to evenly distribute cells.
 - Place cells in incubator, and change media the next day to CMM (no Y-27632)
- For remainder of time in culture: supply cells with cardiomyocyte maintenance media every 2 days.

Novel Differentiation Protocols Developed By Our Lab:															
9 uM/24 hrs CHIR-IWR	DAY 0	DAY 1	DAY 2	DAY 3	DAY 4	DAY 5	DAY 6	DAY 7	DAY 8	DAY 9	DAY 10	DAY 11	DAY 12	DAY 13	DAY 14
Basal Media Formulation:	B27 (-) Ins.								B27 (+) Ins.		B27 (+) Ins. No glu		B27 (+) Ins.		
CHIR99021	9 uM	x	x	x	x	x	x	x	x	x	x	x	x	x	x
IWR-1	x	x	10 uM	10 uM	10 uM	10 uM	x	x	x	x	x	x	x	x	x
Lactate	x	x	x	x	x	x	x	x	x	x	4 uM	4 uM	x	x	x
Variation of CHIR-Activin 2/IWR (with EDTA treatment)															
CHIR-Activin-E/IWR	DAY 0	DAY 1	DAY 2	DAY 3	DAY 4	DAY 5	DAY 6	DAY 7	DAY 8	DAY 9	DAY 10	DAY 11	DAY 12	DAY 13	DAY 14
Basal Media Formulation:	B27 (-) Ins.								B27 (+) Ins.		B27 (+) Ins. No glu		B27 (+) Ins.		
CHIR99021	6 uM	x	x	x	x	x	x	x	x	x	x	x	x	x	x
Y-27632	10 uM	x	x	x	x	x	x	x	x	x	x	x	x	x	x
Activin A	10 ng/ml	x	x	x	x	x	x	x	x	x	x	x	x	x	x
Ascorbic acid	50 ug/ml	x	x	x	x	x	x	x	x	x	x	x	x	x	x
IWR-1	x	x	10 uM	10 uM	10 uM	10 uM	x	x	x	x	x	x	x	x	x
Lactate	x	x	x	x	x	x	x	x	x	x	4 uM	4 uM	x	x	x

Table 8: Successful Differentiation Methods

2.4.4 Immunohistochemical Analysis

The differentiation effectiveness of hiPSCs to hiPSC-CMs is determined by immunofluorescent staining for cardiac specific markers. iPSC-CMs are characterized based on protein expression of the cardiac marker TNNI3 (cytoplasmic) and IRX4 (nuclear). DAPI is also added to image the nucleus of cells. The following protocol is used in fluorescent immunofluorescent analysis of hiPSC-CMs, and is for one 35mm cell culture dish with coverslip. Cells must be passed onto coverslips one to two days prior to staining. hiPSC-CMs are very adherent to one another, so it can take more pipetting effort or longer incubation time with dissociation reagent to dissociate cells enough for staining. Cells will also need to be diluted when replated in order to produce good quality images.

To pass cells onto coverslips:

- Remove cardiomyocyte maintenance media
- Wash cells with 1 mL DPBS
 - Add 1 mL TrypLE to well
 - Incubate for 1-2 minutes
- Pipette cells vigorously until large chunks are dissociated
- Add cells to 3 mL cardiomyocyte maintenance media
- Centrifuge at 500g for 5 minutes
- Remove excess media from cell pellet
- Add 3 mL fresh cardiomyocyte maintenance media
- Pipette vigorously to dislodge and dissociate cells from pellet
- Prepare a 35mm cell culture dish with a coverslip and 2 mL cardiomyocyte maintenance media

- Add 250 uL of cell mixture to well on top of coverslip
- Shift well around side to side in order to evenly distribute cells
- Place in incubator – allow cells to recover for 1-2 days prior to imaging.

To prepare cells for imaging:

- Remove cell media
- Add 750 ul fixative solution
 - Incubate 15 minutes at RT
 - Remove fixative solution
- Add 750 ul permeabilization solution
 - Incubate 15 minutes at RT
 - Remove permeabilization solution
- Add 750 ul blocking buffer
 - Incubate 30 minutes at RT
- Add primary antibodies to the same well
- Incubate overnight in fridge (4°C) or 3 hrs at RT
- Remove solution containing primary antibodies
- Add 1 ml wash buffer
 - Allow to sit for 3 minutes
 - Remove wash buffer
- Repeat twice (3 washes total)
- Add 750 ul blocking buffer with appropriate secondary antibody to each well.
- Incubate (covered from light) for 1 hr at RT

- Remove solution containing secondary antibodies
- Add 1 ml wash buffer
 - Allow to sit for 3 minutes
 - Remove wash buffer
- Repeat twice (3 washes total)
- In final wash, add one drop of DAPI-containing solution
- Secure coverslip to glass slide
- Image cells

Results

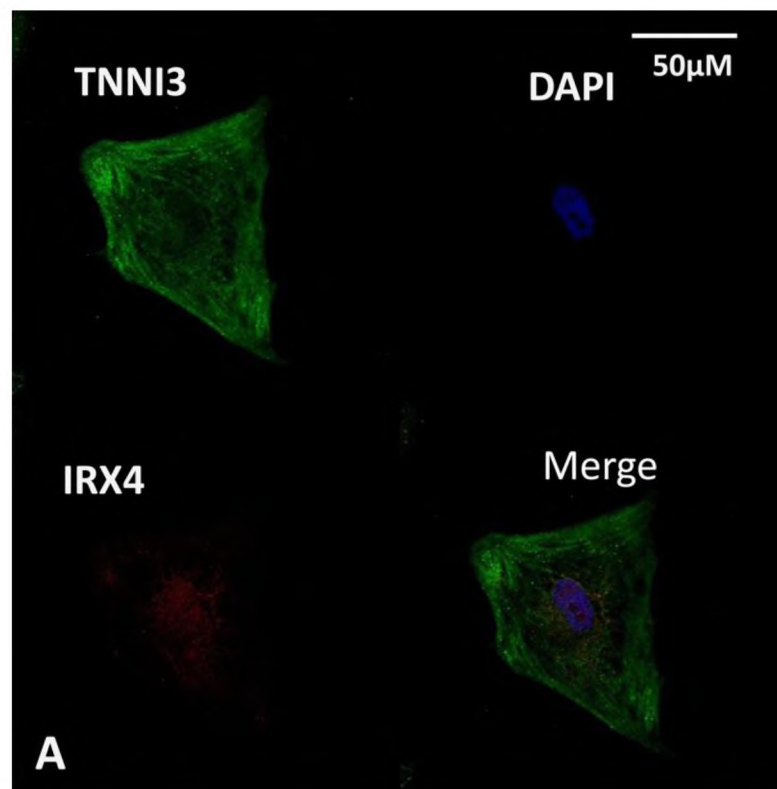


Figure 23a: TNNI3, IRX4, and DAPI Staining of hiPSC-CMs

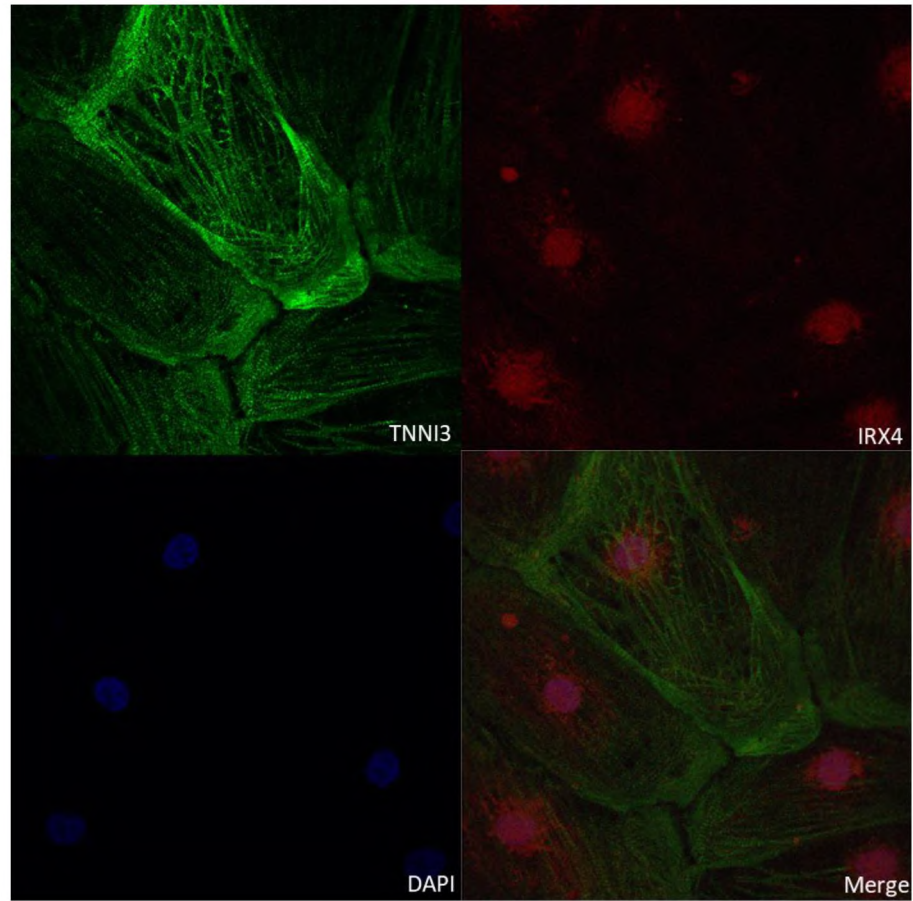
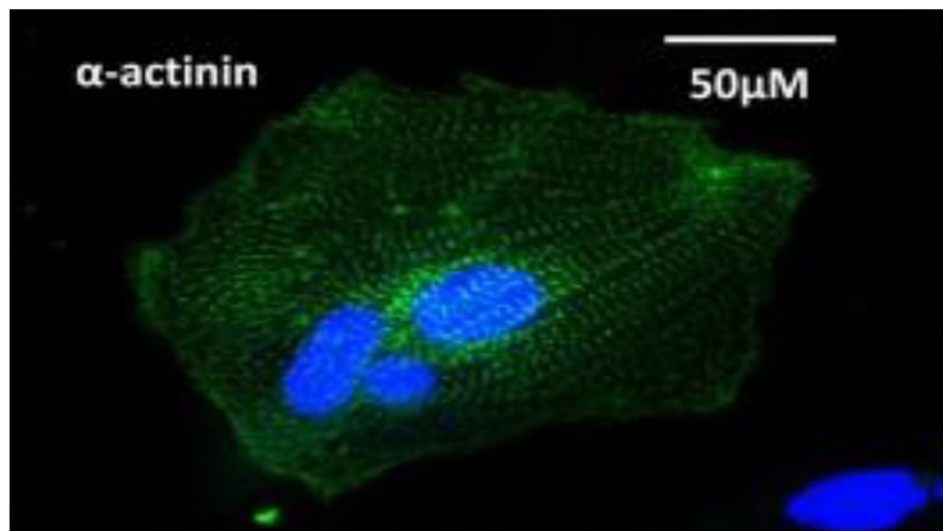


Figure 23b: TNNI3, IRX4, and DAPI Staining of hiPSC-CMs



**Figure 24: α -actinin and DAPI Staining of multi-nucleated hiPSC-CMs.
Multi-nucleation is a sign of higher hiPSC-CM maturity.**

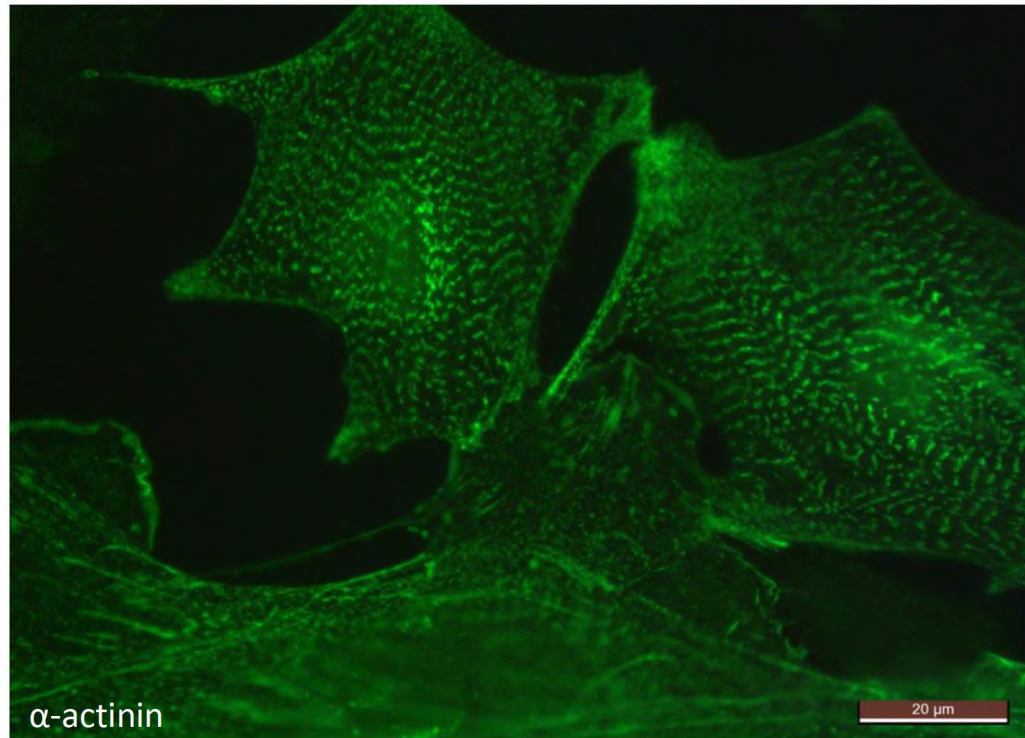


Figure 25a: α -actinin Staining of hiPSC-CMs

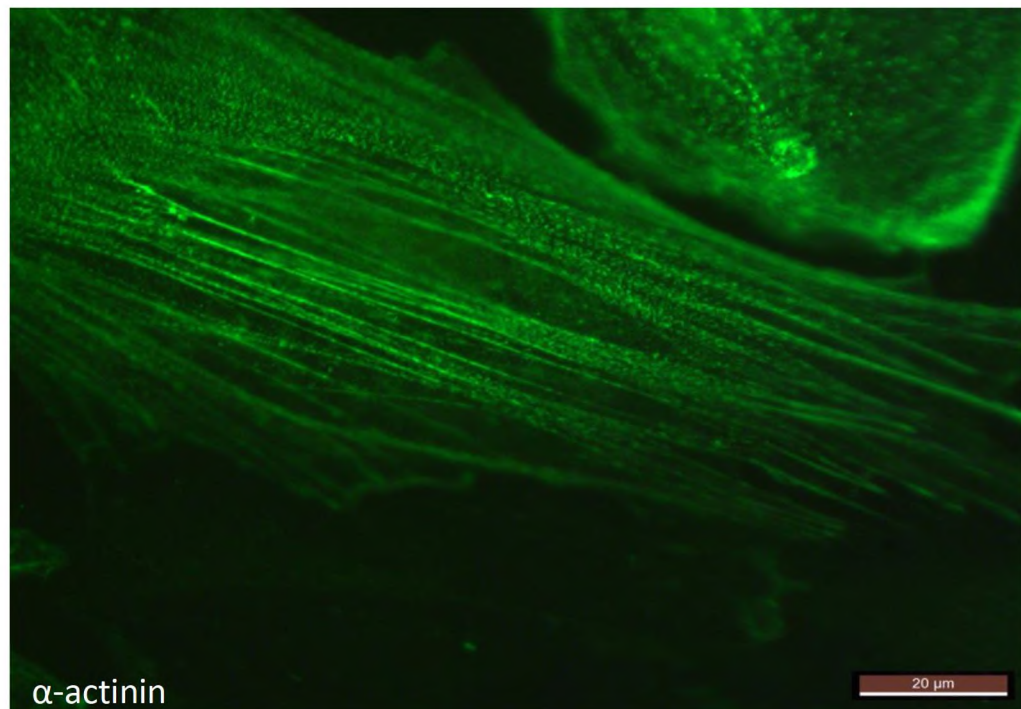


Figure 25b: α -actinin Staining of hiPSC-CMs

2.5 Conclusion

We have performed twenty-one different differentiation protocols. Most of the protocols did not yield functional cardiomyocytes which were able to be used for metabolic studies.

Two robust and successful protocols for iPSC cells under our study were developed. Through these developed protocols we were able successfully to differentiate iPSC cell lines to the functional cardiomyocytes. The obtained iPSC-CM are spontaneously beating and are positive to specific cardiac markers. The immunostaining analysis also reveals that many cardiomyocytes are presented by rod-shape cells and distinct z-lines which is consistent with a mature iPSC-CM phenotype. Expression of IRX-4 protein is consistent with ventricular-like cardiomyocytes. Taken together these results indicate that we created in our laboratory a powerful cellular model for study of cardiac metabolism in Barth syndrome.

CHAPTER III

MASS SPECTROMETRY ASSAYS FOR EVALUATING METABOLIC ACTIVITY

3.1 Introduction

Due to the cardiomyopathy that occurs in BTHS patients, the model of iPSC-CMs with the BTHS genotype provides an excellent source of cellular material which recapitulates the disease genotype and provides a platform for evaluating the disease phenotype using mass spectrometry-based assays. This type of characterization has previously not been established in TAZ-iPSC, and our goal has been to develop and establish biochemical characterization assays for this purpose.

The technical innovation of this project is derived from the fact that there has not yet been established a method of metabolic profiling of hiPSC-CMs as a model of BTHS. There are established methods of performing metabolomics assays on clinical patient material such as plasma or urine, however the development of methods to extract small metabolites from iPSC-CMs as a starting material is a novel concept, and in this case, we were successful in doing so. These assays provide an additional method of analysis to the currently established methods of investigation BTHS, such as gene and protein analysis, and electrophysical measurements (*Barth Syndrome Foundation : Research : Animal and*

Cellular Models of Barth Syndrome, n.d.; Zweigerdt et al., 2014). Additionally, as the field of iPSC-involved research is still relatively new, these assays are an innovative way by which the metabolic and overall biochemical nature of iPSCs can be investigated (House et al., 2020), as demonstrated in publication based on the work of this project.

3.1.1 LC-MS/MS

Metabolic profiling largely uses mass spectrometry as the method of instrumental analysis. In this work, gas chromatography-mass spectrometry (GC-MS) and liquid chromatography-tandem mass spectrometry (LC-MS/MS) are used. This section provides a brief introduction to the method and instruments.

Mass spectrometry is an analytical method which detects molecules based on their mass to charge ratio (m/z). The primary operation of a mass spectrometer is to break down large molecules into smaller fragments to then be detected by the instrument. Each molecule will have an individual fragmentation pattern which is specific to the molecule and allows it to be detected and distinguished from other molecules. The three main components of a mass spectrometer are the ion source, mass analyzer, and ion detector. Liquid chromatography tandem mass spectrometry (LC-MS/MS) is an analytical method which uses a high-pressure liquid chromatography (HPLC) instrument in connection with a triple quadrupole mass spectrometer. Prior to reaching the ionization source, molecules will undergo separation via liquid chromatography, which separates them based on their relative polarity.

The AB Sciex Qtrap 5500 uses electrospray ionization (ESI), which applies a high voltage to analytes in solution, causing the droplets to become charged and the solvent to evaporate, resulting in a stream of charged molecules. A triple quadrupole mass analyzer

is one in which three single quadrupoles are connected in tandem. The first and last cells, Q1 and Q3, are mass filters while the second cell, Q2, is the collision cell in which the original parent ions undergo fragmentation. The ions are then detected, and data is sent to the user interface. The instrument used in this project is a Shimadzu HPLC system (Shimadzu, Tokyo, Japan) and AB Sciex Qtrap 5500 mass spectrometer (ABI Sciex, Toronto, Canada).

3.1.2 GC-MS

Gas chromatography mass spectrometry (GC-MS) is an analytical method which separates molecules based on their relative volatility as they travel through a glass capillary column. This requires the conversion of analytes to a volatile, or gaseous, form attained by a process called derivatization. As the molecules exit the chromatography instrument, they enter the ion source of the mass spectrometer. After ionization, they enter the mass filter and reach the detector. Data pertaining to the retention time and m/z of the sample components is then sent to the user interface. The instrument used in this project is a 7890B Gas Chromatograph instrument coupled to a 5977A Mass Spectrometer controlled by MassHunter and analyzed via ChemStation software (Agilent, Santa Clara, CA).

The primary steps of our metabolomics workflow of evaluating iPSC-CM include cell harvesting, metabolite extraction, derivatization, and analysis.

3.2 Derivatization Methods

Derivatization is a chemical reaction that increases sensitivity and specificity during analysis by mass spectrometry, and thus increases the detection of analytes. Furthermore, derivatization process is an essential step in GCMS for polar and non-volatile metabolites.

3.2.1 MOX-TMS Derivatization

MOX (Methoxamine hydrochloride) is a derivatization reagent used in gas chromatography which produces oximes from ketone or aldehyde-containing metabolites (*Methoxyamine Hydrochloride for GC Derivatization, LiChropurTM, 97.5-102.5% (AT) | 593-56-6, n.d.*). This step is required to stabilize chemically labile functional groups.

BSTFA (N,O-Bis(trimethylsilyl)trifluoroacetamide) is a derivatization reagent which reacts with hydroxy and amine groups in small metabolites to increase both volatility of the compound and sensitivity of the mass spectrometer (*Bstfa | C₈H₁₈F₃NOSi₂ - PubChem, n.d.*).

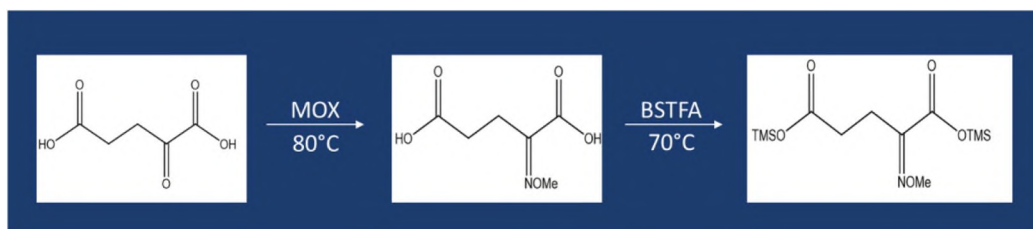


Figure 26: MOX-TMS Derivatization

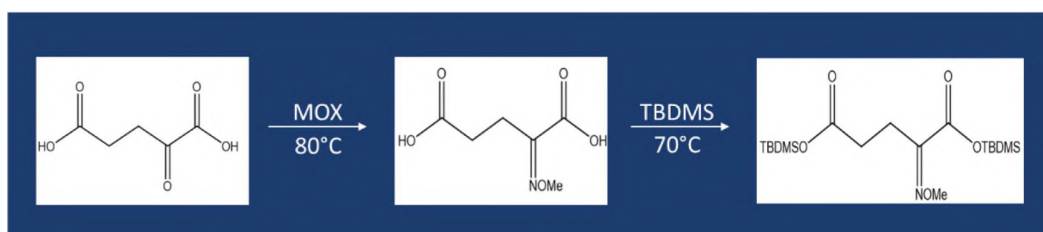


Figure 27: MOX-TBDMS Derivatization

3.2.2 Butyl-Esterification

Butyl-esterification adds a butyl group to the hydroxyl groups of compounds. This allows for classes of compounds such as amino acids and acylcarnitines to be detected as a group due to identical fragmentation patterns, thus increasing the throughput of metabolomics assays.

a. Amino Acids

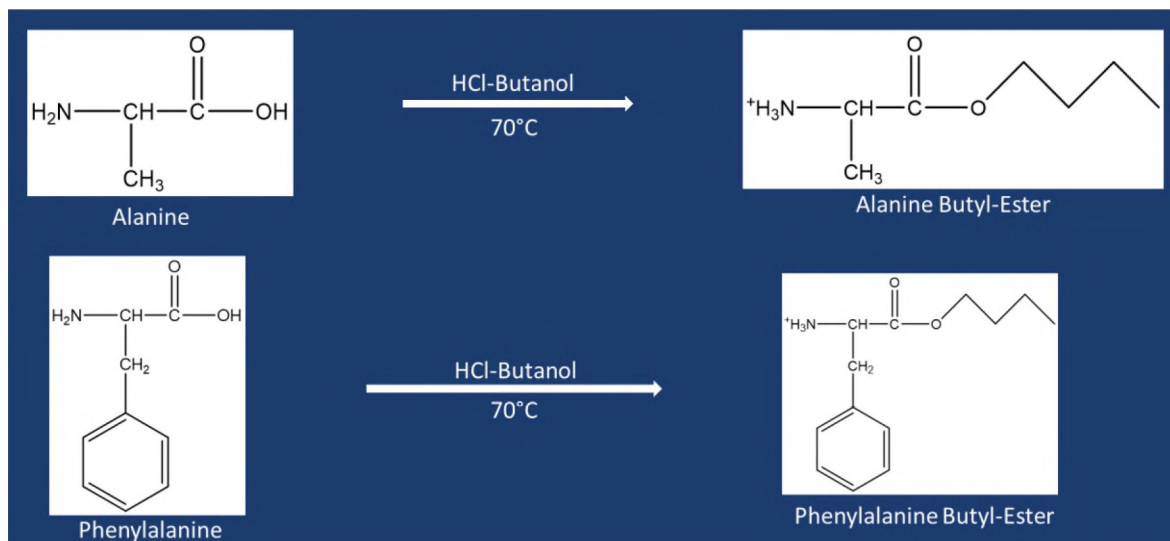


Figure 28: Butyl-Esterification of Amino Acids

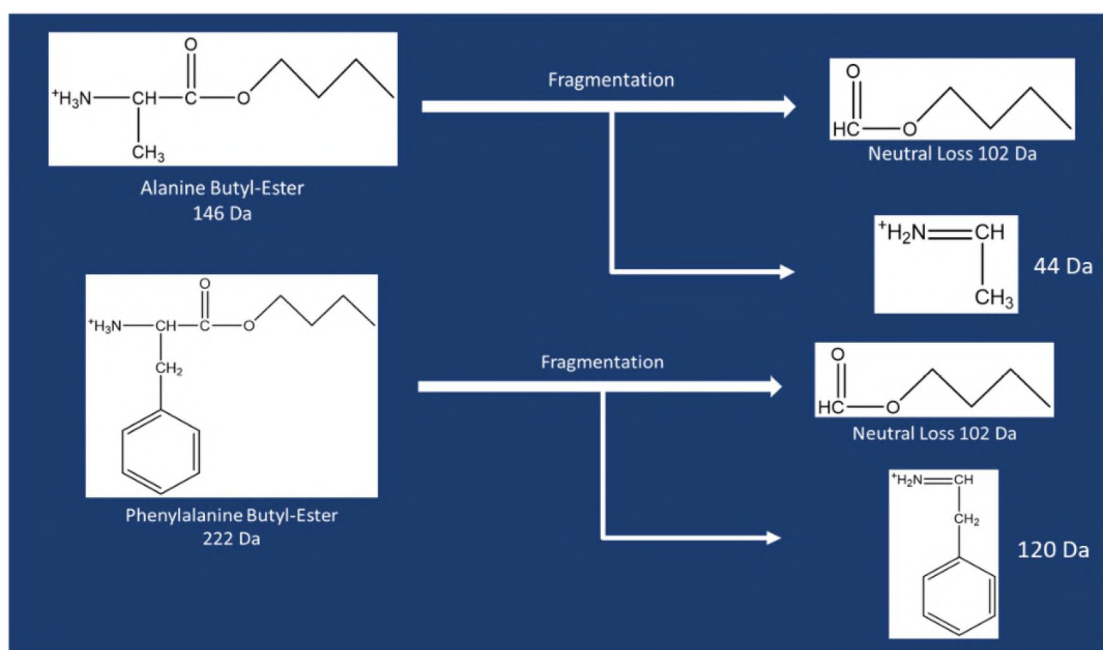


Figure 29: Fragmentation of Amino Acids (Neutral Loss 102 Da)

b. Acylcarnitines

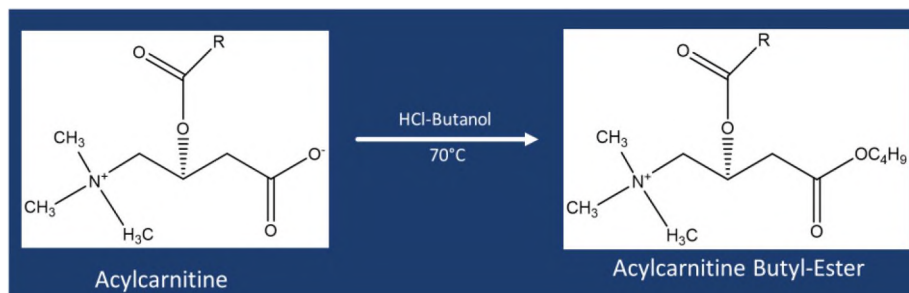


Figure 30: Butyl-Esterification of Acylcarnitines

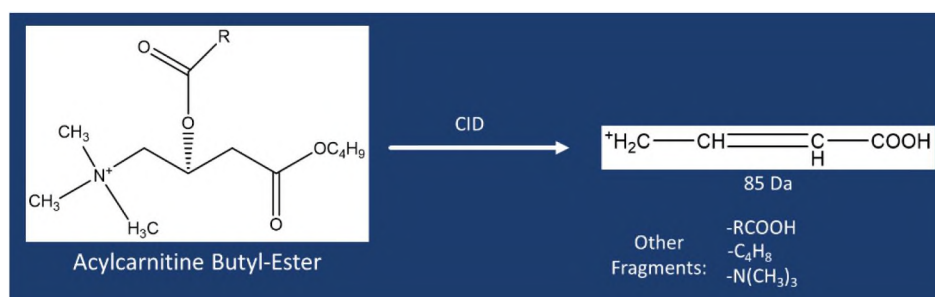


Figure 31: Fragmentation of Acylcarnitines (Precursor Ion 85 Da)

3.3 Mass Spectrometry Assays

We have developed mass spectrometry assays that allow biochemical analysis of small metabolites from iPSC-CMs. The developed assays are highly relevant to the TAZ phenotype. We found that the Bligh-Dyer method was likely to be the most successful method of metabolite extraction, and our extraction method models this well-known method. The assays for small metabolites, citric acid cycle intermediates, amino acids, and acylcarnitines use the same cell harvesting and extraction method and is streamlined to allow for a single extraction to provide material for all analyses at once. The following text describes these assays.

3.3.1 Cell Harvesting and Metabolite Extraction

Materials:

- Labeled amino acids mixture:
 - (Cambridge isotopes laboratories cat.no NSK-A)
 - See note 1 for preparation information
- Labeled acylcarnitines mixture:
 - (Cambridge isotopes laboratories, cat.no NSK-B)
 - See note 2 for preparation information
- Tricarballic acid (Sigma-Aldrich cat.no T53503)
 - Prepare 1 mM in water
- Acetonitrile (VWR, cat.no BDH83640.100E LC/MS grade)
- Chloroform (VWR, cat.no BDH83627 HPLC grade)
- Water (VWR, cat.no BDH23595.100E HPLC grade)
- Phosphate Buffered Saline (PBS), (VWR, cat.no 97063-658)

(Protocols are for 1 well of a 6-well cell culture dish)

Cell Harvesting:

- Place cells on ice and aspirate media
- Wash quickly with ice cold PBS (2x)
- Wash once with ice cold diH₂O
 - *Ensure diH₂O remains on cells for no longer than 30s*
- Add to cell well: 1 mL ice cold ACN
 - Place in freezer: -20c/20 mins

- *White protein precipitate will appear on bottom of cell culture well*
- Add to cell well: 750 uL ice cold diH₂O
 - Scrape cell well, remove harvested cell material to centrifuge tube
- Add to cell well: 1 mL ice cold ACN
 - Place in freezer: -20c/20 mins
- Add to cell well: 750 uL ice cold diH₂O
 - Scrape cell well, remove harvested cell material to same centrifuge tube from first scraping

Metabolite Extraction:

- Add 1 ml cold (-20c) chloroform to each tube
- Vortex and centrifuge: 5,000 rpm/15 minutes
- Ensure clear separation between phases
 - *A clear separation will be observed between the polar (upper) phase, non-polar (lower) phase, and the inter-phase pellet that contains proteins and DNA*
- From the upper polar phase, take an aliquot of 250 mL for acylcarnitines and amino acids assay and transfer to the clean tube.
 - *Label: "Amino Acids and Acylcarnitines".*

- Carefully remove and combine the rest of the upper polar phase with the bottom non-polar phase in a clean tube.
 - *Label: "Small Metabolites by GC/MS".*
- Add 50 mL methanol to the remaining protein pellet.
 - Evaporate solvent under nitrogen stream at room temperature.
 - Reconstitute protein with buffer.
 - Perform protein analysis by protein assay such as Bradford or bicinchoninic acid (BCA).

3.3.2 *Small Metabolite Scan and Citric Acid Cycle Intermediates*

Materials:

- 1 mM Tricarballic Acid in water
- Anhydrous pyridine (Sigma-Aldrich cat.no 270970)
- Methoxyamine hydrochloride (Sigma-Aldrich cat.no 226904)
 - Prepare 20 mg/mL in anhydrous pyridine.
- TMS: N,O-Bis(trimethylsilyl)trifluoroacetamide/BSTFA (Sigma-Aldrich cat.no B-023)

Derivatization:

- Add 100 μ L of 1 mM tricarballic acid to combined polar and non-polar phases (labeled "Small Metabolites by GC/MS").
- Vortex and dry under N₂ at room temperature.
- Add 40 μ L methoxyamine hydrochloride in pyridine (20 mg/mL).

- Cap tubes, vortex and incubate at 80° C for 1 h.
- Cool to the room temperature and add 60 mL TMS
 - Cap tubes, vortex and incubate at 70° C for 30 min.
- Cool to room temperature and transfer to vial for GCMS analysis.

Data analysis. Mass spectra is analyzed by freely available AMDIS software and Fiehn library (Agilent). Identified metabolites are shown in Figure 33. To normalize metabolite levels to the reference standard tricarballic acid (m/z 377 as BSTFA derivative), use the following: use mass spectra to calculate the ratio of peak areas of target metabolites to the reference internal standard (tricarballic acid) and to the total protein amount of each cell pellet as determined by the Bradford assay (Figure 32). The identified small metabolites included amino acids, carbohydrates, fatty acids, and sterols. A full list of identified compounds is included in the appendix.

$$\text{Relative level} = \frac{[\text{Peak area of Metabolite}]}{[\text{Peak area of Reference Standard}]} * \frac{[\text{nmol units of Reference Standard}]}{[\text{Protein Amount}]}$$

Figure 32: Equation for Determining Metabolite Levels in hiPSC-CM

Small Metabolite Scan	
Ion Source	EI (Electron Ionization)
Source Temperature	280°C
Quad Temperature	150°C
Fixed Electron Energy	70eV
Acquisition Type	Scan
Injection Volume	1 µL
Solvent Delay	6 min
Column	HP-5MS 5% Phenyl Methyl Silox (30 m x 250 µm x 0.25µm)
Mode	Splitless
Time Program	
Initial Setpoint	80°C (hold 3 min)
Ramp	15°C/min
Stop	305°C (hold 3 min)

Table 9: GC-MS Parameters for Small Metabolites

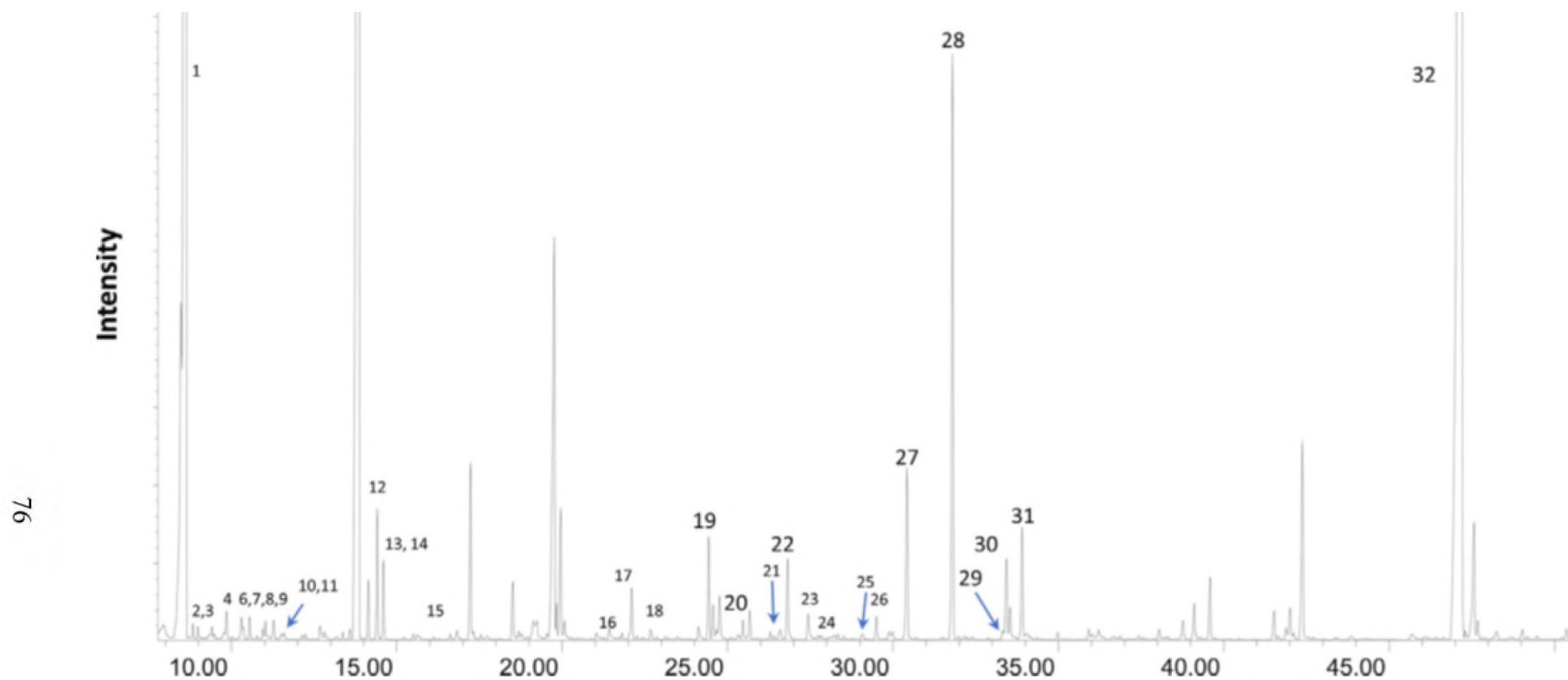


Figure 33: Small Metabolite Scan by GC-MS. (1) Lactate, (2) Glycolic acid, (3) valine, (4) alanine, (5) leucine, (6) 3-hydroxybutyric acid, (7) proline, (8) isoleucine, (9) serine, (10) octanoic acid, (11) glycine, (12) succinate, (13) fumarate, (14) threonine, (15) methionine, (16) aspartic acid, (17) malate, (18) glutamic acid, (19) glycerol-1-phosphate, (20) ornithine, (21) isocitrate (22) citrate, (23) tyrosine, (24) lysine, (25) ascorbic acid, (26) palmitoleic acid (27) palmitic acid, (28) inositol, (29) linoleic acid (30) oleic acid, (31) stearic acid, (32) cholesterol. See Appendix for a full list of detected metabolites.

TCA Cycle Intermediates		
Ion Source	EI (Electron Ionization)	
Source Temperature	280 °C	
Quad Temperature	150 °C	
Fixed Electron Energy	70 eV	
Acquisition Type	SIM (Selected Ion Monitoring)	
Injection Volume	1 uL	
Solvent Delay	4 min	
Column	HP-5MS 5% Phenyl Methyl Silox (30 m x 250 um x 0.25 um)	
Mode	Splitless	
Time Program		
Initial Setpoint	80 °C (hold 3 min)	
Ramp	15 °C/min	
Setpoint	205 °C (hold 0 min)	
Ramp	10°C/min	
Setpoint	220°C (hold 0 min)	
Ramp	15°C/min	
Stop	305°C (hold 3 min)	
Selected Ion Monitoring		
Compound	Ion	Retention Time
Succinate	247	7.3
Fumarate	245	7.4
Malate	233	8.9
α-ketoglutarate	304	9.6
Tricarballic acid	377	10.8
Aconitate	229	10.9
Citrate/Isocitrate	273/245	11.4

Table 10: GC-MS Parameters for Citric Acid Cycle Intermediates

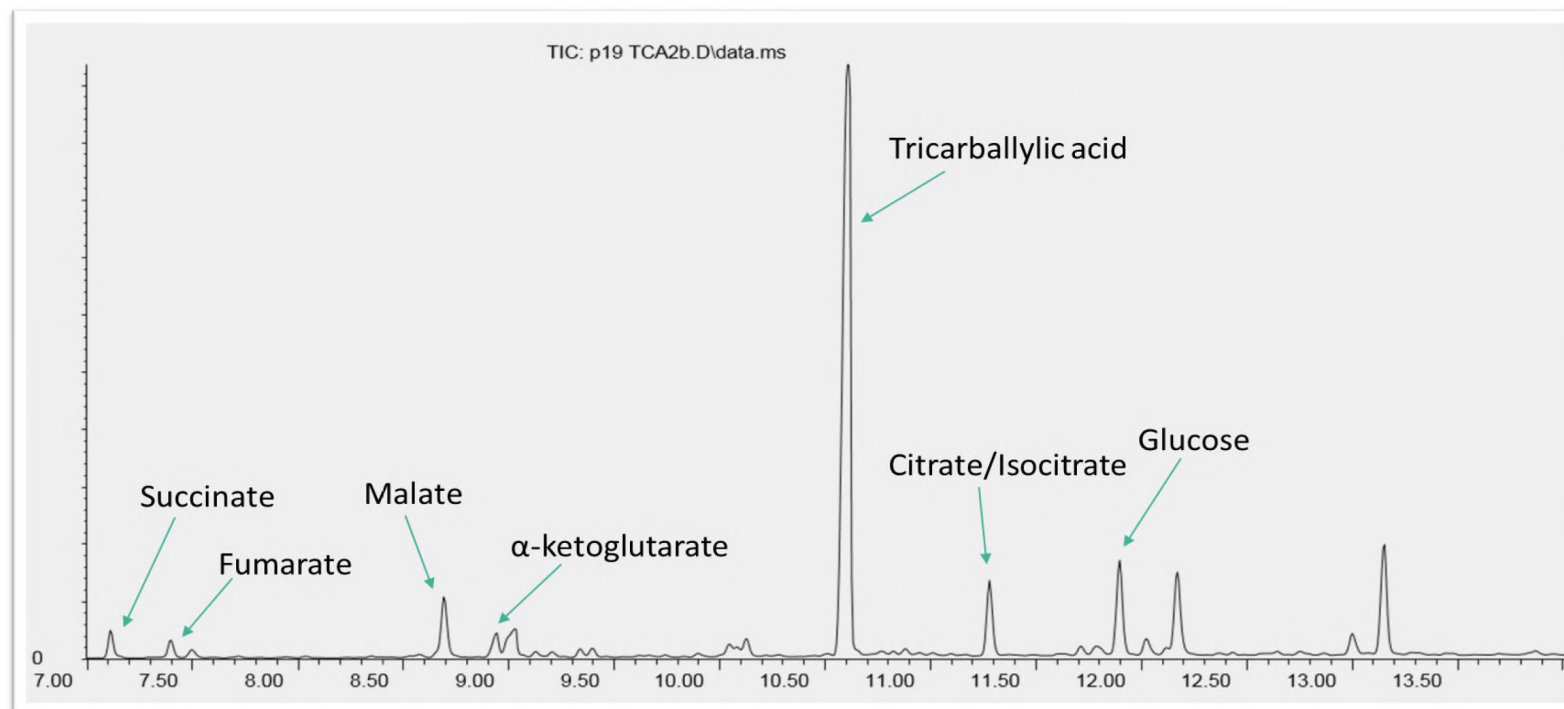


Figure 34: Citric Acid Cycle Intermediates via GC-MS

3.3.3 *Amino Acids and Acylcarnitines*

Materials:

- 3N HCl n-Butanol (Sigma-Aldrich, cat.no 87472)
- Mobile phase for flow infusion:
 - 10% Water (0.1% Formic acid)
 - 90% Acetonitrile (0.1% Formic acid)
- LC inline filter (VWR cat.no 97013-134)

Derivatization:

- Add internal standards working solutions to polar phase labeled "Amino Acids and Acylcarnitines":
 - 50 uL amino acids (NSK-A)
 - 100 uL acylcarnitines (NSK-B)
- Dry under N₂ at room temperature.
- To the dried sample add 60 mL HCl-n-Butanol
 - Cap tubes and incubate at 65 °C for 30 min.
- Cool to room temperature and dry again.
- Reconstitute with 100 uL of mobile phase and transfer to vials for the analysis.

HPLC parameters:

- Introduce derivatized samples directly by the injection to the mass spectrometer instrument through the inline filter with no chromatographic separation:
 - Keep inline filter in HPLC oven at 32 °C.
 - Using isocratic flow inject samples for 1.8 min:
 - Amino Acids: 0.075 mL/min

- Acylcarnitines: 0.090 mL/min

MS/MS-tandem mass spectrometer:

- Use following tandem mass spectrometry scans for the high throughput:
 - Acylcarnitines:
 - Precursor ion scan at m/z 85 (Table 6 and Figure 35).
 - Amino acids:
 - Neutral loss (NL 102, NL 119, NL 56), and single reaction monitoring (SRM) m/z 231.1-m/z 70.1 for arginine (Table 7).

Data analysis:

- Perform data analysis by Chemoview 2.2 software (SCIEX) or comparable software. Calculate peak areas at 50% peak height.

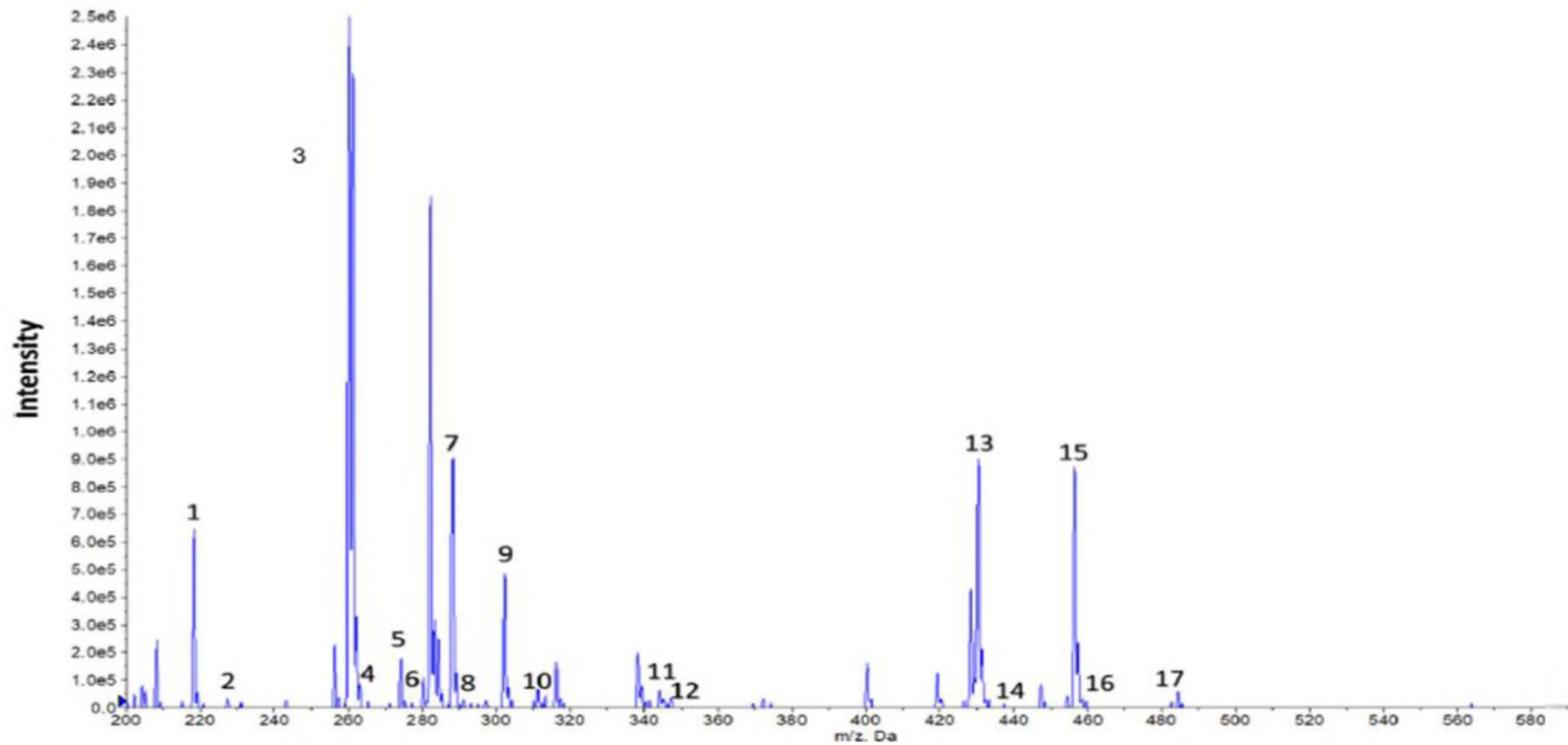


Figure 35: Acylcarnitines Assay: representative precursor ion scan (m/z 85) profile. (1) Free carnitine (C0), (2) C0 ISTD, (3) C2, (4) C2 ISTD, (5) C3, (6) C3 ISTD, (7) C4, (8) C4 ISTD, (9) C5, (10) C5 ISTD, (11) C8, (12) C8 ISTD, (13) C14, (14) C14 ISTD, (15) C16, (16) C16 ISTD, (17) C18. See Table 11 for full list of Acylcarnitines detected.

Acylcarnitines		
Mode of Separation	None – Flow Infusion	
Column	Inline filter	
Oven Temperature	37°C	
Mobile Phase	90% ACN in H ₂ O (0.1% Formic acid)	
Flow Rate	0.075 mL/min isocratic flow	
Mode of Analysis	Precursor Ion Scan	
Abbreviation	Parent Ion (m/z)	Daughter Ion (m/z)
C0	218	85
C0 ISTD	227	85
C2	260	85
C2 ISTD	263	85
C3	274	85
C3 ISTD	277	85
C4	288	85
C4 ISTD	291	85
C5:1	300	85
C5	302	85
C4OH	304	85
C5 ISTD	311	85
C6	316	85
C5OH	318	85
C8:1	342	85
C8	344	85
C8 ISTD	347	85
C3DC	360	85
C10:2	368	85
C10:1	370	85
C10	372	85
C4DC	374	85
C5DC	388	85
C12	400	85
C6DC	402	85
C14:1	426	85
C14	428	85
C14 ISTD	437	85
C16	456	85
C16 ISTD	459	85
C16OH	472	85
C18:1	482	85
C18	484	85
C18:1OH/C18:2OH	498	85
C18OH	500	85

Table 11: LC-MS/MS Parameters for FIA of Acylcarnitines.

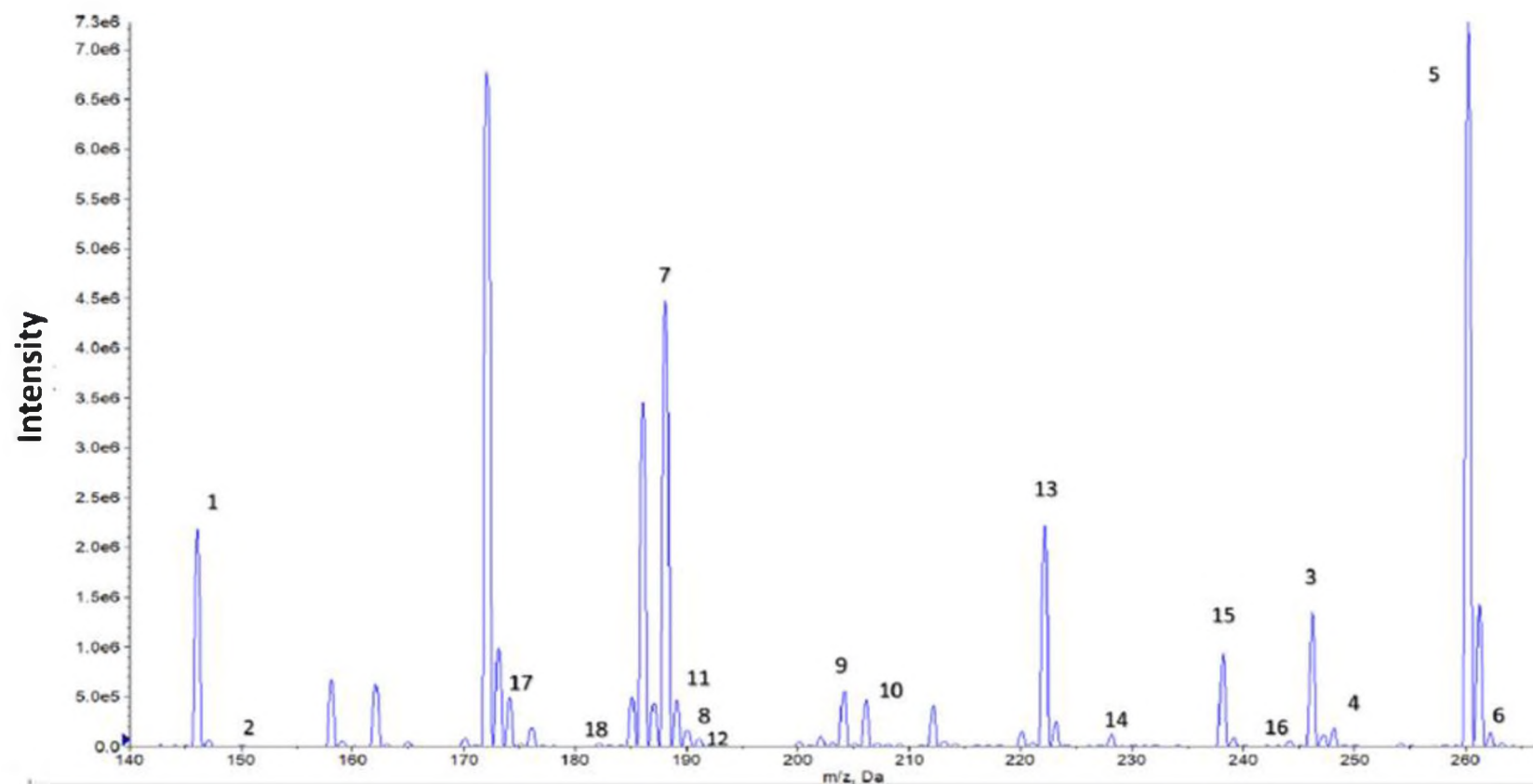


Figure 36: Amino Acids Analysis: representative m/z profile of NL 102 scan (1) alanine, (2) alanine ISTD, (3) aspartic acid, (4) aspartic acid ISTD, (5) glutamic acid (6) glutamic acid ISTD, (7) leucine/isoleucine, (8) leucine/isoleucine ISTD, (9) methionine, (10) methionine ISTD, (11) ornithine, (12) ornithine ISTD, (13) phenylalanine, (14) phenylalanine ISTD, (15) tyrosine, (16) tyrosine ISTD, (17) valine, (17) valine ISTD.

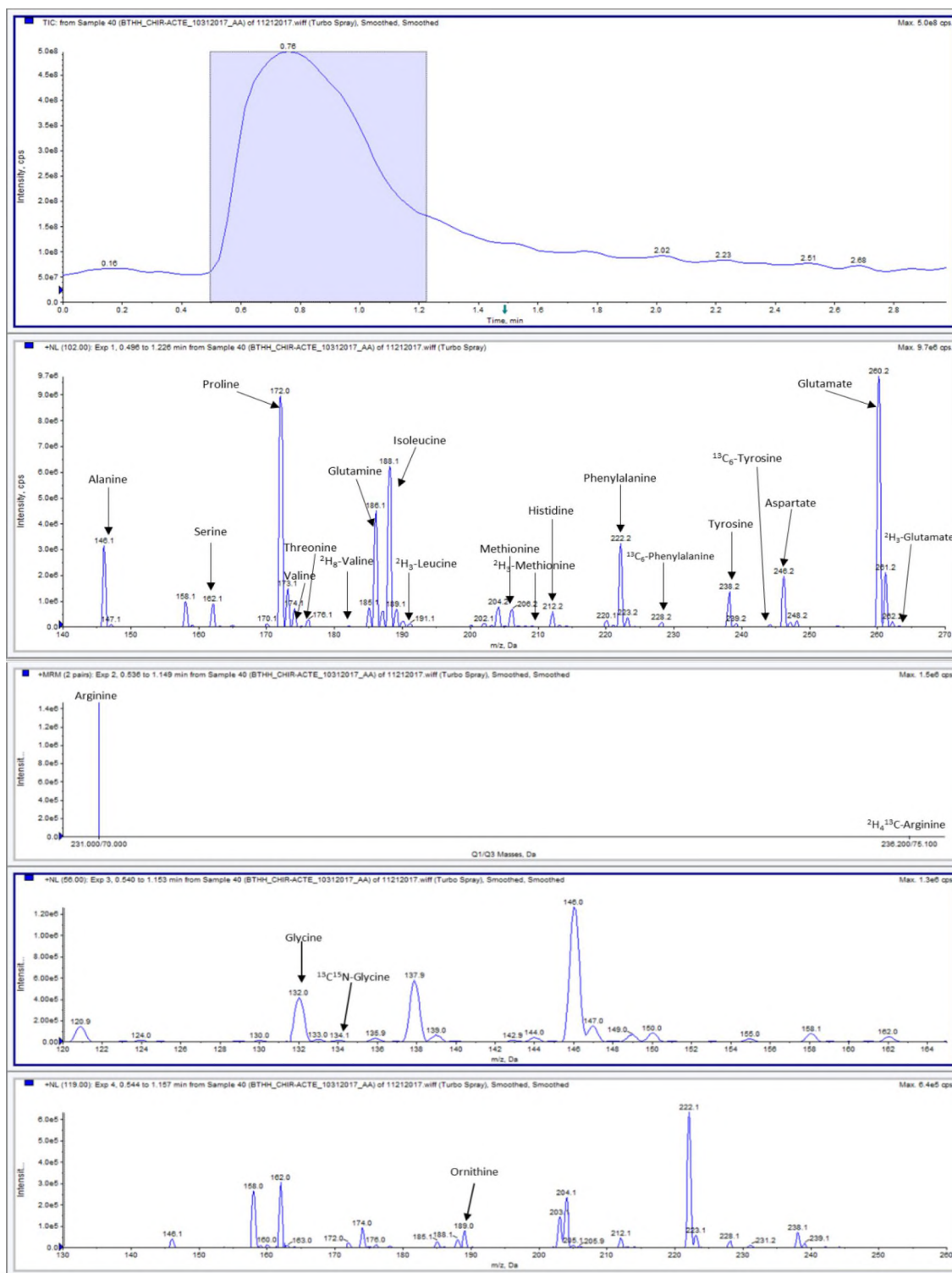


Figure 37: LC-MS/MS spectra of amino acids detected in hiPSC-CMs
 (See table 12 for list of amino acids detectable in hiPSC-CMs.)

Amino Acids		
Mode of Separation	None – Flow Infusion	
Column	Inline filter	
Oven Temperature	37°C	
Mobile Phase	90% ACN in H ₂ O (0.1% Formic acid)	
Flow Rate	0.090 mL/min isocratic flow	
Mode of Analysis	Neutral Loss Scan	
Amino Acid	Parent Ion (m/z)	Fragment Size (m/z)
Alanine	146	102
² H ₄ -Alanine	150	102
Serine	162	102
Proline	172	102
Valine	174	102
Threonine	176	102
² H ₈ -Valine	182	102
Glutamine	186	102
Leucine/Isoleucine	188	102
² H ₃ -Leucine	191	102
Methionine	206	102
² H ₃ -Methionine	209	102
Histidine	212	102
Phenylalanine	222	102
¹³ C ₆ -Phenylalanine	228	102
Tyrosine	238	102
¹³ C ₆ -Tyrosine	244	102
Aspartic Acid	246	102
² H ₃ -Aspartic Acid	249	102
Glutamic Acid	260	102
² H ₃ -Glutamate	263	102
Ornithine	189	119
² H ₂ -Ornithine	191	119
Citrulline	232	119
² H ₂ -Citrulline	234	119
Glycine	132	56
¹⁵ N; 2- ¹³ C-Glycine	134	56
Mode of Analysis	Multiple Reaction Monitoring	
Amino Acid	Precursor Ion (m/z)	Product Ion (m/z)
Arginine	231	70
² H ₄ ; 5- ¹³ C-Arginine	236	75

Table 12: LC-MS/MS Parameters for FIA of Amino Acids.

Note #1: Preparation of working solution NSK-A. Internal standard vial contains labeled standards for amino acids. For the stock solution, reconstitute dry powder in vial with 2 mL of water:methanol (1:1 v%/v%). Complete reconstitution of the contents of one vial in 2 mL produces stock solution of following metabolites. Alanine (2,3,3,3-²H₄) 250 nmol/mL, L-Phenylalanine (ring-¹³C₆) 250 nmol/mL, L-Leucine (5,5,5-²H₃) 250 nmol/mL, L-Valine (²H₈) 250 nmol/mL, L-Arginine: HCl (5-¹³C; 4,4,5,5-²H₄) 250 nmol/L, L-Citrulline (5,5-²H₂) 250 nmol/mL, L-Tyrosine (ring-¹³C₆) 250 nmol/mL, L-Ornithine: HCl (5,5-²H₂) 250 nmol/mL, L-Methionine (methyl-²H₃) 250 nmol/mL, DL-Glutamic Acid (2,4,4-²H₃) 250 nmol/mL, L-Aspartic Acid (2,3,3-²H₃) 250 nmol/mL, Glycine (2-¹³C; ¹⁵N) 500 nmol/mL. For the working solution-dilute stock solution 1:10 in methanol. Add 50 uL of the working solution to the cell lysate.

Note #2: Preparation of working solution NSK-B. Internal standard vial contains labeled acylcarnitines standards. For the stock solution, reconstitute dry powder in vial with 2 mL of methanol. Complete reconstitution of the contents of one vial in 2 mL produces stock solution of following metabolites: Free carnitine (76 nmol/mL), ²H₃-Acetylcarnitine (19 nmol/mL), ²H₃-Propionylcarnitine (3.8 nmol/mL), ²H₃-Butyrylcarnitine (3.8 nmol/mL), ²H₉-Isovalerylcarnitine (3.8 nmol/mL), ²H₃-Octanoylcarnitine (3.8 nmol/mL), ²H₉-Myristoylcarnitine (3.8 nmol/mL), ²H₃-Palmitoylcarnitine (7.6 nmol/mL). For the working solution-dilute stock solution 1:106 in methanol. Add 100 uL of the working solution to the cell lysate.

3.4 Conclusion

In this section, mass spectrometry assays were developed specifically to extract and to analyze a variety of metabolites from hiPSC-CM cells. This step provides a novel and

innovative way of measuring many small metabolites in hiPSC-CM cell culture. The project is technically innovative in a few ways: This has not previously been established as a way of biochemical characterization of a BTHS model derived from hiPSCs. Furthermore, hiPSC-CM is a very challenging cell culture. To the date of the developed protocols there were no published extraction and mass spectrometry protocols specifically optimized for this type of cells. The assays developed include small metabolites (GC-MS), Citric Acid Cycle Intermediates (GC-MS), Amino Acids (LC-MS/MS), and Acylcarnitines (LC-MS/MS). These developed assays build foundation for future hiPSC-CM metabolic studies and will be used as a tool to characterize Barth syndrome hiPSC-CM cellular model.

CHAPTER IV

RANOLAZINE STUDY

In collaboration with the University of Kentucky, this study used ^1H -NMR-assisted metabolomics to develop workflows that can be applied to study the metabolic effect of the anti-angina agent Ranolazine (RanexaTM) on induced pluripotent stem cell-derived cardiomyocytes (hiPSC-CMs). We also used data from non-treated hiPSC-CMs to identify potential targets for a more targeted and hypothesis-based future analysis.

4.1 Ranolazine

Ranolazine (RanexaTM) is an anti-angina agent used to treat chest pressure, pain, and discomfort due to lack of oxygen being supplied to the tissue. This is achieved by lowering the oxygen requirement for the heart. The exact mechanism of action of Ranolazine is not completely understood. So far, researchers know that the drug effect causes an increase in the amount of active pyruvate dehydrogenase (Fillmore & Lopaschuk, 2013). This leads to a shift of cardiac metabolism towards glucose oxidation and away from fatty acid oxidation (Bhandari & Subramanian, 2007), which then causes an increase in the ATP:O₂ ratio. This essentially lowers the heart's demand for oxygen. It has been shown that there is no overall increase in the amount of glycolysis within the heart during

Ranolazine treatment, yet there is an increase in glucose oxidation (McCormack et al., 1996). This indicates that the other forms of glucose oxidation are remaining coupled to glycolysis (Fillmore & Lopaschuk, 2013), and is demonstrated by a lack of lactate, H^+ , and fatty acid buildup in the tissue. This is why Ranolazine is able to decrease chest pressure and pain without having buildup of toxic metabolites, yet the exact mechanism by which the Ranolazine drug acts has yet to be determined (McCormack et al., 1996).

Our rationale to use Ranolazine is based on fact that BTHS affected individuals exhibit lactic acidosis and our model TAZ-hiPSC-CM exhibited increased lactate production (Fatica et al., 2019). Thus, we hypothesized that by increasing pyruvate dehydrogenase (PDH) activity and glucose oxidation using Ranolazine, there will be a positive metabolic effect on TAZ-hiPSC-CM. Specifically, we hypothesized that Ranolazine will decrease lactate levels and increase ATP levels in our model.

The goal of our study was to develop extraction protocol followed by application of untargeted 1H -NMR assisted metabolic profiling (1) to demonstrate technical feasibility of the workflow in hiPSCM and (2) to identify potential metabolic targets for future more targeted studies. This will provide additional insight as to whether Ranolazine has a beneficial effect in TAZ-iPSC-CM. Final goals of the project will be accomplished by analyzing the difference in metabolite levels between wild type and BTHS (TAZ) hiPSC-CMs, and by then analyzing the difference of TAZ mutant hiPSC-CMs when treated with Ranolazine.

4.2 Methods

hiPSC-CM were derived from the differentiation of control (PGP1-TAZ^{WT}) and TAZ mutant (PGP1-TAZ^{517delG}) induced pluripotent stem cells. Stem cells were

differentiated using the CHIR-Activin E/IWR differentiation protocol (see Chapter II) into hiPSC-derived cardiomyocytes. hiPSC-CM were incubated with 100 mM Ranolazine drug for 1 hour, and aliquots of medium from the cell culture well were taken at designated intervals to be used for analysis. After the 1-hour incubation period with Ranolazine, cells were harvested using the method described in Chapter III. Untargeted ^1H -NMR-assisted metabolomics for polar metabolites was performed at the University of Kentucky. Since this experiment represents a pilot and feasibility study, $n=2$ of each experimental condition was used:

- PGP1-TAZ^{WT} not treated with Ranolazine ($n=2$)
- PGP1-TAZ^{WT} treated with Ranolazine ($n=2$)
- PGP1-TAZ^{517delG} not treated with Ranolazine ($n=2$)
- PGP1-TAZ^{517delG} treated with Ranolazine ($n=2$)

^1H -NMR was performed on a Bruker Avance III 16.45 T spectrometer. Measurements from each timepoint were combined into a single measurement of analyte that was present in the cell culture media over the course of the 1 hour in which the cells were treated with Ranolazine.

^1H -NMR is capable of distinguishing unknown molecules from matrices which may be complex or undefined, and it is quantitative and highly reproducible. ^1H -NMR, or nuclear magnetic resonance spectroscopy, works by subjecting the sample to a magnetic field. NMR signals were assigned according to in-house databases. Metabolites were quantified by peak integration and comparison with the internal standard sodium trimethylsilylpropanesulfonate (DSS) with corrections for partial

saturation. The classes of compounds which were detected and identified in this study include:

- Glycolysis Intermediates
- Citric Acid Cycle Intermediates
- Pentose Phosphate Pathway Intermediates
- Sugar Phosphates
- Nucleotides/Hexose Amines
- Miscellaneous compounds

Semi-quantitative comparisons were made in the measured metabolites as the fold change of TAZ^{517delG}-hiPSC-CMs vs. TAZ^{WT}-hiPSC-CMs in order to evaluate the effect of the BTHS (TAZ) mutation on the metabolism of the hiPSC-CMs. The next comparison involved both groups of cells as Nontreated vs. Treated hiPSC-CMs in order to evaluate the effect of Ranolazine on the cellular metabolism in both the presence and absence of the BTHS (TAZ) mutation. Threshold was defined at a cutoff of 1.5 and above for increased levels and 0.5 and below for decreased levels.

Keeping with the general workflow of metabolomics studies, ‘metabolites of interest’ were identified for each class. These will provide possible new therapeutic targets and treatment outcome targets for Ranolazine therapy.

4.3 TAZ^{517delG} vs. TAZ^{WT}-hiPSC-CMs (BTHS vs. Control) (Cell Media ¹H-NMR)

Glycolysis (BTHS vs. WT)

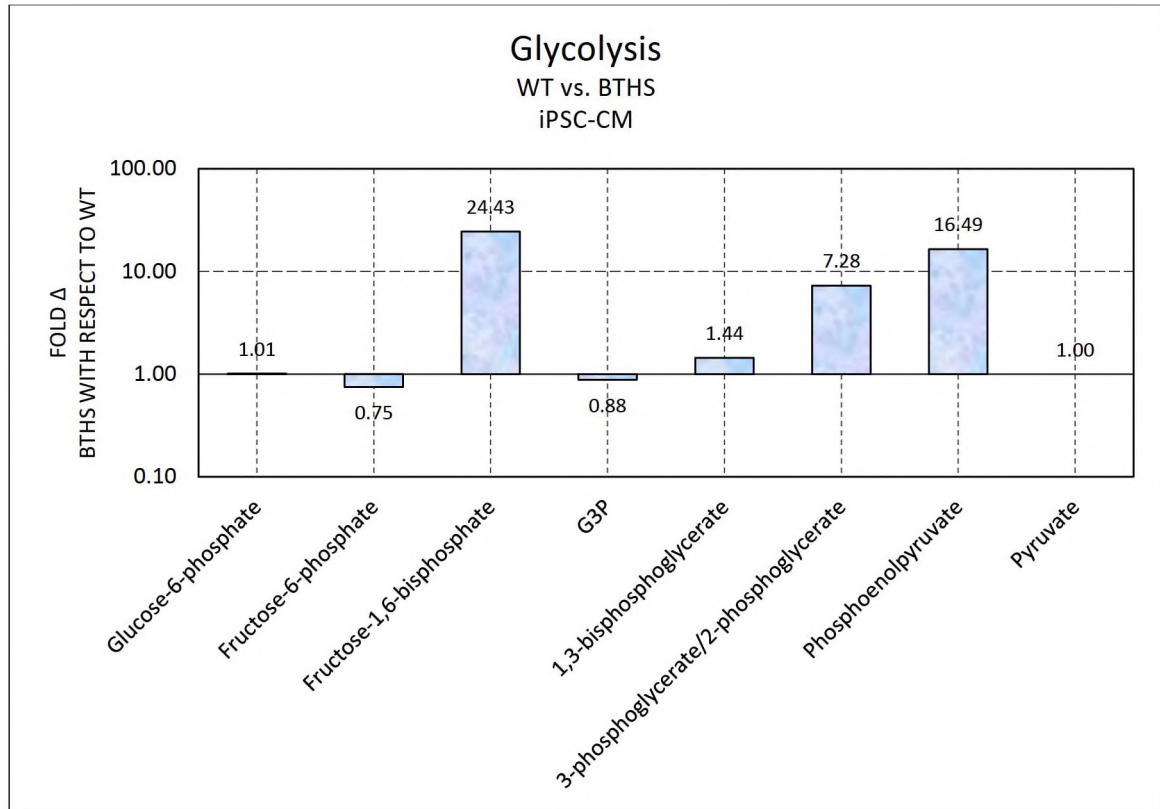


Figure 38: Glycolysis Intermediates in BTHS hiPSC-CMs with respect to WT hiPSC-CMs (cell media)

Potential targets for future studies:

- Fructose-1,6-bisphosphate
- 3-phosphoglycerate/2-phosphoglycerate
- Phosphoenolpyruvate

In BTHS iPSC-CM, there is an overall increase in glycolysis intermediates. This is expected, as the heart will increase glycolysis in order to compensate for disturbed fatty acid oxidation.

Citric Acid Cycle (BTHS vs. WT)

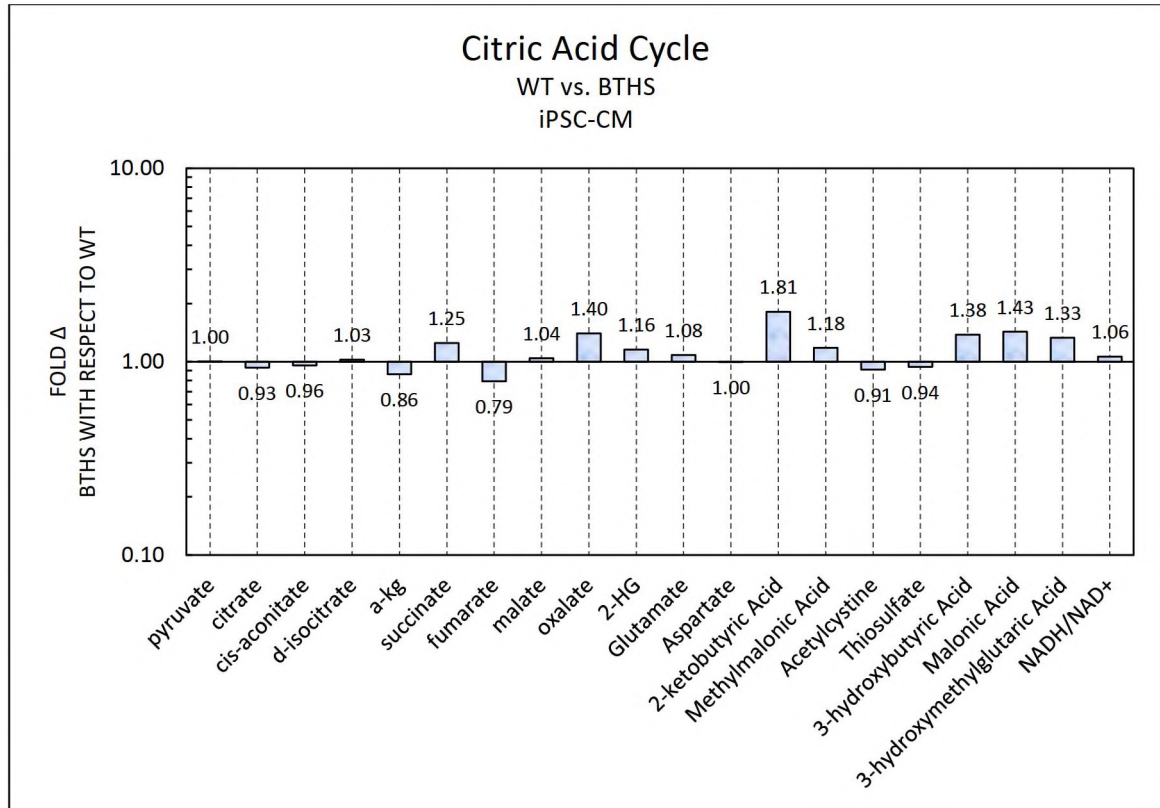


Figure 39: Citric Acid Cycle Intermediates in BTHS hiPSC-CMs with respect to WT hiPSC-CMs (cell media)

Potential targets for future studies:

- 2-ketobutyric Acid
- N-Acetyl-L-Aspartate

Pentose Phosphate Pathway (BTHS vs. WT)

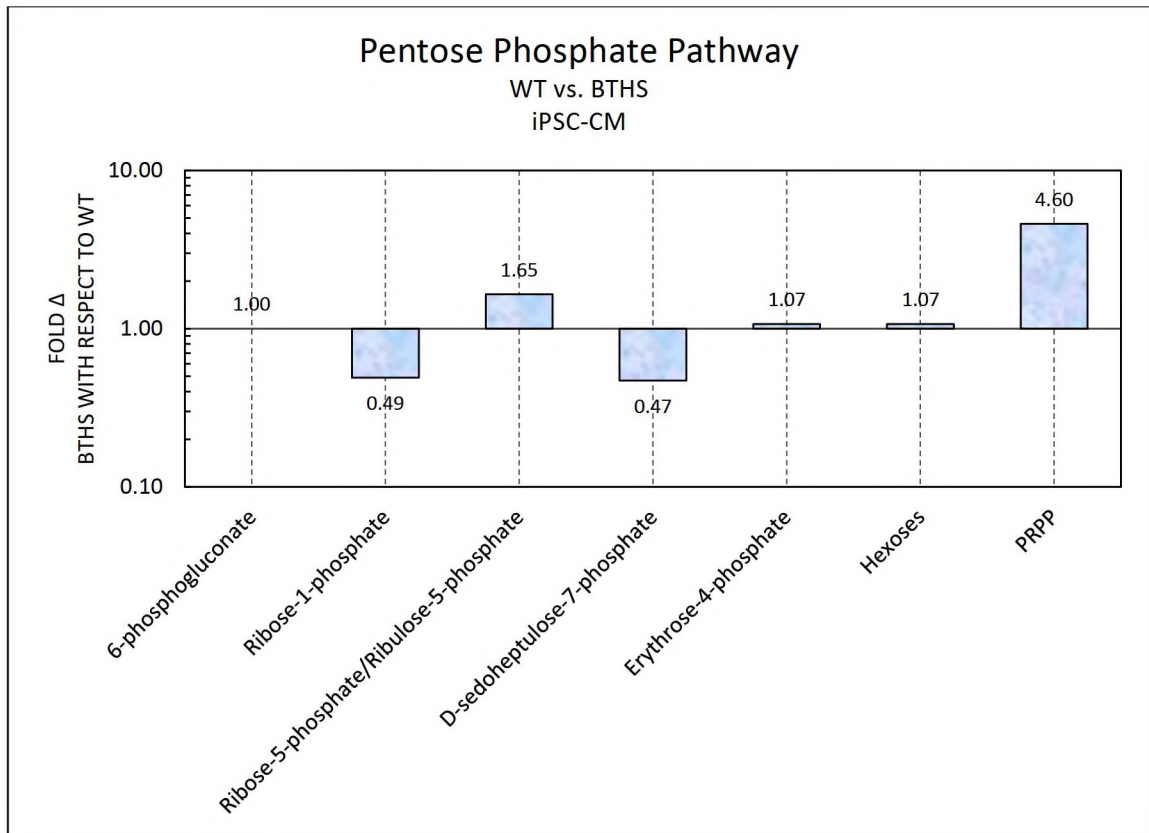


Figure 40: Pentose Phosphate Pathway Intermediates in BTHS hiPSC-CMs with respect to WT hiPSC-CMs (cell media)

Potential targets for future studies:

- Ribose-5-phosphate/Ribulose-5-phosphate
- PRPP

Sugar Phosphates (BTHS vs. WT)

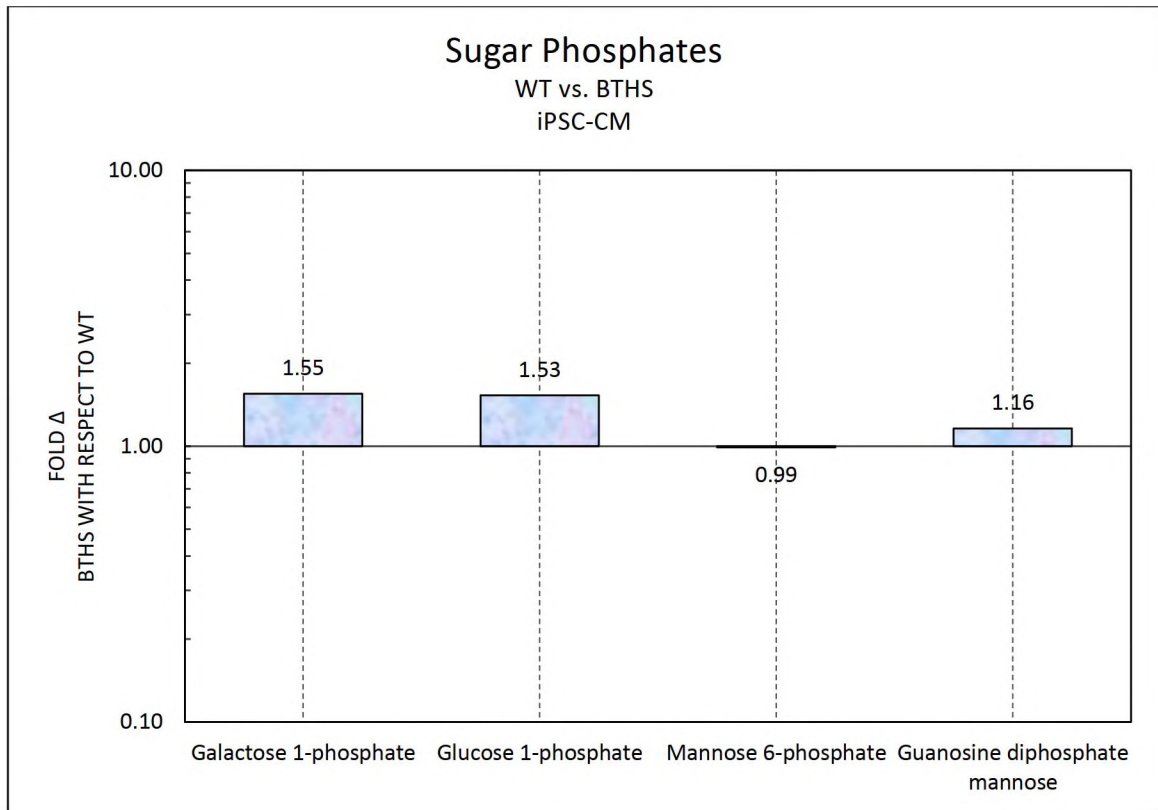


Figure 41: Sugar Phosphates in BTHS hiPSC-CMs with respect to WT hiPSC-CMs (cell media)

Potential targets for future studies:

- Galactose-1-phosphate
- Glucose-1-phosphate

Nucleotides/Hexose Amines (BTHS vs. WT)

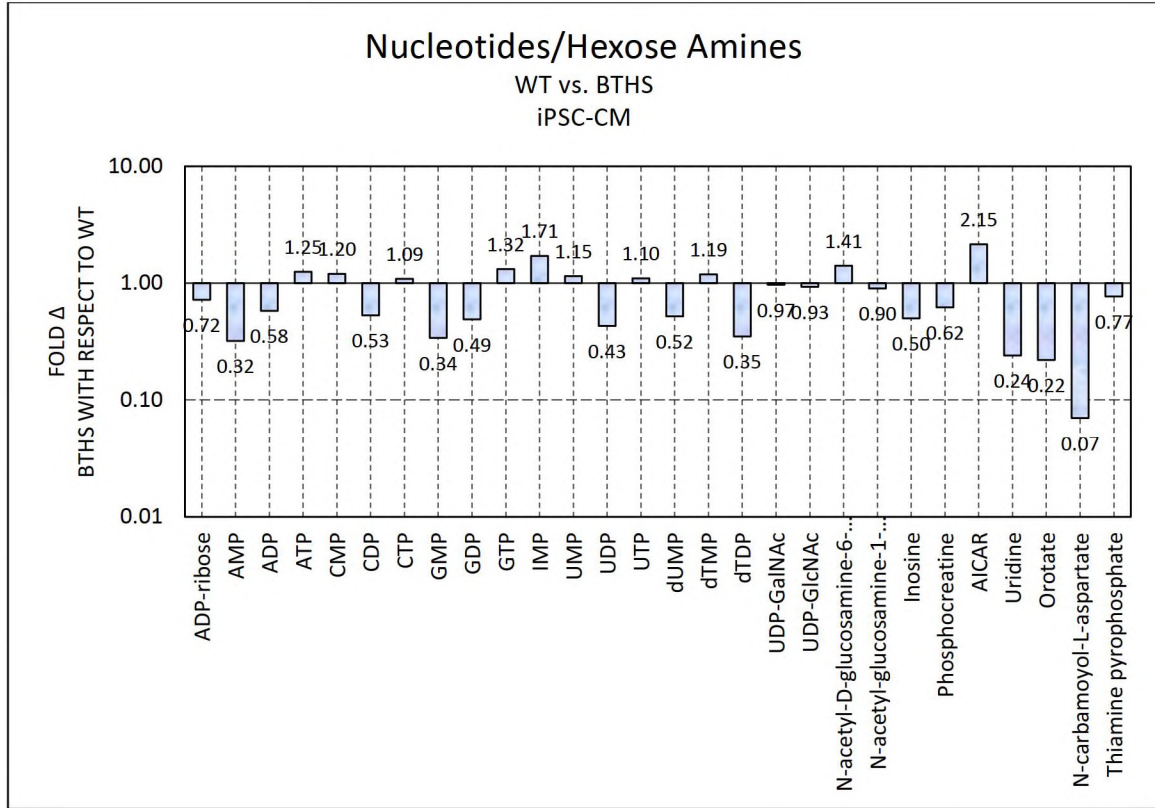


Figure 42: Nucleotides/Hexose Amines in BTHS hiPSC-CMs with respect to WT hiPSC-CMs (cell media)

Potential targets for future studies:

- AMP
- GMP
- GDP
- IMP
- UDP
- dTDP
- Inosine
- AICAR (5-Aminoimidazole-4-carboxamide ribonucleotide)
- Uridine
- Orotate
- N-carbamoyl-L-aspartate

These findings are in agreement with a study which found via statistical analysis of their metabolomics measurements that tRNA synthesis pathway is a site of significant disruption in BTHS patients and can be used to differentiate BTHS subjects from non-diseased subjects (Sandlers et al., 2016).

Miscellaneous Metabolites (BTHS vs. WT)

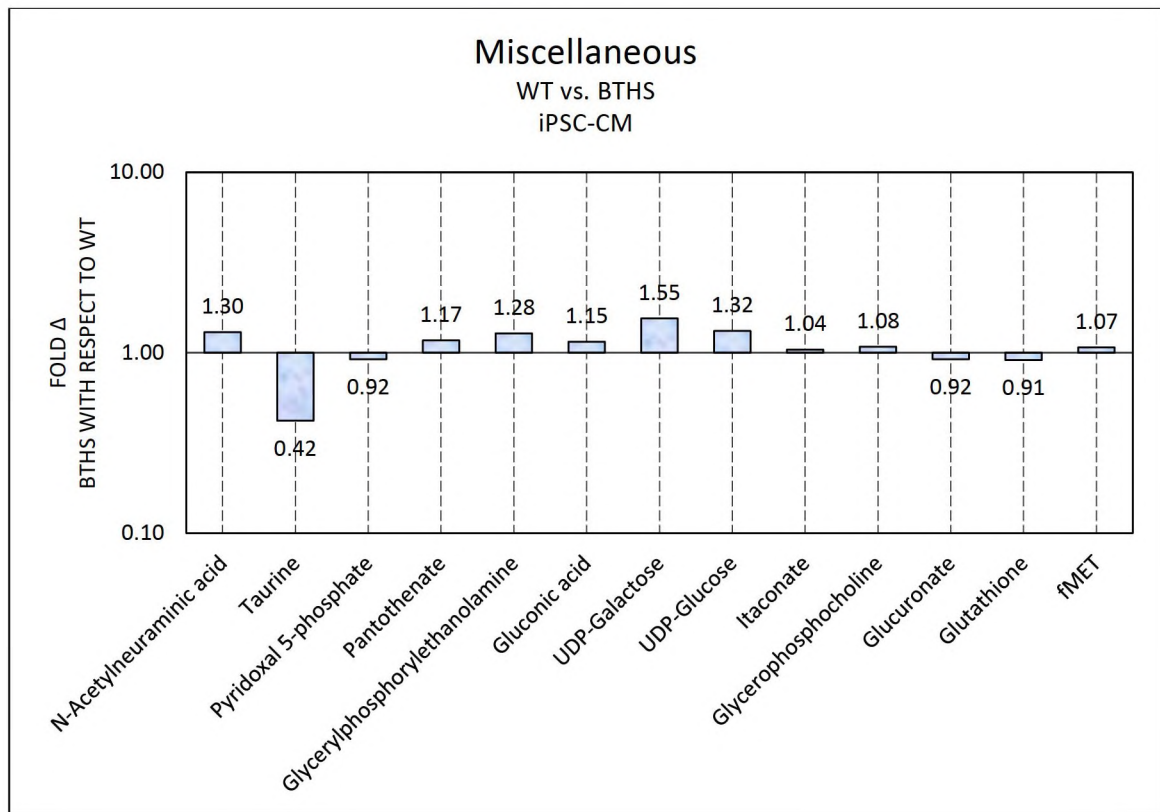


Figure 43: Miscellaneous Metabolites in BTHS hiPSC-CMs with respect to WT hiPSC-CMs (cell media)

Potential targets for future studies:

- Taurine
- UDP-Galactose

Taurine has been shown in previous BTHS studies to be decreased in BTHS patients, so this finding is in agreement with those studies (Oates et al., 2020).

4.4 Ranolazine-treated vs. Control TAZ^{517delG}-hiPSC-CMs (cell media - ¹H-NMR)

Glycolysis (BTHS hiPSC-CM Treated with Ranolazine)

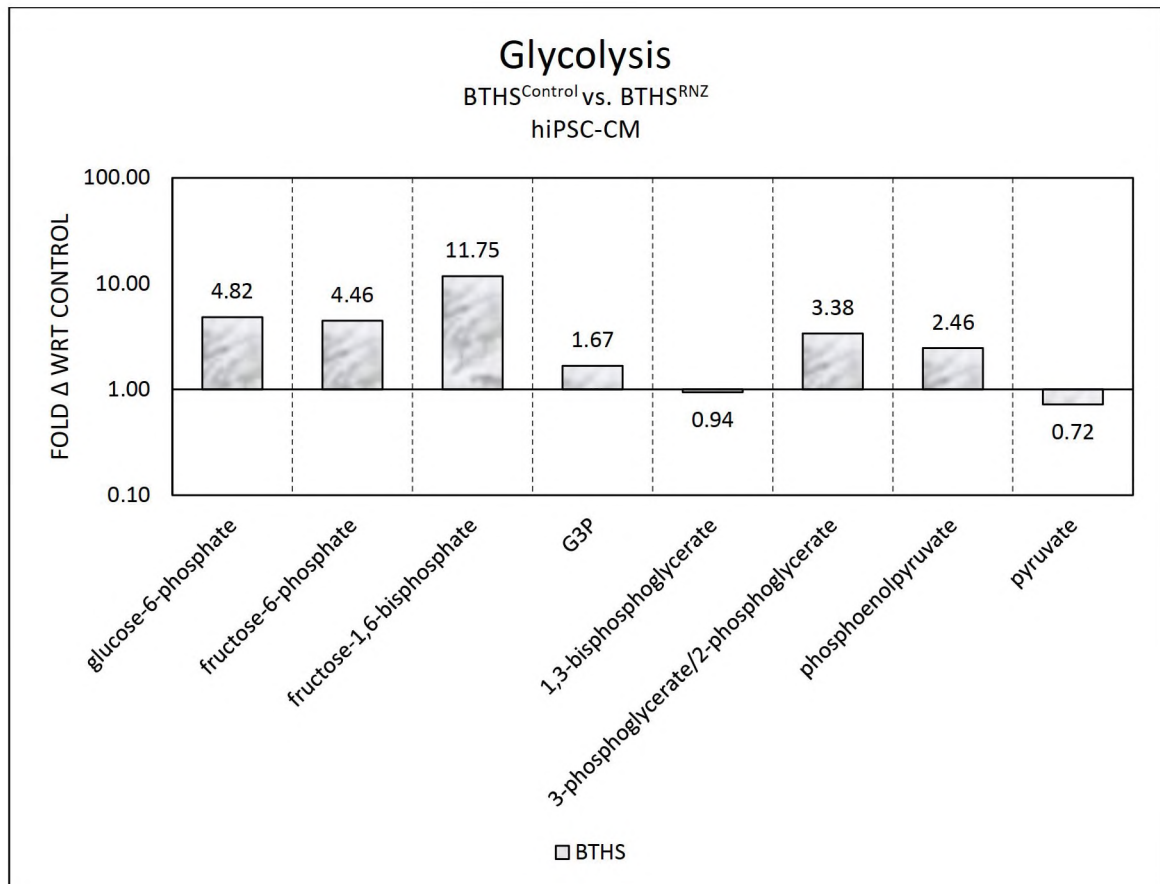


Figure 44: Glycolysis Intermediates in BTHS hiPSC-CMs treated with 100 mM Ranolazine with respect to Non-treated BTHS hiPSC-CMs (cell media)

Potential targets for future studies:

- Glucose-6-phosphate
- Fructose-6-phosphate
- Fructose-1,6-bisphosphate
- G3P
- 3PG/2PG
- Phosphoenolpyruvate

Expectedly, there is an overall increase in glycolysis intermediates in BTHS hiPSC-CM treated with Ranolazine with respect to BTHS hiPSC-CM not treated with Ranolazine. This aligns with our expected results and demonstrates that Ranolazine increases glucose oxidation in hiPSC-CM to alleviate some of the oxygen demand of the heart.

Citric Acid Cycle (BTHS hiPSC-CM treated with Ranolazine)

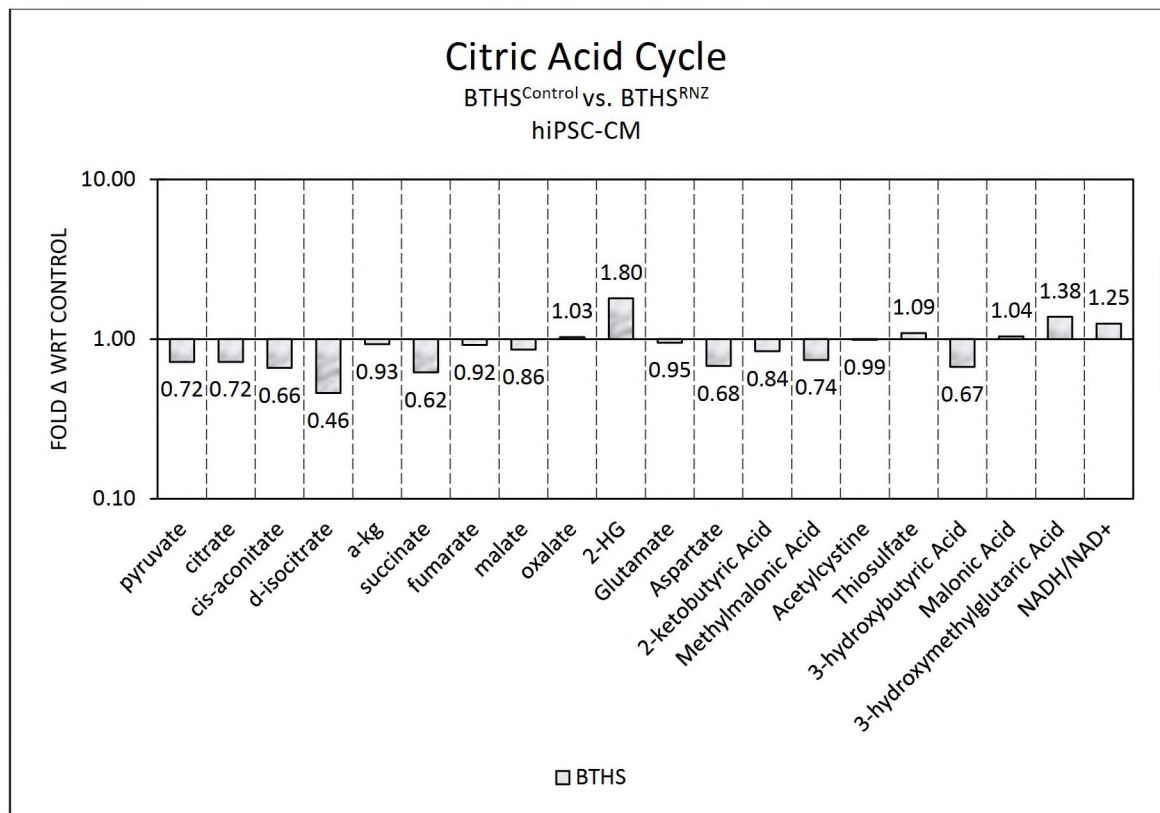


Figure 45: Citric Acid Cycle Intermediates in BTHS hiPSC-CMs treated with 100 mM Ranolazine with respect to Non-treated BTHS hiPSC-CMs (cell media)

Potential targets for future studies:

- D-isocitrate
- 2-HG

Pentose Phosphate Pathway (BTHS hiPSC-CM treated with Ranolazine)

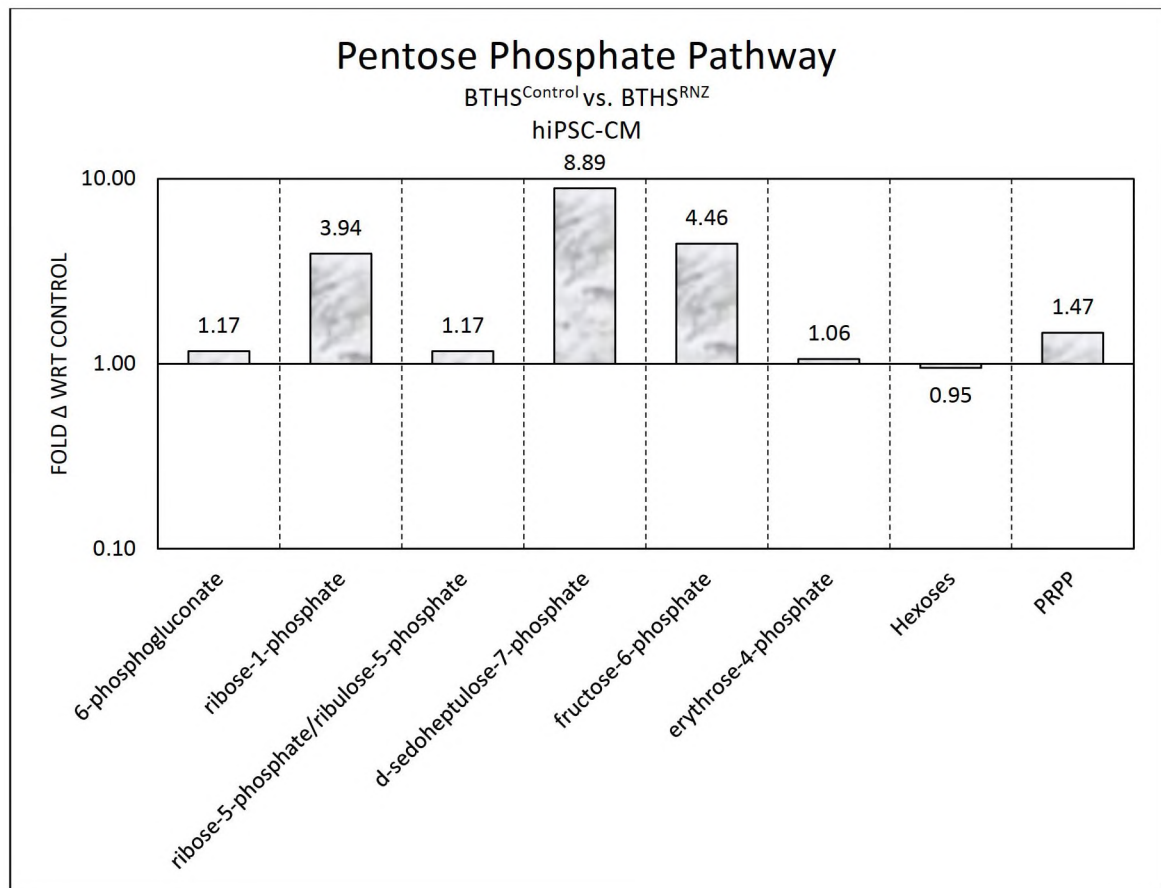


Figure 46: Pentose Phosphate Pathway Intermediates in BTHS hiPSC-CMs treated with 100 mM Ranolazine with respect to Non-treated BTHS hiPSC-CMs (cell media)

Potential targets for future studies:

- Ribose-1-phosphate
- D-sedoheptulose-7-phosphate
- Fructose-6-phosphate
- Fructose-1,6-bisphosphate

Sugar Phosphates (BTHS hiPSC-CM treated with Ranolazine)

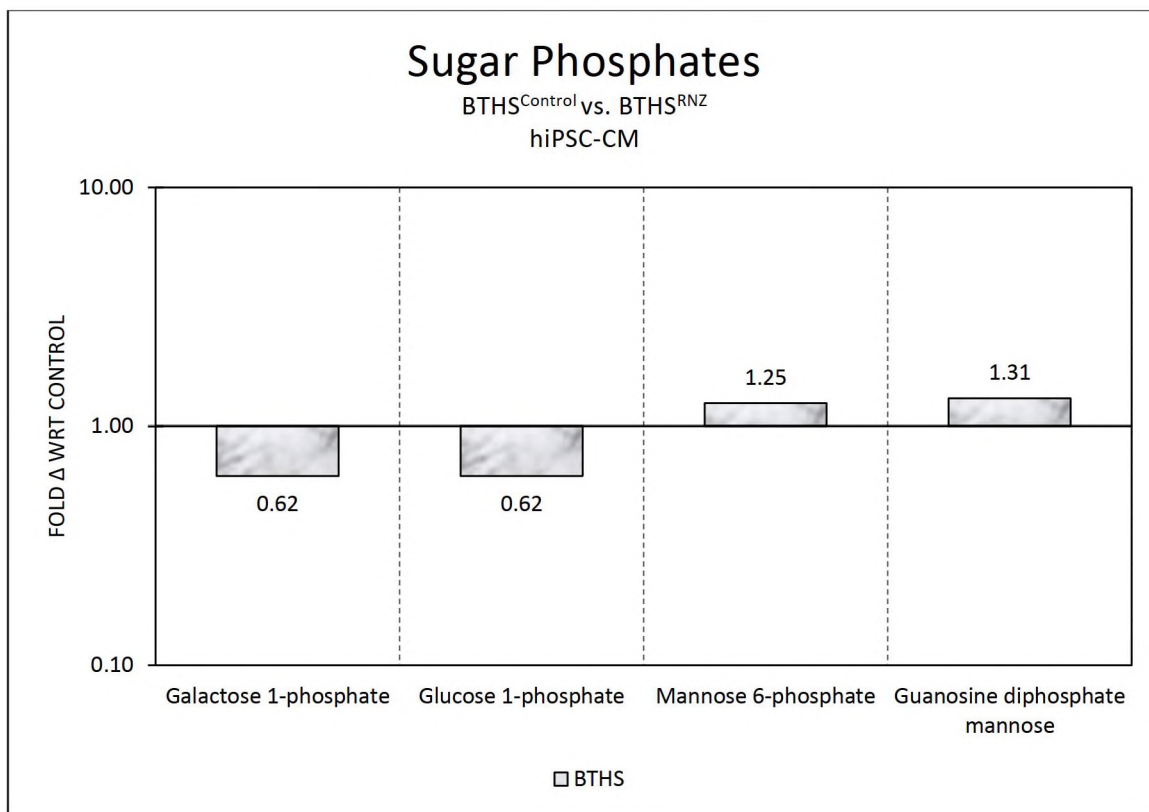


Figure 47: Sugar Phosphates in BTHS hiPSC-CMs treated with 100 mM Ranolazine with respect to Non-treated BTHS hiPSC-CMs (cell media)

No metabolites of interest were identified.

Nucleotides/Hexose Amines (BTHS hiPSC-CM treated with Ranolazine)

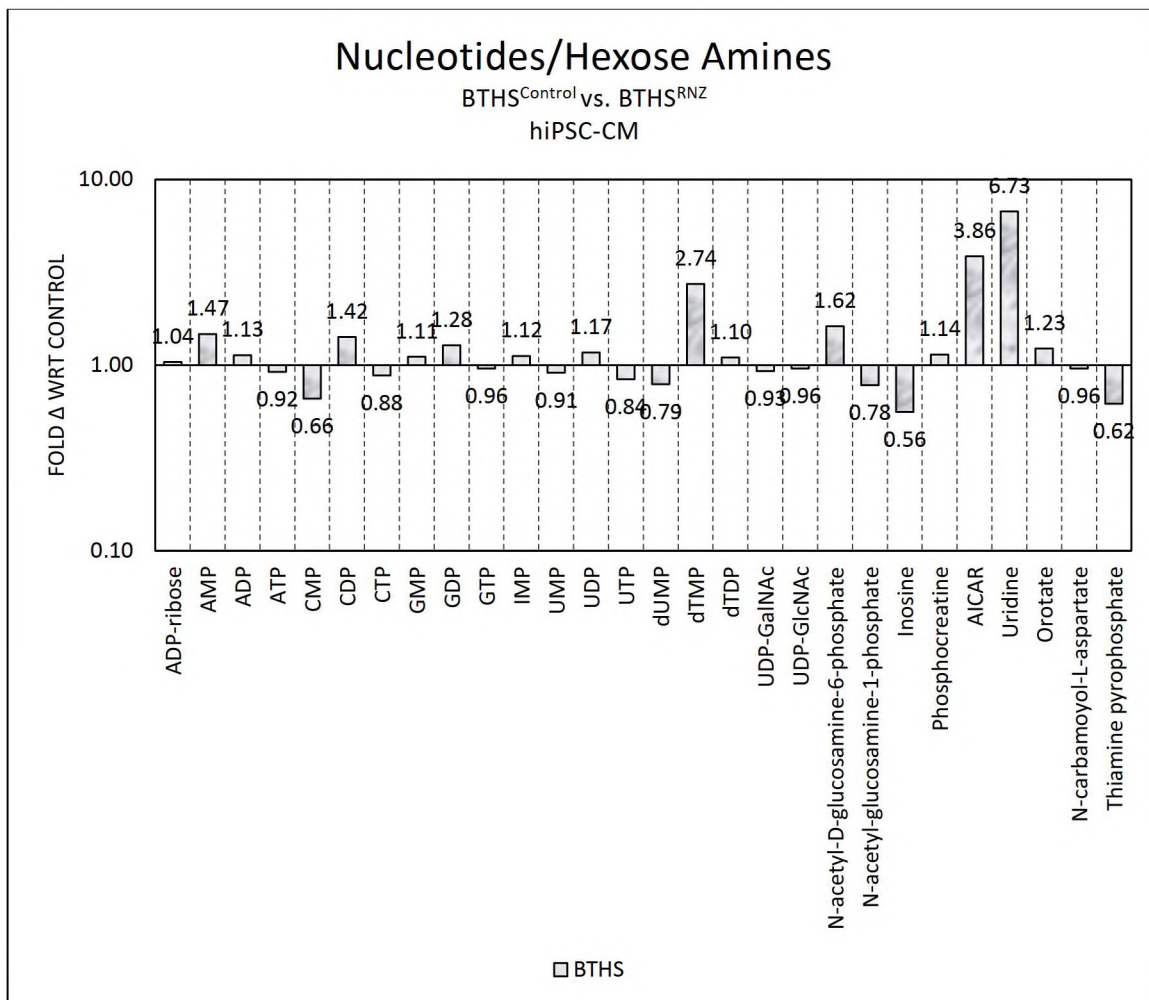


Figure 48: Nucleotides/Hexose Amines in BTHS hiPSC-CMs treated with 100 mM Ranolazine with respect to Non-treated BTHS hiPSC-CMs (cell media)

Potential targets for future studies:

- dTMP
- N-acetyl-D-glucosamine-6-phosphate
- AICAR (5-Aminoimidazole-4-carboxamide ribonucleotide)
- Uridine

Miscellaneous Metabolites (BTHS hiPSC-CM treated with Ranolazine)

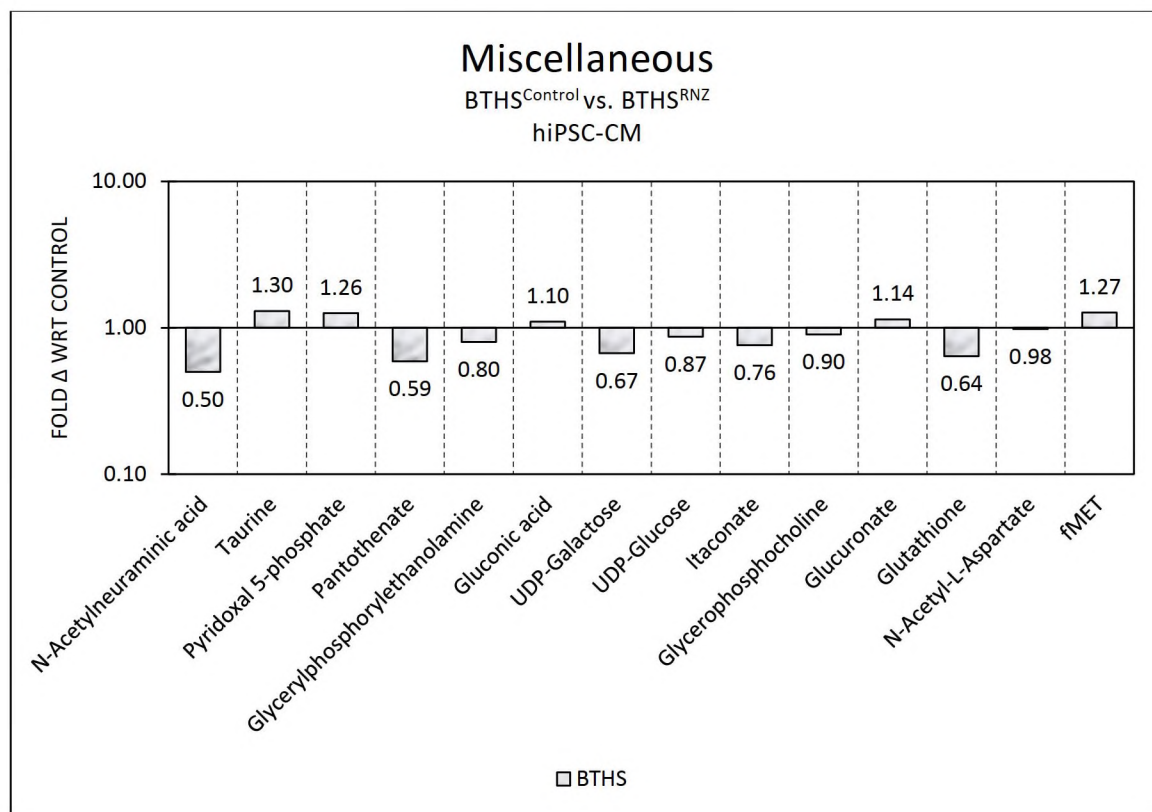


Figure 49: Miscellaneous Metabolites in BTHS hiPSC-CMs treated with 100 mM Ranolazine with respect to Non-treated BTHS hiPSC-CMs (cell media)

Potential targets for future studies:

- N-Acetylneuraminic acid

4.5 Technical Feasibility

This study demonstrates the technical feasibility of extraction protocol followed by ^1H -NMR metabolomics assays to evaluate the effect of drug treatment or disease state on hiPSC-CMs. This provides an innovative way of evaluating the cellular model (hiPSC-CMs) of BTHS, as we have identified 85 metabolites which can be measured and used to evaluate the effect of TAZ mutation and drug treatment.

A limitation of this study is that due to the discovery stage of the project, the sample size is small ($n=2$), however this serves as a pilot study in order to verify the feasibility of the assays and also to identify compounds which are targets for future studies. It is not possible to make a statistically significant mechanistic or biochemical conclusions from this data, however there are several metabolites which support the feasibility and scientific soundness of the assays, as the metabolite changes were validated with other studies by our laboratory. These metabolites will be pointed out in the next section, which highlights metabolite changes in the cell lysate, measured by LC-MS/MS.

4.5.1 *Metabolic Abnormalities Due to TAZ Mutation and Effect of Ranolazine*

Treatment on TAZ^{517delG} hiPSC-CMs (cell lysate – LC-MS/MS)

This section discusses selected metabolites that were found to be significant from the measurement of cell lysate metabolite levels. A full chart of detected metabolites can be found in the Appendix (Figures 55 and 56).

To summarize our findings, we found from this experiment that the increased succinate levels which are shown to be present in BTHS hiPSC-CM are normalized when treated with Ranolazine (Figure 50). Also, we observed expected decreased levels of the antioxidant glutathione in BTHS cells, and a subsequent increase in levels due to

Ranolazine treatment. Although for neither of these metabolites were the levels completely normalized, it does show that Ranolazine has a positive metabolic effect on BTHS hiPSC-CMs during treatment.

Succinate

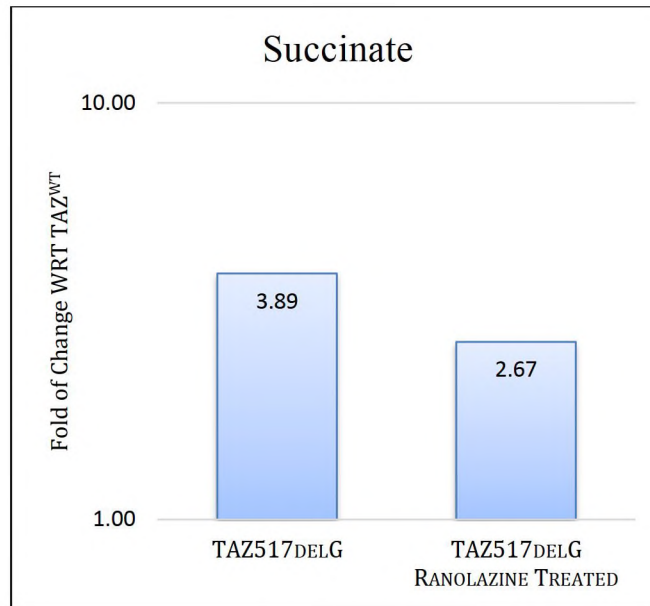


Figure 50: Succinate Levels in TAZ^{517delG} vs. TAZ^{517delG} 100 mM Ranolazine-treated hiPSC-CMs (cell lysate)

In Barth Syndrome cardiomyocytes, succinate dehydrogenase activity has been shown to be diminished (Dudek et al., 2016). Succinate dehydrogenase links the citric acid cycle to the respiratory chain, as the enzyme is a part of Complex II. As shown above, our study indicates that there is an accumulation of succinate in TAZ-iPSC-CM, in agreement with another published study from our lab (Fatica et al., 2019), and that Ranolazine treatment leads to a decrease in these elevated succinate levels.

Additionally, several studies have indicated that an increase in succinate levels is routinely seen in models of heart failure and is linked to an increase in ketone-body

metabolism (Aguiar et al., 2014). Presumably, the levels of succinate are increased to supply the reaction of acetoacetate to acetoacetyl-CoA. This is downstream of C4OH-carnitine production, which is common to be seen increased during heart failure and Barth Syndrome in particular (Cotter et al., 2013).

GSH+GSSG

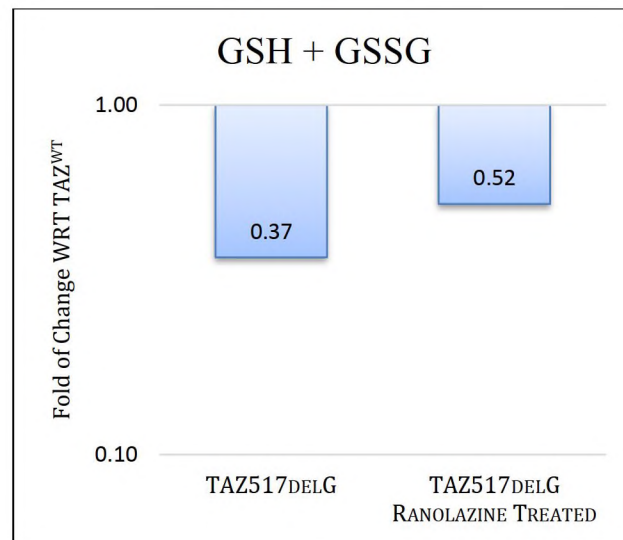


Figure 51: GSH + GSSG Levels in TAZ^{517delG}, and TAZ^{517delG} 100 mM Ranolazine-Treated hiPSC-CMs (cell lysate)

Glutathione (GSH + GSSG) is an important antioxidant in the cell. The reduced form of glutathione is GSH, and the oxidized form, which contains 2 GS- molecules, is GSSG. These two forms together work to regulate the redox status of the cell (*GSH and GSSG - Creative Proteomics*, n.d.). In Figure 51, it is demonstrated that there is a decrease in GSH + GSSG in TAZ-iPSC-CMs in comparison to WT hiPSC-CMs. This finding is consistent with a recent study (J. Kodger, Y.I. Sandler – unpublished results, Figure 52) that shows a decrease in GSH+GSSG in TAZ hiPSCs as compared to WT iPSCs. The total glutathione level is increased when hiPSC-CMs are treated with Ranolazine, though not

completely rescued to the level of the wild type cells. This decreased level of glutathione is consistent with a study which found that cardiolipin (CL) deficient cells have reduced glutathione levels (Patil et al., 2020) and this was found to be linked to diminished cysteine levels due to CL deficiency. We propose that glycine deficiency also contributes to low levels of glutathione.

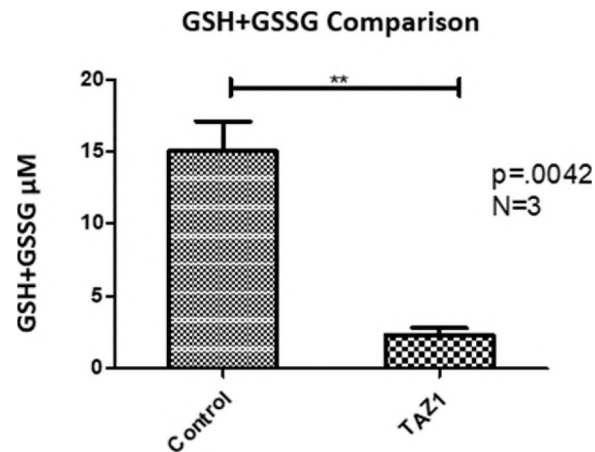


Figure 52: GSH+GSSG Levels in Undifferentiated iPSCs (WT vs. BTHS) (J. Kodger, Y.I. Sandler – Unpublished Data)

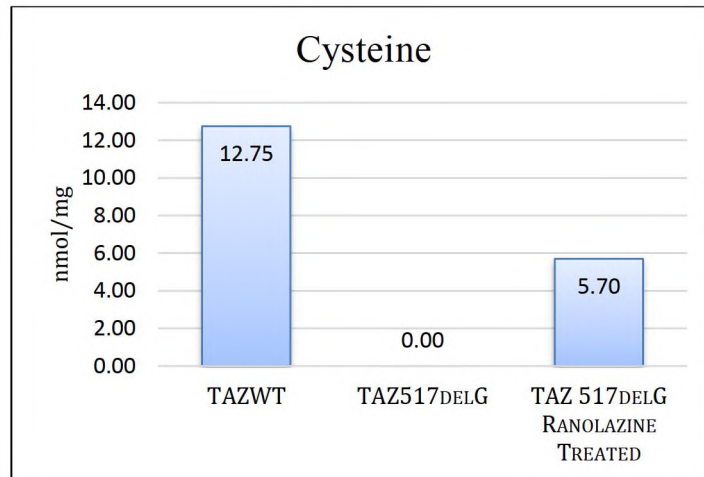


Figure 53: Cysteine Levels in WT, TAZ^{517delG}, and TAZ^{517delG} 100 mM Ranolazine-Treated hiPSC-CMs (cell lysate - absolute values shown because fold-of-change cannot be calculated)

Glutathione is comprised of 3 amino acids – cysteine, glycine, and glutamate. In Figure 53 it is shown that the cysteine levels follow the same pattern – a decrease in TAZ cells, and a subsequent increase when treated with Ranolazine. The deficient cysteine levels of TAZ hiPSC-CMs could contribute to the low levels of glutathione in the cells, as the availability of cysteine is the limiting factor of glutathione synthesis (Matuz-Mares et al., 2021).

4.6 Conclusion

We have identified many metabolites of interest from both BTHS hiPSC-CM vs. WT hiPSC-CM and BTHS hiPSC-CM treated with Ranolazine vs. BTHS hiPSC-CM not treated with Ranolazine. As a limitation to this study, the small sample size (n=2) limits our ability to make definitive conclusions as to the biochemical or mechanistic causes of changes in metabolite levels. For this reason, each metabolite class was calculated as a fold-of-change with respect to the control, and significance was determined at 1.5 (increase) or 0.5 (decrease). The outcome of this study is not sufficient to draw any concrete biological or mechanistic conclusions, however as a pilot study it has identified metabolites which are of interest in both the study of BTHS as well as Ranolazine treatment of hiPSC-CMs and has demonstrated the technical feasibility of using ^1H -NMR metabolomics on cultured cells (hiPSC-CMs) in order to evaluate metabolic differences.

CHAPTER V

CONCLUSION AND FUTURE DIRECTIONS

This proof of principle idea and technically innovative project has demonstrated the ability of NMR based metabolomics to be used to evaluate the (TAZ^{517delG}) mutation and Ranolazine treatment in a powerful cellular model of Barth syndrome. This project will pave a pathway for a new method of evaluating Barth syndrome cellular models and contributes to the understanding of metabolic disease phenotype. It is our hope that the development of these metabolomic assays will provide a means to expand our understanding of BTHS and inherited cardiomyopathies in general.

With regards to this project, there are a few aspects which leave room for future developments. On the level of differentiation of iPSCs to iPSC-CMs, additional analysis of cells (iPSC-CMs) should be performed if either of the differentiation methods are to be established for routine use. Although immunohistochemical imaging was performed, and the existence of cardiac proteins (TNNT3) and ventricular proteins (IRX4) was demonstrated, it would be helpful to perform flow cytometry analysis of the iPSC-CMs to establish the percentage of cardiac cells in the culture. Flow cytometry also provides a means to purify a population of cells, so if the ratio of cardiac to non-cardiac cells was

found to be insufficient, the ratio could be increased by performing flow cytometry cell sorting.

In the future, it would be interesting to evaluate different TAZ mutations using these assays to establish genotype-phenotype correlations and to determine whether the metabolic effect of Ranolazine is different amongst the varying mutations. It can be expected that the metabolic effect would indeed be different, as BTHS is a “mystery disease” from which patients can present with widely different symptoms, however it leaves the potential to find a metabolic intersection at which the various mutations converge. If a metabolic common denominator were to be found, this would pave the way for developing therapeutics specific to the BTHS disease, and for expanding our understanding the exact cause of the BTHS phenotype on the metabolome level. Overall, this project has produced advancements in the realm of metabolomics assay development for cultured cellular samples, in particular iPSC-CM.

BIBLIOGRAPHY

- About Inborn Errors of Metabolism*. (n.d.). Retrieved March 18, 2021, from <https://www.genome.gov/Genetic-Disorders/Inborn-Errors-of-Metabolism>
- Aguilar, C. J., Rocha-Franco, J. A., Sousa, P. A., Santos, A. K., Ladeira, M., Rocha-Resende, C., Ladeira, L. O., Resende, R. R., Botoni, F. A., Melo, M. B., Lima, C. X., Carballido, J. M., Cunha, T. M., Menezes, G. B., Guatimosim, S., & Leite, M. F. (2014). Succinate causes pathological cardiomyocyte hypertrophy through GPR91 activation. *Cell Communication and Signaling: CCS*, 12(1). <https://doi.org/10.1186/S12964-014-0078-2>
- Aisenbrey, E. A., & Murphy, W. L. (2020). Synthetic alternatives to Matrigel. *Nature Reviews. Materials*, 5(7), 539. <https://doi.org/10.1038/S41578-020-0199-8>
- Aubert, G., Martin, O. J., Horton, J. L., Lai, L., Vega, R. B., Leone, T. C., Koves, T., Gardell, S. J., Krüger, M., Hoppel, C. L., Lewandowski, E. D., Crawford, P. A., Muoio, D. M., & Kelly, D. P. (2016). The Failing Heart Relies on Ketone Bodies as a Fuel. *Circulation*, 133(8), 698–705. <https://doi.org/10.1161/CIRCULATIONAHA.115.017355>
- Barth Syndrome Foundation : Research : Animal and Cellular Models of Barth Syndrome*. (n.d.). Retrieved October 26, 2021, from <https://www.barthsyndrome.org/research/animalandcellularmodelsofBarthsyndrome.html>
- Bashir, A., Bohnert, K. L., Reeds, D. N., Peterson, L. R., Bittel, A. J., de las Fuentes, L., Pacak, C. A., Byrne, B. J., & Cade, W. T. (2017). Impaired cardiac and skeletal muscle bioenergetics in children, adolescents, and young adults with Barth

- syndrome. *Physiological Reports*, 5(3), e13130.
<https://doi.org/10.14814/PHY2.13130>
- Batalov, I., & Feinberg, A. W. (2015). Differentiation of Cardiomyocytes from Human Pluripotent Stem Cells Using Monolayer Culture. *Biomarker Insights*, 10(Suppl 1), 71–76. <https://doi.org/10.4137/BMI.S20050>
- Bhandari, B., & Subramanian, L. (2007). Ranolazine, a partial fatty acid oxidation inhibitor, its potential benefit in angina and other cardiovascular disorders. *Recent Patents on Cardiovascular Drug Discovery*, 2(1), 35–39.
<https://doi.org/10.2174/157489007779606095>
- Bhattacharya, S., Burridge, P. W., Kropp, E. M., Chuppa, S. L., Kwok, W.-M., Wu, J. C., Boheler, K. R., & Gundry, R. L. (2014). High Efficiency Differentiation of Human Pluripotent Stem Cells to Cardiomyocytes and Characterization by Flow Cytometry. *Journal of Visualized Experiments : JoVE*, 91, 52010. <https://doi.org/10.3791/52010>
- Bruneau, B. G., Bao, Z.-Z., Tanaka, M., Schott, J.-J., Izumo, S., Cepko, C. L., Seidman, J. G., & Seidman, C. E. (2000). Cardiac Expression of the Ventricle-Specific Homeobox Gene *Irx4* Is Modulated by *Nkx2-5* and *dHand*. *Developmental Biology*, 217(2), 266–277. <https://doi.org/https://doi.org/10.1006/dbio.1999.9548>
- Bstfa* | *C8H18F3NOSi2* - *PubChem*. (n.d.). Retrieved November 2, 2021, from <https://pubchem.ncbi.nlm.nih.gov/compound/BSTFA>
- Budi, E. H., Duan, D., & Derynck, R. (2017). Transforming Growth Factor- β Receptors and Smads: Regulatory Complexity and Functional Versatility. In *Trends in Cell Biology*. <https://doi.org/10.1016/j.tcb.2017.04.005>
- Burke, M. A., Chang, S., Wakimoto, H., Gorham, J. M., Conner, D. A., Christodoulou,

- D. C., Parfenov, M. G., DePalma, S. R., Eminaga, S., Konno, T., Seidman, J. G., & Seidman, C. E. (2016). Molecular profiling of dilated cardiomyopathy that progresses to heart failure. *JCI Insight*, 1(6).
<https://doi.org/10.1172/jci.insight.86898>
- Cao, N., Liu, Z., Chen, Z., Wang, J., Chen, T., Zhao, X., Ma, Y., Qin, L., Kang, J., Wei, B., Wang, L., Jin, Y., & Yang, H. T. (2012). Ascorbic acid enhances the cardiac differentiation of induced pluripotent stem cells through promoting the proliferation of cardiac progenitor cells. *Cell Research*, 22(1), 219–236.
<https://doi.org/10.1038/cr.2011.195>
- Chatham, J. C. (2002). Lactate – the forgotten fuel! *The Journal of Physiology*, 542(Pt 2), 333. <https://doi.org/10.1113/JPHYSIOL.2002.020974>
- Clarke, S. L. N., Bowron, A., Gonzalez, I. L., Groves, S. J., Newbury-Ecob, R., Clayton, N., Martin, R. P., Tsai-Goodman, B., Garratt, V., Ashworth, M., Bowen, V. M., McCurdy, K. R., Damin, M. K., Spencer, C. T., Toth, M. J., Kelley, R. I., & Steward, C. G. (2013). Barth syndrome. *Orphanet Journal of Rare Diseases*, 8(1), 23. <https://doi.org/10.1186/1750-1172-8-23>
- Corkey, B. E., & Shirihai, O. (2012). Metabolic master regulators: sharing information among multiple systems. *Trends in Endocrinology & Metabolism*, 23(12), 594–601.
<https://doi.org/https://doi.org/10.1016/j.tem.2012.07.006>
- Cotter, D. G., Schugar, R. C., & Crawford, P. A. (2013). Ketone body metabolism and cardiovascular disease. *American Journal of Physiology-Heart and Circulatory Physiology*, 304(8), H1060–H1076. <https://doi.org/10.1152/ajpheart.00646.2012>
- Dilated cardiomyopathy - Symptoms and causes - Mayo Clinic.* (n.d.). Retrieved

- December 2, 2021, from <https://www.mayoclinic.org/diseases-conditions/dilated-cardiomyopathy/symptoms-causes/syc-20353149>
- Doenst, T., Nguyen, T. D., & Abel, E. D. (2013). Cardiac Metabolism in Heart Failure. *Circulation Research*, 113(6), 709–724.
<https://doi.org/10.1161/CIRCRESAHA.113.300376>
- Dudek, J., Cheng, I.-F., Chowdhury, A., Wozny, K., Balleininger, M., Reinhold, R., Grunau, S., Callegari, S., Toischer, K., Wanders, R. J., Hasenfuß, G., Brügger, B., Guan, K., & Rehling, P. (2016). Cardiac-specific succinate dehydrogenase deficiency in Barth syndrome. *EMBO Molecular Medicine*, 8(2), 139–154.
<https://doi.org/10.15252/EMMM.201505644>
- Ebert, A. D., Diecke, S., Chen, I. Y., & Wu, J. C. (2015). Reprogramming and transdifferentiation for cardiovascular development and regenerative medicine: where do we stand? *EMBO Molecular Medicine*, 7(9), 1090–1103.
<https://doi.org/10.15252/emmm.201504395>
- Emwas, A. H., Roy, R., McKay, R. T., Tenori, L., Saccenti, E., Nagana Gowda, G. A., Raftery, D., Alahmari, F., Jaremko, L., Jaremko, M., & Wishart, D. S. (2019). NMR Spectroscopy for Metabolomics Research. *Metabolites*, 9(7).
<https://doi.org/10.3390/METABO9070123>
- Fatica, E. M., Deleonibus, G. A., House, A., Kodger, J. V., Pearce, R. W., Shah, R. R., Levi, L., & Sandler, Y. (2019). Barth Syndrome: Exploring Cardiac Metabolism with Induced Pluripotent Stem Cell-Derived Cardiomyocytes. *Metabolites*, 9(12).
<https://doi.org/10.3390/METABO9120306>
- Fillmore, N., & Lopaschuk, G. D. (2013). Targeting mitochondrial oxidative metabolism

- as an approach to treat heart failure. *Biochimica et Biophysica Acta (BBA) - Molecular Cell Research*, 1833(4), 857–865.
<https://doi.org/10.1016/J.BBAMCR.2012.08.014>
- Finsterer, J. (2019). Barth syndrome: mechanisms and management. *The Application of Clinical Genetics*, 12, 95. <https://doi.org/10.2147/TACG.S171481>
- Gessert, S., & Kuhl, M. (2010). The Multiple Phases and Faces of Wnt Signaling During Cardiac Differentiation and Development. *Circulation Research*, 107(2), 186–199.
<https://doi.org/10.1161/CIRCRESAHA.110.221531>
- GSH and GSSG - Creative Proteomics*. (n.d.). Retrieved November 13, 2021, from
<https://www.creative-proteomics.com/services/gsh-and-gssg.htm>
- Gwaltney, C., Stokes, J., Aiudi, A., Mazar, I., Ollis, S., Love, E., & Shields, A. (2021). Development and content validity of the Barth Syndrome Symptom Assessment (BTHS-SA) for adolescents and adults. *Orphanet Journal of Rare Diseases*, 16(1), 1–13. <https://doi.org/10.1186/S13023-021-01897-Z/TABLES/5>
- Hershberger, R. E., Morales, A., & Siegfried, J. D. (2010). Clinical and genetic issues in dilated cardiomyopathy: A review for genetics professionals. *Genetics In Medicine*, 12, 655. <http://dx.doi.org/10.1097/GIM.0b013e3181f2481f>
- House, A., Fatica, E., Shah, R., Stergar, J., Pearce, R., & Sandler, Y. (2020). A protocol for metabolic characterization of human induced pluripotent stem cell-derived cardiomyocytes (iPS-CM). *MethodsX*, 7, 100572.
<https://doi.org/10.1016/J.MEX.2019.05.028>
- Jain, A., Norton, N., Bruno, K. A., Cooper, L. T., Atwal, P. S., & Fairweather, D. (2021). Sex Differences, Genetic and Environmental Influences on Dilated Cardiomyopathy.

- Journal of Clinical Medicine*, 10(11), 2289. <https://doi.org/10.3390/JCM10112289>
- Jefferies, J. L. (2013). Barth syndrome. *American Journal of Medical Genetics. Part C, Seminars in Medical Genetics*, 163C(3), 198–205.
<https://doi.org/10.1002/AJMG.C.31372>
- Kamdar, F., Kamdar, A. K., Koyano-Nakagawa, N., Garry, M. G., & Garry, D. J. (2015). Cardiomyopathy in a dish: Using human inducible pluripotent stem cells to model inherited cardiomyopathies. *Journal of Cardiac Failure*, 21(9), 761–770.
<https://doi.org/10.1016/j.cardfail.2015.04.010>
- Katsuragi, S., & Ikeda, T. (2021). Dilated Cardiomyopathy. *Maternal and Fetal Cardiovascular Disease*, 97–106. https://doi.org/10.1007/978-981-10-1993-7_9
- Kattman, S. J., Witty, A. D., Gagliardi, M., Dubois, N. C., Niapour, M., Hotta, A., Ellis, J., & Keller, G. (2011). Stage-specific optimization of activin/nodal and BMP signaling promotes cardiac differentiation of mouse and human pluripotent stem cell lines. *Cell Stem Cell*, 8(2), 228–240. <https://doi.org/10.1016/j.stem.2010.12.008>
- Kelley, R. I., Cheatham, J. P., Clark, B. J., Nigro, M. A., Powell, B. R., Sherwood, G. W., Sladky, J. T., & Swisher, W. P. (1991). X-linked dilated cardiomyopathy with neutropenia, growth retardation, and 3-methylglutaconic aciduria. *The Journal of Pediatrics*, 119(5), 738–747. [https://doi.org/https://doi.org/10.1016/S0022-3476\(05\)80289-6](https://doi.org/10.1016/S0022-3476(05)80289-6)
- Kiebish, M. A., Yang, K., Liu, X., Mancuso, D. J., Guan, S., Zhao, Z., Sims, H. F., Cerqua, R., Cade, W. T., Han, X., & Gross, R. W. (2013). Dysfunctional cardiac mitochondrial bioenergetic, lipidomic, and signaling in a murine model of Barth syndrome. *Journal of Lipid Research*, 54(5), 1312–1325.

<https://doi.org/10.1194/jlr.M034728>

Kim, M. S., Horst, A., Blinka, S., Stamm, K., Mahnke, D., Schuman, J., Gundry, R., Tomita-Mitchell, A., & Lough, J. (2015). Activin-A and Bmp4 levels modulate cell type specification during CHIR-induced cardiomyogenesis. *PLoS ONE*, *10*(2).

<https://doi.org/10.1371/journal.pone.0118670>

Kitzenberg, D., Colgan, S. P., & Glover, L. E. (2016). Creatine kinase in ischemic and inflammatory disorders. *Clinical and Translational Medicine* *2016 5:1*, *5*(1), 1–10.

<https://doi.org/10.1186/S40169-016-0114-5>

Kolwicz, S. C., Airhart, S., & Tian, R. (2016). Ketones Step to the Plate. *Circulation*, *133*(8), 689–691. <https://doi.org/10.1161/CIRCULATIONAHA.116.021230>

Kolwicz, S. C., Purohit, S., & Tian, R. (2013). Cardiac Metabolism and its Interactions With Contraction, Growth, and Survival of Cardiomyocytes. *Circulation Research*, *113*(5), 603–616. <https://doi.org/10.1161/CIRCRESAHA.113.302095>

Lian, X., Hsiao, C., Wilson, G., Zhu, K., Hazeltine, L. B., Azarin, S. M., Raval, K. K., Zhang, J., Kamp, T. J., & Palecek, S. P. (2012). Robust cardiomyocyte differentiation from human pluripotent stem cells via temporal modulation of canonical Wnt signaling. *Proceedings of the National Academy of Sciences of the United States of America*. <https://doi.org/10.1073/pnas.1200250109>

Lian, X., Zhang, J., Azarin, S. M., Zhu, K., Hazeltine, L. B., Bao, X., Hsiao, C., Kamp, T. J., & Palecek, S. P. (2013). Directed cardiomyocyte differentiation from human pluripotent stem cells by modulating Wnt/ β -catenin signaling under fully defined conditions. *Nature Protocols*, *8*(1), 162. <https://doi.org/10.1038/NPROT.2012.150>

Lu, Y.-W., & Claypool, S. M. (2015). Disorders of phospholipid metabolism: an

- emerging class of mitochondrial disease due to defects in nuclear genes . In *Frontiers in Genetics* (Vol. 6, p. 3).
<https://www.frontiersin.org/article/10.3389/fgene.2015.00003>
- Malik, N., & Rao, M. S. (2013). A Review of the Methods for Human iPSC Derivation. *Methods in Molecular Biology (Clifton, N.J.)*, 997, 23. https://doi.org/10.1007/978-1-62703-348-0_3
- Matuz-Mares, D., Riveros-Rosas, H., Vázquez-Meza, H., & Vilchis-Landeros, M. M. (2021). Glutathione Participation in the Prevention of Cardiovascular Diseases. *Antioxidants*, 10(8). <https://doi.org/10.3390/ANTIOX10081220>
- Mazzotta, S., Neves, C., Bonner, R. J., Bernardo, A. S., Docherty, K., & Hoppler, S. (2016). Distinctive Roles of Canonical and Noncanonical Wnt Signaling in Human Embryonic Cardiomyocyte Development. *Stem Cell Reports*, 7(4), 764–776.
<https://doi.org/10.1016/J.STEMCR.2016.08.008>
- McCormack, J. G., Barr, R. L., Wolff, A. A., & Lopaschuk, G. D. (1996). Ranolazine Stimulates Glucose Oxidation in Normoxic, Ischemic, and Reperfused Ischemic Rat Hearts. *Circulation*, 93(1), 135–142. <https://doi.org/10.1161/01.CIR.93.1.135>
- McLaren, A. (2001). Ethical and social considerations of stem cell research. *Nature*, 414, 129. <http://dx.doi.org/10.1038/35102194>
- McNally, E. M., Golbus, J. R., & Puckelwartz, M. J. (2013). Genetic mutations and mechanisms in dilated cardiomyopathy. *The Journal of Clinical Investigation*, 123(1), 19–26. <https://doi.org/10.1172/JCI62862>
- McNally, E. M., & Mestroni, L. (2017). Dilated cardiomyopathy: genetic determinants and mechanisms. *Circulation Research*, 121(7), 731–748.

- <https://doi.org/10.1161/CIRCRESAHA.116.309396>
- Methoxyamine hydrochloride for GC derivatization, LiChropur™, 97.5-102.5% (AT) | 593-56-6. (n.d.). Retrieved November 2, 2021, from <https://www.sigmaaldrich.com/US/en/product/sial/89803>*
- National Center for Biotechnology Information. (n.d.). *(R)-trans-4-(1-Aminoethyl)-N-(4-pyridyl) cyclohexanecarboxamide | C14H21N3O - PubChem*. PubChem Compound Database. <https://doi.org/CID=448042>
- Neely, J. R., & Morgan, H. E. (1974). Relationship Between Carbohydrate and Lipid Metabolism and the Energy Balance of Heart Muscle. *Annual Review of Physiology*, 36(1), 413–459. <https://doi.org/10.1146/annurev.ph.36.030174.002213>
- Nocito, L., Kleckner, A. S., Yoo, E. J., Jones IV, A. R., Liesa, M., & Corkey, B. E. (2015). The Extracellular Redox State Modulates Mitochondrial Function, Gluconeogenesis, and Glycogen Synthesis in Murine Hepatocytes. *PLOS ONE*, 10(3), e0122818. <https://doi.org/10.1371/journal.pone.0122818>
- Oates, P. J., Brown, D. A., Vernon, H. J., Gangoiti, J. A., & Barshop, B. A. (2020). Metabolomic biomarkers from patients with Barth syndrome treated with elamipretide: insights from the TAZPOWER study. *MedRxiv*, 2020.11.20.20235580. <https://doi.org/10.1101/2020.11.20.20235580>
- OMIM Entry - # 302060 - BARTH SYNDROME; BTHS. (n.d.). Retrieved March 27, 2022, from <https://www.omim.org/entry/302060>*
- Paradies, G., Paradies, V., Ruggiero, F. M., & Petrosillo, G. (2019). Role of Cardiolipin in Mitochondrial Function and Dynamics in Health and Disease: Molecular and Pharmacological Aspects. *Cells*, 8(7), 728. <https://doi.org/10.3390/CELLS8070728>

- Patil, V. A., Li, Y., Ji, J., & Greenberg, M. L. (2020). Loss of the mitochondrial lipid cardiolipin leads to decreased glutathione synthesis. *Biochimica et Biophysica Acta. Molecular and Cell Biology of Lipids*, 1865(2), 158542. <https://doi.org/10.1016/J.BBALIP.2019.158542>
- Raja, V., & Greenberg, M. L. (2014). THE FUNCTIONS OF CARDIOLIPIN IN CELLULAR METABOLISM – POTENTIAL MODIFIERS OF THE BARTH SYNDROME PHENOTYPE. *Chemistry and Physics of Lipids*, 179, 49–56. <https://doi.org/10.1016/j.chemphyslip.2013.12.009>
- Raval, K. K., & Kamp, T. J. (2014). Cardiomyopathy, mitochondria and Barth syndrome: iPSCs reveal a connection. *Nature Medicine*, 20, 585. <http://dx.doi.org/10.1038/nm.3592>
- Roberts, L. D., Souza, A. L., Gerszten, R. E., & Clish, C. B. (2012). Targeted Metabolomics. *Current Protocols in Molecular Biology*, 98(1), 30.2.1-30.2.24. <https://doi.org/10.1002/0471142727.mb3002s98>
- Rony, I. K., Baten, A., Bloomfield, J. A., Islam, M. E., Billah, M. M., & Islam, K. D. (2015). Inducing pluripotency in vitro: recent advances and highlights in induced pluripotent stem cells generation and pluripotency reprogramming. *Cell Proliferation*, 48(2), 140–156. <https://doi.org/10.1111/cpr.12162>
- Ross, S. B., Fraser, S. T., Nowak, N., & Semsarian, C. (2017). Generation of induced pluripotent stem cells (iPSCs) from a hypertrophic cardiomyopathy patient with the pathogenic variant p.Val698Ala in beta-myosin heavy chain (MYH7) gene. *Stem Cell Research*, 20, 88–90. <https://doi.org/10.1016/J.SCR.2017.02.015>
- Sandlers, Y., Mercier, K., Pathmasiri, W., Carlson, J., McRitchie, S., Sumner, S., &

- Vernon, H. J. (2016). Metabolomics Reveals New Mechanisms for Pathogenesis in Barth Syndrome and Introduces Novel Roles for Cardiolipin in Cellular Function. *PLOS ONE*, 11(3), e0151802. <https://doi.org/10.1371/journal.pone.0151802>
- Saric, A., Andreau, K., Armand, A.-S., Møller, I. M., & Petit, P. X. (2015). Barth Syndrome: From Mitochondrial Dysfunctions Associated with Aberrant Production of Reactive Oxygen Species to Pluripotent Stem Cell Studies. *Frontiers in Genetics*, 6, 359. <https://doi.org/10.3389/fgene.2015.00359>
- Saric, A., Andreau, K., Armand, A.-S., Møller, I. M., & Petit, P. X. (2016). Barth Syndrome: From Mitochondrial Dysfunctions Associated with Aberrant Production of Reactive Oxygen Species to Pluripotent Stem Cell Studies. *Frontiers in Genetics*, 6, 359. <https://doi.org/10.3389/fgene.2015.00359>
- Schlame, M., & Greenberg, M. L. (2017). Biosynthesis, remodeling and turnover of mitochondrial cardiolipin. *Biochimica et Biophysica Acta*, 1862(1), 3. <https://doi.org/10.1016/J.BBALIP.2016.08.010>
- Schlame, M., & Ren, M. (2006). Barth syndrome, a human disorder of cardiolipin metabolism. *FEBS Letters*, 580(23), 5450–5455. <https://doi.org/https://doi.org/10.1016/j.febslet.2006.07.022>
- Sharma, A., Li, G., Rajarajan, K., Hamaguchi, R., Burrridge, P. W., & Wu, S. M. (2015). Derivation of Highly Purified Cardiomyocytes from Human Induced Pluripotent Stem Cells Using Small Molecule-modulated Differentiation and Subsequent Glucose Starvation. *JoVE (Journal of Visualized Experiments)*, 2015(97), e52628. <https://doi.org/10.3791/52628>
- Sigma Aldrich. (n.d.). *IWR-1 ≥98% (HPLC) | Sigma-Aldrich*. Retrieved November 7,

- 2018, from
<https://www.sigmaaldrich.com/catalog/product/sigma/i0161?lang=en®ion=US>
 STEMCELL Technologies. (n.d.). *CHIR99021* | *STEMCELL Technologies*. Retrieved
 November 7, 2018, from <https://www.stemcell.com/chir99021.html>
- Taegtmeyer, H. (2004). Cardiac metabolism as a target for the treatment of heart failure.
Circulation, *110*(8), 894–896.
<https://doi.org/10.1161/01.CIR.0000139340.88769.D5>
- Takahashi, K., Tanabe, K., Ohnuki, M., Narita, M., Ichisaka, T., Tomoda, K., &
 Yamanaka, S. (2007). Induction of Pluripotent Stem Cells from Adult Human
 Fibroblasts by Defined Factors. *Cell*, *131*(5), 861–872.
<https://doi.org/10.1016/j.cell.2007.11.019>
- Valianpour, F., Wanders, R. J. A., Barth, P. G., Overmars, H., & van Gennip, A. H.
 (2002). Quantitative and Compositional Study of Cardiolipin in Platelets by
 Electrospray Ionization Mass Spectrometry: Application for the Identification of
 Barth Syndrome Patients. *Clinical Chemistry*, *48*(9), 1390 LP – 1397.
<http://clinchem.aaccjnls.org/content/48/9/1390.abstract>
- Vallins, W. J., Brand, N. J., Dabhade, N., Butler-Browne, G., Yacoub, M. H., & Barton,
 P. J. R. (1990). Molecular cloning of human cardiac troponin I using polymerase
 chain reaction. *FEBS Letters*, *270*(1), 57–61.
[https://doi.org/https://doi.org/10.1016/0014-5793\(90\)81234-F](https://doi.org/https://doi.org/10.1016/0014-5793(90)81234-F)
- Vaz, F. M., Houtkooper, R. H., Valianpour, F., Barth, P. G., & Wanders, R. J. A. (2003).
 Only One Splice Variant of the Human TAZ Gene Encodes a Functional Protein
 with a Role in Cardiolipin Metabolism. *Journal of Biological Chemistry*, *278*(44),

43089–43094. <https://doi.org/10.1074/JBC.M305956200>

Vernon, H. J., Sandler, Y., McClellan, R., & Kelley, R. I. (2014). Clinical laboratory studies in Barth Syndrome. *Molecular Genetics and Metabolism*, 112(2), 143–147.

<https://doi.org/https://doi.org/10.1016/j.ymgme.2014.03.007>

Wang, G., McCain, M. L., Yang, L., He, A., Pasqualini, F. S., Agarwal, A., Yuan, H., Jiang, D., Zhang, D., Zangi, L., Geva, J., Roberts, A. E., Ma, Q., Ding, J., Chen, J., Wang, D.-Z., Li, K., Wang, J., Wanders, R. J. A., ... Pu, W. T. (2014). Modeling the mitochondrial cardiomyopathy of Barth syndrome with induced pluripotent stem cell and heart-on-chip technologies. *Nature Medicine*, 20, 616.

<http://dx.doi.org/10.1038/nm.3545>

Weng, Z., Kong, C.-W., Ren, L., Karakikes, I., Geng, L., He, J., Chow, M. Z. Y., Mok, C. F., Chan, H. Y. S., Webb, S. E., Keung, W., Chow, H., Miller, A. L., Leung, A. Y. H., Hajjar, R. J., Li, R. A., & Chan, C. W. (2014). A Simple, Cost-Effective but Highly Efficient System for Deriving Ventricular Cardiomyocytes from Human Pluripotent Stem Cells. *Stem Cells and Development*.

<https://doi.org/10.1089/scd.2013.0509>

Werner, C., Doenst, T., & Schwarzer, M. (2016). *Chapter 4 - Metabolic Pathways and Cycles* (M. Schwarzer & T. B. T.-T. S. G. to C. M. Doenst (Eds.); pp. 39–55).

Academic Press. [https://doi.org/https://doi.org/10.1016/B978-0-12-802394-5.00004-](https://doi.org/https://doi.org/10.1016/B978-0-12-802394-5.00004-2)

2

Wortmann, S. B., Kluijtmans, L. A., Engelke, U. F. H., Wevers, R. A., & Morava, E.

(2012). The 3-methylglutaconic acidurias: what's new? *Journal of Inherited*

Metabolic Disease, 35(1), 13–22. <https://doi.org/10.1007/s10545-010-9210-7>

- Yan, Y., & Kang, B. (2012). The Role of Cardiolipin Remodeling in Mitochondrial Function and Human Diseases. *Journal of Molecular Biology Research*, 2(1).
<https://doi.org/10.5539/jmbr.v2n1p1>
- Yang, L., Soonpaa, M. H., Adler, E. D., Roepke, T. K., Kattman, S. J., Kennedy, M., Henckaerts, E., Bonham, K., Abbott, G. W., Linden, R. M., Field, L. J., & Keller, G. M. (2008). Human cardiovascular progenitor cells develop from a KDR+ embryonic-stem-cell-derived population. *Nature*, 453, 524.
<http://dx.doi.org/10.1038/nature06894>
- Zweigerdt, R., Gruh, I., & Martin, U. (2014). Your Heart on a Chip: iPSC-Based Modeling of Barth-Syndrome-Associated Cardiomyopathy. *Cell Stem Cell*, 15(1), 9–11. <https://doi.org/10.1016/j.stem.2014.06.015>

Retention Time	Compound	Retention Time	Compound	Retention Time	Compound	Retention Time	Compound
7.9965	2-hydroxypyridine	14.1458	phosphate	23.4125	N-acetyl-L-aspartic acid	29.9662	isopropyl beta-D-1-thiogalactopyranoside
8.1343	Pyruvate	14.8924	glycine	23.878	pyrophosphate	30.1162	C11 dioic acid
8.4309	pyruvic acid	15.0446	succinic acid	25.3057	beta-glycerolphosphate	30.4062	pantothenic acid 2
8.7542	lactic acid	15.3612	methysuccinate	25.8489	dihydroxyacetone phosphate	31.0394	palmitic acid
8.7587	lactate	15.6934	glyceric acid	26.0456	glycerol-1-phosphate	31.1039	cytidine-5'-monophosphate 1
9.0231	glycolic acid	15.8734	fumaric acid	26.27	O-phosphocolamine	31.2005	gluconic acid
9.6752	L-alanine	16.4511	L-serine 2	26.9177	L-ornithine 2	32.446	allo-inositol
10.3118	3-hydroxypyridine	16.7666	2,3-dihydroxypyridine	26.991	3-phosphoglycerate	32.7037	N-acetyl-D-mannosamine
10.4629	oxalate	17.1466	L-threonine 2	26.9932	3-phosphoglyceric acid	32.7804	heptadecanoic acid
10.6951	3 OH propanoic acid	17.2099	hydroquinone	27.0399	citrulline	34.0369	oleic acid
10.7051	4-hydroxypyridine	18.0676	2-hydroxybenzyl alcohol	27.1621	citric acid	34.5124	stearic acid
10.8684	L-norleucine	18.0676	3-hydroxybenzyl alcohol	27.1621	citrate	36.6921	D-glucose-6-phosphate
11.1195	BHiB	19.0942	1-methyl nicotinamide	27.2021	myristic acid	37.7165	arachidic acid
11.1195	malonic acid 1	19.1986	citramalic acid	27.6554	adenine	40.7117	behenic acid
11.2751	L-proline	19.3052	4-hydroxymandelonitrile	28.0409	tyrosine 1	41.7238	sucrose
11.395	DL-isoleucine	19.6874	D-malic acid	28.4575	tagatose	42.2248	5'-deoxy-5'(methylthio)adenosine
11.9661	L-mimosine	19.9052	O-acetylsalicylic acid	28.6508	C16 methyl palmitate	42.4737	lactose
12.5594	L-valine 2	20.3118	L-pyroglutamic acid	28.9441	D-allose	43.1847	maltose
12.7682	DL-glyceraldehyde 2	20.4084	aspartic acid	29.063	D-mannose	43.3381	squalene
13.1082	benzoic acid	20.6184	phenylalanine 1	29.1786	D (+)altrose 2	44.619	uridine-5'-monophosphate
13.1871	norvaline 2	21.0417	creatinine	29.3785	D-glucose	45.0556	isomaltose
13.707	nicotinic acid	21.6861	2-hydroxyglutarate	29.4585	1-hexadecanol	46.9599	adenosine-5-monophosphate
13.8947	urea	22.2649	3-hydroxy-3-methylglutaric acid	29.5107	dehydroascorbic acid 3	47.7231	cholesterol
14.0425	L-leucine 2	22.6982	L-glutamic acid	29.7074	D-sorbitol	49.8617	lanosterol
						53.5558	maltotriose

Figure 54: Complete list of compounds measured by GC-MS small metabolite scan

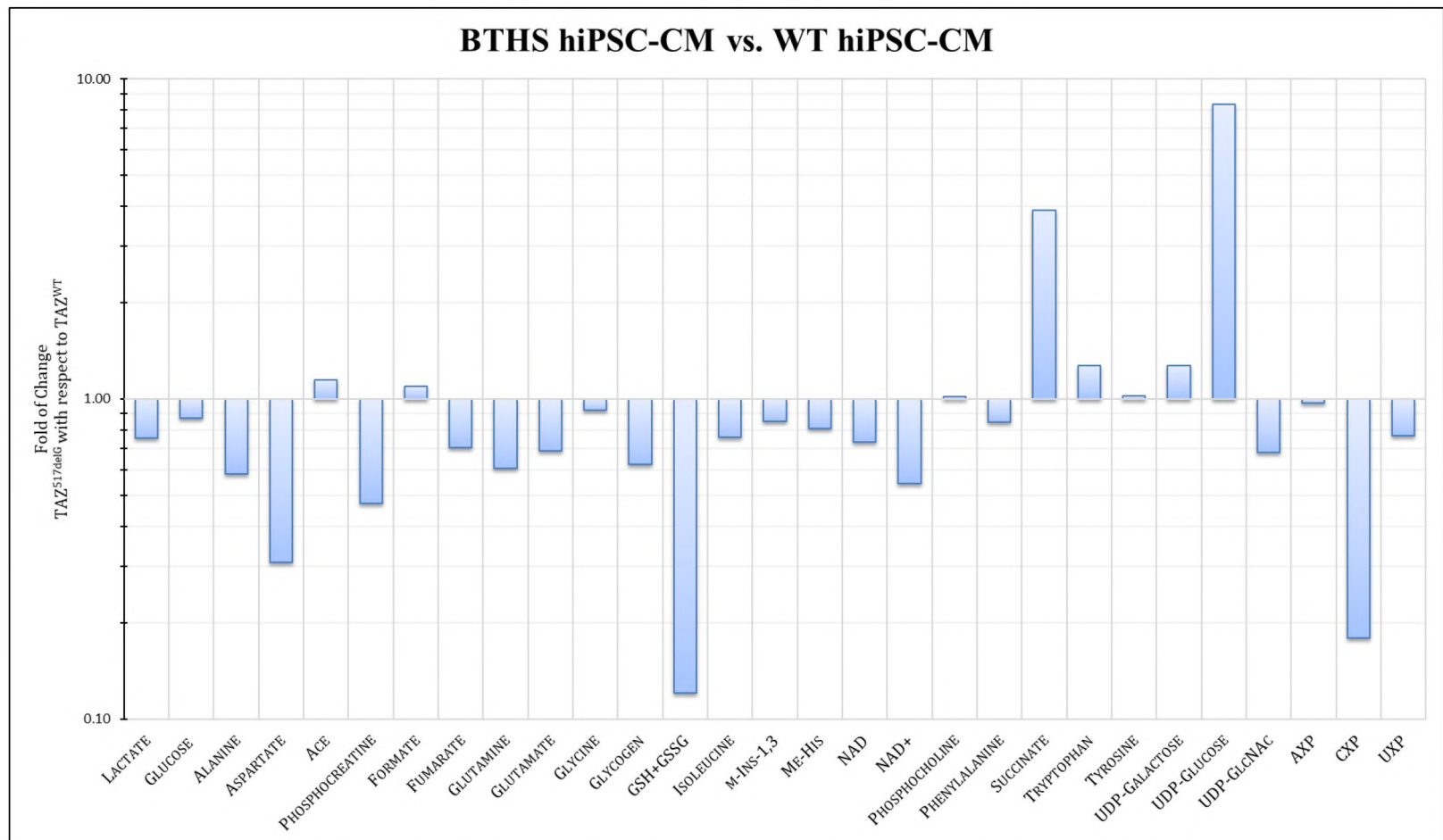


Figure 55: hiPSC-CM: TAZ^{WT} vs. TAZ^{517delG} (cell lysate)

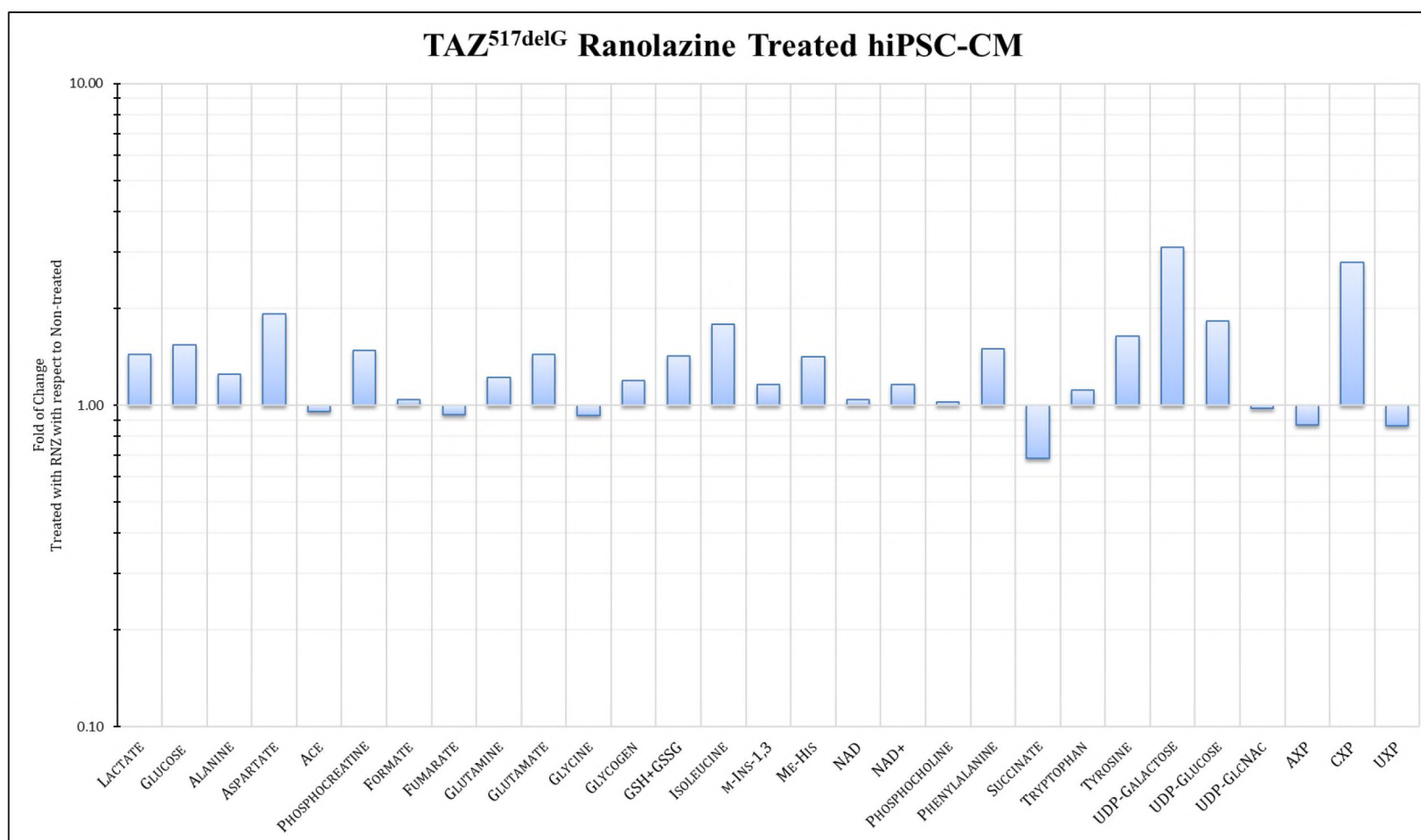


Figure 56: hiPSC-CM: TAZ^{517delG} vs. TAZ^{517delG} Ranolazine-treated (cell lysate)